NOTICE

The quality of this microfiche is heavily dependent upon the quality of the original thesis submitted for microfilming. Every effort has been made to ensure the highest quality of reproduction possible.

If pages are missing, contact the university which granted the degree.

Some pages may have indistinct print especially if the original pages were typed with a poor typewriter ribbon or if the university sent us a poor photocopy.

Previously copyrighted materials (journal articles, published tests, etc.) are not filmed.

Reproduction in full or in part of this film is governed by the Canadian Copyright Act, R.S.C. 1970, c. C-30. Please read the authorization forms which accompany this thesis.

THIS DISSERTATION
HAS BEEN MICROFILMED
EXACTLY AS RECEIVED

AVIS

La qualité de cette microfiche dépend grandement de la qualité de la thèse soumise au microfilmage. Nous avons tout fait pour assurer une qualité supérieure de reproduction.

S'il manque des pages, veuillez communiquer avec l'université qui a conféré le grade.

La qualité d'impression de certaines pages peut laisser à désirer, surtout si les pages originales ont été dactylographiées à l'aide d'un ruban usé ou si l'université nous a fait parvenir une photocopie de mauvaise qualité.

Les documents qui font déjà l'objet d'un droit d'auteur (articles de revue, examens publiés, etc.) ne sont pas microfilmés.

La reproduction, même partielle, de ce microfilm est soumise à la Loi canadienne sur le droit d'auteur, SRC 1970, c. C-30. Veuillez prendre connaissance des formules d'autorisation qui accompagnent cette thèse.

LA THÈSE A ÉTÉ
MICROFILMÉE TELLE QUE
NOUS L'AVONS REÇUE

A STUDY OF THE BED LOAD TRANSPORT OF A GRAVEL-BED RIVER

by

NICK TYWONIUK

Submitted in partial fulfillment

of the requirements of the degree of

Doctor of Philosophy

Department of Civil Engineering

School of Graduate Studies

University of Ottawa

Ottawa Canada

March 1979

UNIVERSITÉ D'OTTAWA
UNIVERSITY OF OTTAWA

ABSTRACT

A research program of the bed load transport of a gravel-bed river, the Vedder River in British Columbia, was undertaken in 1971 and 1972, and continued through to 1975. Research objectives included instrumentation development (specifically, a hydrophone system), data collection, and specific and comparative analyses of bed load transport results.

The program was designed to be a field research undertaking. Field observations, carried out during the summers of 1971 and 1972 on a six mile river reach, included the collection of bed material, bed load and suspended sediment data, hydrometric data, channel geometry data and hydrophone data. The development of a hydrophone system and operations technique for the collection of acoustical information at or near the bottom of a gravel-bed river formed a significant component of the field investigations.

Estimates of bed load transport were made by (a) direct measurements utilizing two types of bed load samplers, (b) the application of bed load equations, including discharge, tractive force, relative roughness and statistics-based equations, (c) volumetric measurements from channel geometry data, and (d) qualitative hydrophone measurements.

The hydrophone system and operations were developed; the experiments, however, in a quantitative technique of bed load transport measurement. The analyses involving bed load transport equations were useful both in illustrating their applications and limitations and in illustrating the levels and ranges of results among the equations. The volumetric measurements provided a useful base for comparison with the other

techniques or methodologies utilized. The overall study provided acoustic and bed-load transport information as well as information on the sediment transport characteristics for a river reach requiring reliable data for river engineering purposes.

A continuation of bed load transport research is recommended, both in the areas of instrumentation development and in the further research into bed load transport phenomena, particularly in gravel-bed rivers. It is suggested that there is a further need for field research, on rivers other than the Vedder River, to add to the information already available. In view of more efficient and more accurate survey techniques, volumetric measurements are recommended for future studies, together with other data collection which would enable a sediment balance analysis.

ACKNOWLEDGEMENTS

This study was undertaken while the author was on the staff at Water Resources Branch, Environmental Management Service, Fisheries and Environment Canada, Ottawa. The author acknowledges the assistance provided by many members of the Branch, particularly W. Stichling and G. Tofte, and assistance given by the staff of the Canada Center for Inland Waters, particularly C. K. Jonys, and, further, the assistance of other Inland Waters Directorate Staff.

Early drafts of the report were reviewed by W. Stichling, G. Tofte, W. Chin, C. K. Jonys, K. Adamowski and R. G. Warnock. The author appreciates the time and effort spent in reviewing these and in suggesting areas of improvement.

The author is indebted to Dr. R. G. Warnock who supervised the author's academic work at the University of Ottawa and advised on the preparation of this thesis. Dr. Warnock's time and effort in guidance provided during the research and preparation of the thesis are greatly appreciated.

TABLE OF CONTENTS

		Page
ABSTRACT		i
ACKNOWLEDGEMENTS		iii
TABLE OF CONTENTS		iv
LIST OF TABLES		vii
LIST OF FIGURES		viii
NOTATIONS		x
CHAPTER 1	INTRODUCTION	1
1.1	Motivation	1
1.2	Objectives	3
1.3	Procedures	3
CHAPTER 2	THEORETICAL OVERVIEW	8
2.1	Bed Load Transport	8
2.2	Bed Load Transport Equations	11
2.2.1	Discharge Equations	14
2.2.1.1	Schoklitsch (1934) Equation	14
2.2.1.2	Meyer-Peter (1934) Equation	16
2.2.2	Tractive Force Equations	17
2.2.2.1	Meyer-Peter and Muller (1948) Equation	17
2.2.2.2	Straub (1935) Equation	19
2.2.3	Relative Roughness Equation	21
2.2.3.1	Rottner (1959) Equation	21
2.2.4	Equation Based on Statistical Considerations	23
2.2.4.1	Einstein (1950) and Modified Einstein Procedure (1955)	23
2.3	Acoustic Detection of Bed Load Transport	27
2.3.1	Historical Review	27
2.3.2	Basic Acoustical Concepts	30
2.3.3	Theoretical Feasibility Analysis	34
2.3.3.1	Modelling Concepts	34
2.3.3.2	Acoustic Bed Load Transport Function	37
2.3.3.3	Numerical Simulation Results	40
2.3.3.4	General Observations	44
CHAPTER 3	EXPERIMENTAL PROCEDURES	47
3.1	Hydrophone System	47
3.1.1	General Design Concepts	47
3.1.2	Operational Details	48
3.1.3	Laboratory Calibrations	51
3.1.3.1	September, 1971, Calibration	51
3.1.3.2	February, 1972, Calibration	55
3.1.4	Field Procedures	61

3.2	Field Meausrements (Direct)		62
	3.2.1	Instrumentation	62
	3.2.1.1	Hydrometric Instrumentation	62
	3.2.1.2	Bed Load Sampling Equipment	63
	3.2.1.3	Suspended Sediment Sampling Equipment	64
	3.2.1.4	Other Instrumentation Requirements	64
	3.2.2	Field Procedures	65
	3.2.2.1	Hydrometric Procedures	65
	3.2.2.2	Bed Load Sampling Procedures	65
	3.2.3	Complementary Data	66
	3.2.3.1	Cross-Section Profiles	66
	3.2.3.2	Slope Data	67
	3.2.3.3	Particle Size Data	68
CHAPTER 4	COMPUTATIONS PROCEDURES		69
4.1	Hydrology		69
4.2	Channel Geometry		71
4.3	Hydraulics Data		72
	4.3.1	Bed Material and Bed Load Data	76
	4.3.2	Suspended Sediment Data	76
4.4	Discharge Equations		82
	4.4.1	Schoklitsch (1934) Equation	82
	4.4.2	Meyer-Peter (1934) Equation	82
4.5	Tractive Force Equations		83
	4.5.1	Meyer-Peter and Muller (1948) Equation	83
	4.5.2	Straub (1935) Equation	86
4.6	Relative Roughness Equations		88
	4.6.1	Rottner (1959) Equation	88
4.7	Equation Based on Statistical Conciserations		88
	4.7.1	Modified Einstein Procedure (1955)	88
	4.7.2	Einstein (1950) Equation	91
CHAPTER 5	DATA ANALYSIS AND RESULTS		100
5.1	Hydrophone Measurements		100
5.2	Direct Measurement Results		108
	5.2.1	Bed Load Discharge Results	108
	5.2.2	Bed Load Particle Size	111
	5.2.3	Suspended Sediment Data	112
	5.2.4	Bed Material Sample Data	112
	5.2.5	Volumetric Measurement Results	116
5.3	Results of Equations		116
5.4	Comparisons of Bed Load Discharge Results		123
	5.4.1	Comparison of Equation and Sampling Bed Load Discharges	123
	5.4.2	Comparison of Volumetric and Direct (Sampling) Measurements	124

CHAPTER 6	CONCLUSIONS AND RECOMMENDATIONS	127
6.1	Conclusions	127
6.2	Recommendations	130
BIBLIOGRAPHY		131
APPENDIX A	SPECIFICATIONS AND OPERATIONAL DETAILS OF HYDROPHONE SYSTEM	135
APPENDIX B	DATA FROM DIRECT FIELD MEASUREMENTS	157
APPENDIX C	PHOTOGRAPHS ILLUSTRATING INSTRUMENTATION AND SITE CONDITIONS	205

LIST OF TABLES

Table		Page
2.1	Characteristics of various grades of sediment	20
3.1	Summary of calibration tests, Sept., 1971	53
3.2	Summary of calibration tests, Feb., 1972	56
4.1	Bed material analysis data, Vedder and Chilliwack Rivers, 1970	79
4.2	Bed load particle size analysis data, cross-section six, 1971	80
4.3	Bed load analysis data, cross-section six, 1972	81
4.4	Sample calculation of effective diameter	84
4.5	Bed load calculation results, Schoklitsch (1934) equation	85
4.6	Bed load calculation results, Meyer-Peter (1934) equation	85
4.7	Bed load calculation results, Meyer-Peter and Muller (1948) equation	89
4.8	Bed load calculation results, Straub (1935) equation	89
4.9	Bed load calculation results, Rottner (1959) equation	90
4.10	Hydraulic calculations for a channel without bank friction	92
4.11	Calculations for determining bed load discharge (Einstein, 1950)	96
4.12	Bed load discharge by Einstein method	99
5.1	1972 Hydrophone measurements at cross-section six	101
5.2	Summary of bed load measurements at cross-section six, 1971 and 1972	110
5.3	Bed load discharge results from direct measurements	114
5.4	Bed material particle size versus distance along study reach	117
5.5	Net sediment deposition and scour at cross sections	118

LIST OF FIGURES

Figure		Page
1.1	Site plan: Vedder River study reach	6
2.1	Sediment load classification (from Cooper, et al, 1970)	10
2.2	Physical model for theoretical feasibility analysis	36
2.3	SPL versus distance of hydrophone from the bed, and width of moving bed (from Jonys, 1975)	41
2.4	SPL versus g_s for different pebble jump lengths and different aerial concentrations (from Jonys, 1975)	43
2.5	SPL versus g_s for different pebble velocities and aerial concentrations (from Jonys, 1975)	45
3.1	Schematic illustrating hydrophone system	49
3.2	Schematic illustrating acoustical parameters	50
3.3	Recorded output in decibels versus velocity for shown frequency ranges. (Data from Sept., 1971, calibration tests)	54
3.4	Recorded output in decibels versus frequency for shown velocities. (Data from Feb., 1972, calibration tests)	57
3.5	Recorded output in decibels versus frequency for shown velocities. (Data from Feb., 1972, calibration tests)	59
4.1	Flow duration curve for Vedder River at Vedder Crossing	70
4.2	Discharge versus area for cross-section 6	73
4.3	Discharge versus surface breadth for cross-section 6	73
4.4	Discharge versus mean velocity for cross-section 6	74
4.5	Discharge versus depth for cross-section 6	74
4.6	Longitudinal profile of the Vedder River study reach	75
4.7	Hydrographs for 1971 and 1972	77
4.8	Comparison of critical tractive force derivations	87
5.1	1971 and 1972 data summary (cross-section six)	102
5.2	Cross-sectional sound intensities (detailed), May 31, 1972	103
5.3	Cross-sectional sound intensities, bed load rates, velocities and depths, May 30 and 31, 1972	104
5.4	Depth - velocity - sound intensity relations, June 12 and 15, 1972	106

5.5	Flow versus bed load discharge, from measurements	110 (a)
5.6	Bed load particle size distribution versis location	113
5.7	Flow versus bed load discharge results from computations using bed load formulae	121

NOTATIONS

The following abbreviations and symbols are used in this study:

Abbreviations:

BL	band level
C	centigrade
cfs	cubic feet per second
cm	centimeter
cps	cycles per second
db	decibel
fig	figure
fps	feet per second
ft	foot
gm	gram
hz	hertz
K	thousand
lb	pound
log	logarithm to the base 10
min	minute
mm	millimeter
psi	pounds per square inch
sec	second
SPL	spectrum level
sta	station
vs	versus
%	percent

Symbols:

The symbols used in the text and the various equations are defined at the time of their use. A partial list of the symbols used is outlined below.

Symbol	Meaning	Dimensions
A	Cross-sectional area of flow	L^2
b	Channel breadth, general	L
b_w	Water surface breadth	L
b_s	Width of bed contributing to bed load discharge	L
c	Propogation velocity wave	L/T
D	Particle diameter or equivalent diameter	L
D_x	The specified size at which x percent of the total sample weight is smaller than	L
d	Depth of flow, general	L
E	Energy flux density	F/T^2
G_s	Sediment discharge, dry weight	F/T
G_s'	Sediment discharge, submerged weight	F/T
g	Gravitational acceleration	L/T^2
g_s	Sediment discharge per unit width, dry weight	F/LT
i_b	Fraction of specified size range of total bed sample by weight	
I	Intensity of wave	F/T^3
k_s	Equivalent sand-grain roughness	L
p	Sound pressure	F/LT^2
P	Wetter perimeter of channel cross section	L
p	Root mean square pressure	F/L^2
Q	Fluid discharge	L^3/T
q	Fluid discharge per unit width	L^2/T
R	Hydraulic radius of channel cross section	L

R'	Partial hydraulic radius with respect to grain size roughness	L
R''	Partial hydraulic radius for channel irregularities	L
S	Slope, general	
t	time	T
U	Velocity of fluid particles	L/T
V	Velocity, general	L/T
V_m	Mean velocity	L/T
V_*	Shear velocity	L/T
y	Distance from bed	L
γ	Specific weight of fluid	F/L^3
γ_s	Specific weight of solids	F/L^3
γ'_s	Submerged specific weight of solids	F/L^3
δ	Boundary layer thickness	L
Δ	Apparent roughness diameter	L
μ	Dynamic viscosity of fluid	FT/L^2
ν	Kinematic viscosity of fluid	L^2/T
ρ	Mass density of fluid	FT^2/L^4
ρ_s	Mass density of solids	FT^2/L^4
τ	Shear stress at boundary	F/L^2
τ_c	Boundary shear stress for beginning of motion	F/L^2
ϕ	Intensity of transport	
ψ	Intensity of shear on particle	

CHAPTER 1

INTRODUCTION

1.1 Motivation

Many natural rivers and streams, particularily in the mountainous and foothills regions of Western Canada, have mobile beds consisting of non-cohesive granular materials of a wide range of sand and gravel sizes. These materials are capable of being eroded, transported and deposited by the flow, thereby altering the geometry of the flow and tending to adjust the channel bed to a configuration that is in equilibrium with the flow. Channels of this type are referred to as alluvial channels and when a state of equilibrium is reached, the channel is referred to as a regime or stable channel (Cooper, 1970).*

In an alluvial channel, flow consists of the combined movement of water and bed material. Bed material particles are transported by flow in one or more of the following ways: (1) by surface creep (rolling or sliding on the bed); (2) by saltation (leaping into the flow and then resting on the bed); and (3) by suspension (suspended and supported by the surrounding fluid during its entire motion) (Tywoniuk, 1972). In this study, emphasis is on the bed load, the material which moves in almost continuous contact with the streambed, being rolled or pushed along the bottom by the force of the water. The phenomena of flow and of bed load discharge is extremely complex in a gravel-bed channel because of the two-phase nature of the flow, the distinct pattern of bed-forms for each flow, and the variability in the natural flows.

---

*Details in parentheses refer to corresponding references in the Bibliography

Bed load data are required in the proper engineering and economic design of projects related to erosion and shoaling of rivers, irrigation canals and nagivation channels. The economic life of reservoirs depends on the amount and type of sediment transported and on the rate and degree of deposition in the reservoir. The hydrodynamic behaviour of sediment also affects the boundary resistance to flow and therefore the stage-discharge relationships in channels with mobile beds. More recently the significance of sediment pollution has been realized. Assessment of pollution effects requires not only knowledge of the efficiency of the sediment as a carrier, but also knowledge of quantities and rates of sediment transport.

With very few exceptions, most recent research in river mechanics has emphasized the development of reliable theories for the solution of problems related to channel design, sediment discharge prediction and the prediction of the future behavior of natural streams. In spite of the large number of theories which now exist, there is a general lack of confidence concerning their ability to produce reliable solutions to these types of engineering problems (Cooper, 1970).

The unreliability was also the author's experience in the application of various theories to sediment discharge prediction. This factor, and the adamant insistence by some researchers (Shulits et al, 1968) that "only studies on actual rivers will give the answer" and that "computer results must be checked by field determinations" led to the planning of research on bed load transport reported herein. With recent emphasis on "remote sensing" applications in hydrological studies, and the nature of the bed load transport measurement problem, there appeared to be merit in measurement of bed load measurement by non-direct means, such as by acoustic detection.

1.2 Objectives

The research of bed load transport of a gravel-bed river was based on a number of specific objectives. The requirement of larger amounts of quantitative data necessitated researching new applications of technology, hence the development of a hydrophone system and operations technique for the collection of acoustical information at or near the bottom of a gravel-bed river. Secondly, it was intended to assess the feasibility of using this instrumentation for bed load measurement by obtaining acoustical field data together with hydraulic and geometric data for use as a qualitative base. Thirdly, there was a direct requirement to obtain bed load and other hydraulic data to provide a basis for a scientific evaluation of the complex Vedder River system.

The research related to the hydrophone system was at least partly based on the hypothesis that the bed load discharge at a point in a river cross-section is some function of the sound intensity at that point. Since the intent was that of practical "acoustical" measurement of bed load, it was desirable to measure only those additional variables which are normally measured during hydrometric and sediment surveys. These data (flow, particle size, slope, etc.) would enable consideration of the bed load transport as determined by equations, direct measurement, and by acoustic detection methods.

1.3 Procedures

A direct request for bed load data for Canadian streams first arose in about 1964. A government agency responsible for river dredging in the lower Fraser River requested the Water Survey of Canada to obtain sediment data in the lower river reaches. These data were to include the bed load component. This first demand was followed by numerous demands in the provinces of British Columbia, Alberta and Ontario. As a result, an emphasis was placed on the development of sampling equipment and procedures and on applied research into the study of bed load movement.

In requesting bed load information, staff of other agencies generally requested that the bed load component be computed by one or more of the many equations developed and available for this purpose. Of the variety of equations or methods available, these were found to be far from satisfactory, even for purposes of preliminary estimates. In most cases the river hydraulics engineers relied strongly on experience and judgement rather than on established design procedure.

It became evident that the development of sampling equipment and procedures was required. While computations, or predictions, by means of equations were a very useful tool in the extrapolation of measured data and in the interpolation of data, design engineers preferred direct measurement data. Existing measurement procedures were relatively inefficient and had other shortcomings related to hydraulic and sampling efficiencies. In the initial stages of development, two main types of sampling equipment evolved; the basket type and the pressure-difference type. Measurement procedures were made relatively efficient by introducing motorized equipment, automatic and continuous measurement recorders, provision of stable working boats or catamarans, and by utilization of a relatively large amount of staff. It became evident that even more efficient procedures needed to be developed in the case of measurement of bed load if one was to obtain an appropriate level of knowledge of the nature of bed load movement; the nature of which appeared to be highly erratic in space and time. An acoustic detection technique appeared to have merit.

In discussing the need for field research, Shulits and Hill (Shulits et al, 1968) cautioned: "as this is very expensive research of a long-range character, it

should be administered on a regional basis by devoted and competent individuals with adequate assistants. There should be opportunity to consult experts." The procedures followed in performing the research reported herein heeded this advice. In discussing these, it is useful to discuss the research procedures firstly and separately from the organizational procedures involving the planning, logistics, scheduling and consultation with experts.

Thus, at the outset it was established that the applied research of the process of bed load transport in a gravel-bed river should be primarily a field study. With this decided, a five- or six-mile length of river reach of the Vedder River in British Columbia, a tributary of the Fraser River and immediately upstream of the Vedder Canal, was selected as the study site. The site plan is shown in Figure 1.1. This site was already partly instrumented, and even more important from the point of view of initiating a study, bed load data for this stream were required for purposes of flood protection (dyke design).

Having selected a study site, procedures as follows were developed:

(a) preparation and instrumentation of the study site,

(b) development and calibration of the hydrophone system,

(c) collection of acoustical information for a wide range of flow conditions,

(d) collection of corresponding hydrometric, sediment and geometric data,

(e) performance of the required analyses in evaluating bed load transport as determined by equations, direct measurement, and by acoustic detection, and

(f) assessment of the degree of success in fulfillment of established objectives.

With respect to organizational procedure, the research (and the sequence of procedural events which resulted) was substantially supported by a number of water resources agencies.

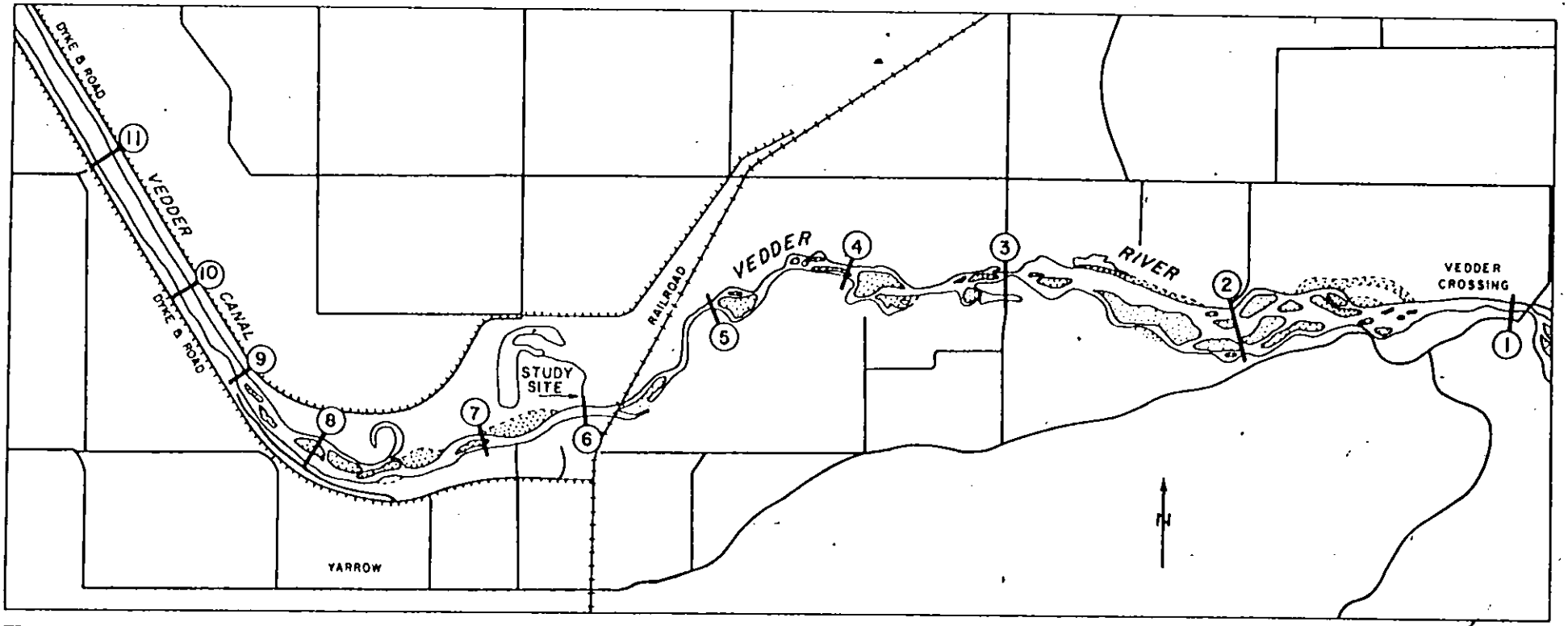

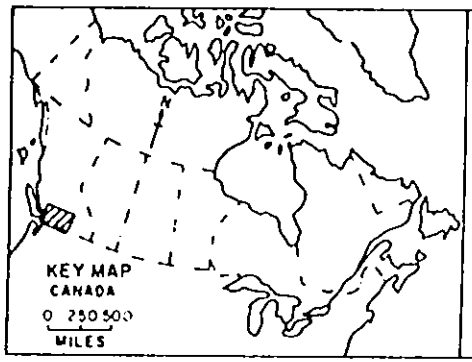

FIGURE 1.1: SITE PLAN: VEDDER RIVER STUDY REACH

0 1/2 1
MILES

The study was initiated in 1970 by the Water Survey of Canada as a joint program between the region and the head office. The participation was later expanded to include the Applied Hydrology Division, Water Survey of Canada, Canada Center for Inland Waters and the Univeristy of Ottawa. This arrangement provided the regional representation, devoted and competent individuals with competent assistants and the opportunity to consult with experts.

It should be further noted that progress reports were prepared in 1971 (Tywoniuk, 1972) and in 1972 (Tywoniuk et al, 1973). These provided a basis for discussion with provincial officials in British Columbia, with staff of the Operations and Management Branch, Department of the Environment, as well as with staff of the participating agencies identified above. Additionally, the progress reports formed a basis for internal review and assessment of the program and for review and guidance from participating agencies. Further progress reports and reports on research conducted were also prepared subsequent to 1972 and subsequent to the initial work of 1971 and 1972.

Finally, additional opportunity to consult experts arose in May, 1973, at a national hydrology symposium on fluvial processes and sedimentation. A paper describing the acoustic detection of bed load transport was presented at this symposium and, perhaps even more important, the various aspects of bed load transport were discussed with the experts present.

CHAPTER 2

THEORETICAL OVERVIEW

2.1 Bed Load Transport

The amount of bed load transported by a river is generally in the order of 5 percent to 25 percent of the suspended load (Tywoniuk, 1972). Although the amount of bed load may be small as compared with the total sediment load, it is of considerable significance because it shapes the bed and influences the stability of the channel, the form of sediment bed surface, and the flow parameters.

At the outset, it is useful to define terms such as bed load, bed material, and others. Such terms, as used throughout this document, and frequently in literature, are illustrated in figure 2.1 and are defined as follows (Tywoniuk, 1972):

Bed load - The material which moves in almost continuous contact with the streambed, being rolled or pushed along the bottom by the force of the water.

Suspended load - Sediment that is supported by the upward components of turbulent currents and that stays in suspension for appreciable lengths of time.

Bed layer - A flow layer immediately above the bed of thickness equivlent to the thickness of two grain diameters. The thickness of the bed layers varies with particle size.

Bed material - The sediment mixture of which the streambed is composed.

Wash load - That part of the suspended load which consists of grain sizes finer than those of the bed.

Bed material load - That part of the total sediment load which consists of grain sizes represented in the bed and equals the sediment transport capability of the flow.

Total sediment load - Bed load plus suspended load or bed material load plus wash load.

Bed load equation - The general relationship between bed load rate, flow condition, and composition of the bed material.

Total sediment load has also been defined as consisting of wash load, suspended bed material load and bed load. Further, on the basis of mechanism of transport, total load consists of suspended load and bed load; and on the basis of particle size, total load consists of wash load and bed material load. In the first case, suspended load equals wash load plus suspended bed material load; in the latter case, bed material load equal suspended bed material load plus bed load.

Section 1.1 makes reference to the modes by which bed material particles are transported: by surface creep, by saltation and/or by suspension.

There is no sharp line of distinction between saltation and suspension. This distinction however, is important as it delimits two methods of hydraulic transportation which follow different laws: (a) sediments moving as surface creep and saltation are supported by the river bed (bed load) and (b) sediments travelling in suspension are supported by the flow (suspended load). Similarly, there are no clear divisions among those sediments travelling as surface creep, saltation or as suspended sediments. Experiments have shown that an exchange relationship exists between the particles involved in the bed load motion and the particles on the bed (Einstein, 1950). It is logical that, in space and time, there is also an exchange between the particles moving as bed load and those moving as suspended load, particularly in cases where net aggredation or degradation occurs. It follows that, over a duration of time, a specific particle can move in suspension for part of the time, along the bed of the river for part of the time, and not at all for the remaining time.

It is evident, therefore, that bed load movement in the form of creep and saltation is a stochastic process with highly variable rates of movement. The

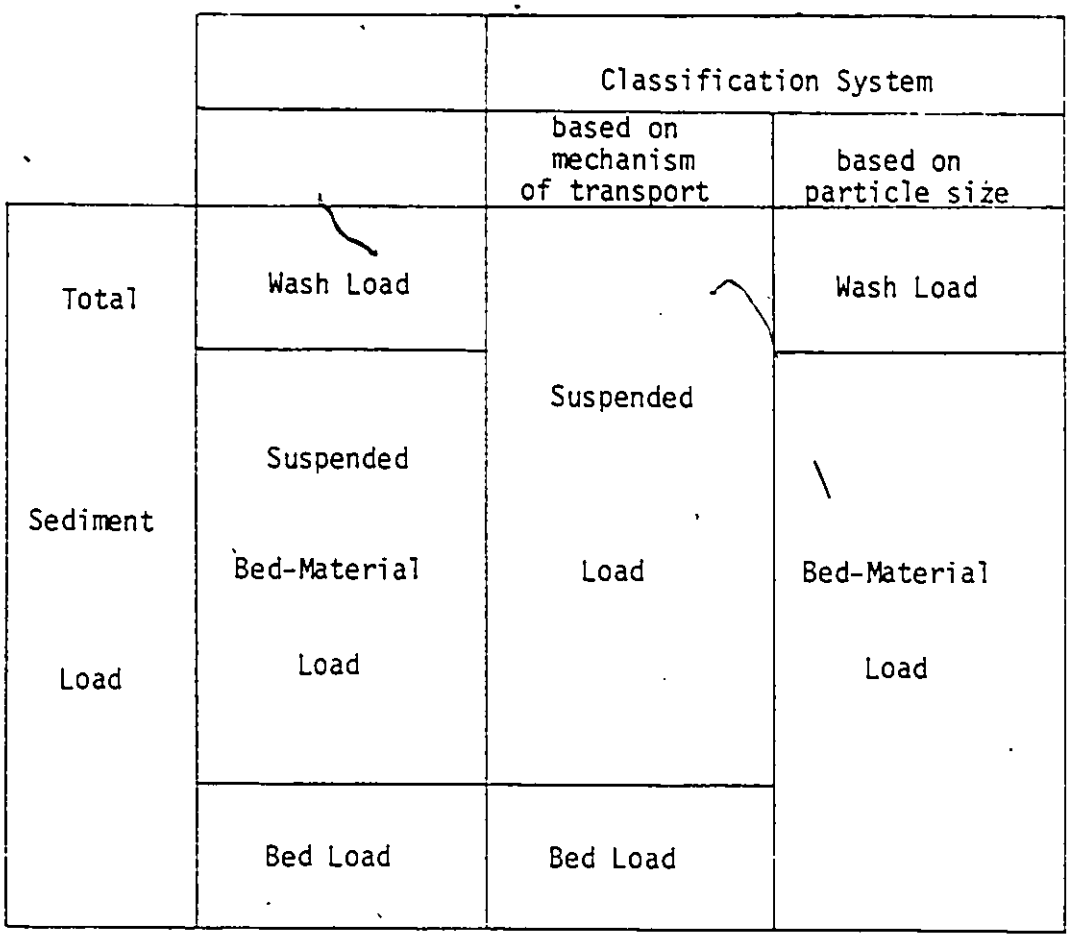

Figure 2.1. Sediment Load Classification (from Cooper, et al, 1970)

rate of movement changes along the channel, across the section and with time. In essence, bed load movement is a three-dimensional stochastic process. Empirical or semi-theoretical equations are basicially numerical models defining the deterministic component of the bed load transport process.

The theoretical considerations of bed load tranpsort, particularly as related to transport equations, are more thoroughly discussed in Section 2.2 below.

2.2 Bed Load Transport Equations

The history of bed load formula or equation development dates back to about DuBoys (1879). Since this date, hundreds of researchers have published theories, equations and related information.

Just as there are numerous bed load transport equations, there are also varied approaches which have been used in the studies which have led to the development of theories of flow in alluvial channels. These have been categorized as follows: (1) studies on the geomorphic aspects of flow in alluvial channels, (2) detailed studies on the dynamics of flow in alluvial channels, and (3) studies intended to determine the relationships among the variables that describe the sediment properties, the fluid properties, the channel geometry, and the characteristics of the flow (Cooper, 1970).

The geomorphic approach involves the qualitative observation of the behavior of natural channels. The results are a qualitative description of the physical processes and their consequences. Some researchers have attempted to correlate some of the more pertinent variables (Leopold et al, 1974). The relationships developed have aided primarily in the qualitative understanding of the behavior of flow in alluvial channels rather than in development of suitable relationships for purposes of accurate design predictions.

Studies of the dynamics of flow have been both theoretical and experimental. These usually examine some narrow aspect of the flow phenomenon,

such as the various forces acting on a sediment particle either in motion or at rest on the boundary. The results of these studies have provided an understanding of the physical laws governing the dynamics of flow and have enabled the development of techniques, such as those for suspended sediment particle size analysis, and of mathematical models of the processes involved. With respect to practical engineering problems, these studies alone have had somewhat limited value.

In the third case the studies deal more directly with sediment transport and have resulted in the majority of the theories now used in engineering practice. The approach has usually involved the development of a mathematical model followed by an empirical evaluation of the model to test its validity, to determine numerical coefficients, and in some cases to determine the mathematical form of the relations (Cooper, 1970).

In outlining the theory of bed load transport equations or formulae, it is essentially the third category of approach as described above which will be discussed.

Numerous text books and other articles have been written about bed load formulae, but none treat the subject in its entirety; and for good reason. For example, Yalin states: "There is no room here to go through all these formulae, nor is it necessary, for many of them now have only an historical meaning" (Yalin, 1972); Shulits and Hill, in their very comprehensive analysis, state "Our intent is not to treat all bed load formulas. Such an encyclopedic goal would really have value as a history of the field" (Shulits et al, 1968); other authors have chosen to indicate simply that they do not give a complete record of all formulae.

In following the advice of these other researchers, it becomes necessary to limit the scope of the theory discussed herein. The selection of bed load equations was based primarily on the work done by Shulits and Hill (Shulits et al, 1968). This appeared appropriate since these were already once carefully selected:

"In an attempt to select and recommend several formulas for immediate use and further substantiation, we look into formulas which are best known or most used or founded on substantial data. Some formulas actually satisfy all three of these criteria. Knowingly not included are formulas based on a scant amount of experimental data and which usually offer no way to evaluate constants; those derived theoretically, usually by postulation, which give the structure or framework of the formula without coefficients; and conjectural formulas, usually of an "approach" nature" (Shulits et al, 1968).

A further criteria in the selection of several equations from those already selected on the above criteria, therefore, was to select those which were familiar (both on a personal and on a Canadian experience basis), and those which varied from a theoretical point of view. Equations selected are as follows:

(1) discharge equations (bed load as a function of discharge):
   (a) Schoklitsch (1934)
   (b) Meyer-Peter (1934)

(2) tractive force equations (bed load as a function of tractive force):
   (a) Meyer-Peter and Muller (1948)
   (b) Straub (1935)

(3) relative roughness equation (use of relative roughness, D/H, as a parameter; where D is the grain diameter and H is the depth of flow):
   (a) Rottner (1959)

(4) equation based on statistical considerations:
   (a) Einstein (1950) and Modified Einstein Procedure (1955).

The discussion of the above is based primarily on the works of Shulits and Hill (Shulits et al, 1968) and on articles specifically related to the particular equations.

2.2.1 Discharge Equations

Discharge equations are those in which the bed load is a function of the discharge. Among the equations which can be so categorized are the Schoklitsch (1934) and the Meyer-Peter (1934) equations.

2.2.1.1 Schoklitsch (1934) Equation

Schoklitsch originally presented his 1934 formula in metric units as follows:

$$G_l = 7000\ (Q_l - Q_{0l})\ S^{2/3}/D^{1/2} \qquad \ldots 2.1$$

in which G_l is the bed load in kg/sec/m, D, the grain size in mm, S, the slope, Q_l, the discharge and Q_{0l}, the critical discharge, respectively in m^3/sec/m (Shulits et al, 1968).

The critical discharge, for a sediment specific gravity of 2.65, is given in metric units by

$$Q_{0l} = 0.00001944D/S^{4/3} \qquad \ldots 2.2$$

The Schoklitsch method of determining this critical discharge was to plot, for a given flow and grain diameter, a curve of bed load as ordinate and slope as abscissa; then to extrapolate the curve to zero bed load to obtain the intercept with the abscissa. This intercept was the critical slope for the particular flow and grain diameter. At this slope intercept, the corresponding discharge identifying the curve was the critical discharge. This method, hence the above equation 2.2, was applicable for uniform grain material only.

For non-uniform grain material, the mixture was considered to be made up of a number of grades of mean grade diameter D_a, D_b, D_c and so on; the division into grades being quite arbitrary. The percentage weight a, b, c and so on, that each grade comprised of the total, was determined. The bed load, G_{la}, G_{lb}, G_{lc}, etc., was then computed for each grain diameter for a given discharge and slope by using the above two equations. The bed load for the mixture was then

$$G_1 = aG_{1a} + bG_{1b} + cG_{1c} + \ldots \qquad \ldots 2.3$$

In using the above procedures, it may happen that Q_{01} for one of the coarse grades will be larger than Q_1. This will result in a "negative" bed load for the particular grade, which is substituted into equation 2.3 with the negative sign.

Schoklitsch attributed this negative bed load to the smoothing of the bed by the finer grains, thus barely permitting motion of the coarser grains which in turn reduced the bed load. In spite of this explanation, the negative load was one of the questioned aspects of this formula. Schoklitsch, to point out that the amount of fines was of great influence in mixtures, showed with Gilbert data how the bed load increases with the percentage of fines.

By computing a number of examples, Schoklitsch found that an effective diameter, D_E, for mixtures, lying roughly between D_{40} and D_{60}, can be inserted in the uniform-grain formulas. The subscripts, 40 and 60 indicate, as usual, the grain diameter for which 40% and 60%, respectively, of the mixture by weight is finer. The median diameter, D_{50}, which is often quoted and applied, cannot be justified rigorously since it was not so specified by Schoklitsch. The proper method is to calculate the mixture bed load by equation 2.3 and then find which D in equation 2.1 yields the same load. This D becomes the effective diameter for the mixture. Only by such a computation for a particular stream site can a sensible and reliable D be determined.

In English units the formula 2.1 becomes

$$G_1 = 25\ (Q_1 - Q_{01})\ S^{2/3}/D^{1/2} \qquad \ldots 2.4$$

where G_1 is the bed load in lb/sec/ft, D is the grain diameter in ft, and Q_1 and Q_{01} the discharge and critical discharge, respectively, in cfs/ft. The critical discharge is

$$Q_{01} = 0.0638D/S^{4/3} \qquad \ldots 2.5$$

2.2.1.2 Meyer-Peter (1934) Equation

In metric units, the Meyer-Peter equation is

$$SQ_{B1}^{2/3}/D = 17 + 0.4\, G_1^{2/3}/D \qquad ...2.6$$

where Q_{B1} is the unit water discharge, G_1 is the dry unit bed load, respectively in kg/sec/m, D is the uniform grain diameter in meters and S is the slope. The constants 17 and 0.4 are valid only for sand with a specific gravity of 2.68.

In the symbol Q_{B1}, the subscript 1 denotes unit width, whereas B denotes the discharge apportioned to the bed. This concept arose from the need to correct for wall roughness, that is, for the fact that the experimental flume-wall is smoother than the sand bed. Composite roughness can be treated by procedures leading to the concept of an hydraulic radius of the channel bottom and of the channel walls, and of apportionment of the total discharge between one for the bottom and one for each wall.

In the above equation, the uniform-grain diameter, D, could be used, or the equivalent diameter for a mixture D_E could be used in its place. The uniform-grain diameter is the geometric mean of the two sieve sizes delimiting the sand. For example, for limiting mesh openings of 24 and 34 mm, the resulting geometric mean of 28.6 mm would be used. The equivalent grain diameter, D_E, of a mixture is D_{35}; that is, 35 percent of the mixture is finer than D_{35}.

The term, $SQ_{B1}^{2/3}/D$, is regarded as the discharge parameter and $G_1^{2/3}/D$ as the transport parameter. Equation 2.6 is not dimensionally homogeneous since these two parameters have different dimensions; however, this is of no practical significance in an empirical equation.

In English units, the Meyer-Peter equation is

$$SQ_{B1}^{2/3}/D = 0.252 - 0.0254\, G_1^{2/3}/D \qquad ...2.7$$

or, in terms of G_1,

$$G_1 = (39.3\, Q_{B1}^{2/3}\, S - 9.94D)^{3/2} \qquad ...2.8$$

where G_1 is in lb/sec/ft, D is in feet, and Q_{B1} is in cfs/ft.

2.2.2 Tractive Force Equations

Tractive force equations are those in which bed load is a function of tractive force. Among these types of equations are the Meyer-Peter and Muller (1948) and the Straub (1935) formulas.

2.2.2.1 Meyer-Peter and Muller (1948) Equation

The original form of the Meyer-Peter and Muller equation in metric units for a rectangular channel is

$$\gamma Q_B/Q(K_B/K_G)^{3/2}\ HS = 0.047\gamma_S'' D_E + 0.25(\gamma/g)^{1/3} G_1''^{2/3} \qquad ...2.9$$

in which γ is the specific weight of water in metric tons per m^3; Q_B the part of the discharge apportioned to the bed and considered responsible for bed load transport in liters/sec; Q the total discharge, also in liters/sec; K_B the so-called particle or grain roughness in $m^{1/3}$/sec; H the depth (m); S the slope; γ_S'' the submerged specific weight of the sediment grain (in water) in metric tons/m^3 which is equal to $\gamma_S - \gamma$, where γ_S is the specific weight (in air) of the sediment grain; D_E the effective diameter of the bed material (m); g the acceleration due to gravity in m/s^2; and G_1'' the bed load weighed under water in metric tons/sec/m.

The bed roughness coefficient, K_B, is for the total bed roughness, that is, it embraces the bed roughness due to the sediment grains and that due to form resistance (bar, ripples, etc.). It should be noted that K_B pertains to the bed only and is different from K_T, the roughness coefficient for the entire cross-section. The value of K_B is either estimated or computed from

$$Q_B/A_B = K_B\, R_B^{2/3}\, S^{1/2} \qquad ...2.10$$

The particle or grain roughness, K_G, is defined as

$$K_G = 26/D_{90}^{1/6} \qquad ...2.11$$

where D_{90} is the particle diameter of the bed material at which 90 percent of the mixture by weight is finer. This coefficient, K_G, is a measure of the friction due to the particle grains on a level bed. Though the equation is often used indiscriminately, it is, according to Meyer-Peter and Muller, strictly applicable only to fully developed turbulence.

The effective diameter, D_E, is the mean diameter by weight or

$$D_E = \Sigma D \Delta p/100 \qquad ...2.12$$

where D is the average size of particles in a size fraction and Δp is the percent in that size fraction.

As each term in equation 2.9 has the dimension of a tractive force, it is illuminating to inquire into the meaning of each. For this purpose the equation is transposed to

$$0.25\,(\Delta/g)^{1/3}\,G_1^{II\,2/3} = (Q_B/Q)\,(K_B/K_G)^{3/2}\,\gamma HS - 0.047\gamma_S^{II}D_E \qquad ...2.13$$

or

$$T_G = T_{QK} - T_0 \qquad ...2.14$$

Consider the term T_{QK} in which the total tractive force (ΔHS) appears. Q_B/Q is a reducing multiplier to account for the fact that only a part (Q_B) of the total discharge acts on the bed. The second reducing factor, $(K_B/K_G)^{3/2}$, denotes that in the presence of form resistances, such as bars and ripples, only another part of the total tractive force is available for bed load transport. The term T_{QK} is then that part of the $T = \gamma HS$ available to start the sediment moving and then keep it moving as bed load.

The last term, $0.047\ \gamma_S''\ D_E$, in equation 2.13 is T_O, the critical tractive force, that at which the bed is just barely at rest. It follows then that $T_G = T_{QK} - T_O$ is the part of the tractive force that transports the bed load.

To further simplify equation 2.9, the symbol Q_K is adopted:

$$Q_K = (Q_B/Q)\,(K_B/K_G)^{3/2} \qquad \ldots 2.15$$

The original equation 2.9 then becomes in English units

$$G_1 = 9.23\,(Q_K T - 4.84\,D_E)^{3/2} \qquad \ldots 2.16$$

in which G_1 is the bed load (dry weight) in lb/sec/ft; T is the tractive force (γHS) in lb/ft, wherein $\gamma = 2.65(62.4)$ lb/ft^3 and H is the depth in ft; and D_E is the effective grain diameter in ft. This form of the formula demonstrates that the Meyer-Peter and Muller formula is of the tractive force type.

For a very wide channel Q closely approximates Q_B, so that $Q_B/Q = 1$. If there is no form roughness, for example, for a level bed, $K_B = K_G$ and K_B/K_G becomes one. Thus; for a very wide and level channel, i.e., with no form roughness, $Q_K = 1$.

2.2.2.2 Straub (1935) Equation

In English units, the Straub equation as given by the author in 1935 is

$$G_1 = (\psi/\gamma^2)\ T\ (T-T_O) \qquad \ldots 2.17$$

where G_1 is the bed load (dry weight) in lbs/sec/ft, ψ is the "sediment characteristic", γ is the specific weight of water in lb/ft^3, T is the tractive force in lb/ft^2 and T_O is the critical tractive force (lb/ft^2) of the sediment. In this equation, T = γHS, where H is the depth in feet and S is the slope.

The values of ψ and T_O for the various particle sizes of Missouri River sand, as originally given by Straub, are shown in Table 2.1. Although Straub states that his value of ψ and T_O are based on the "research work of Schoklitsch, Schaffernak and Gilbert", no numerical or graphical data are included to afford a clear understanding of just how the values were obtained.

TABLE 2.1. Characteristics of Various Grades of Sediment

Mean diameter mm	General Classification	Ψ	T_o lb/ft^2
1/8	Fine sand	523,000	0.0162
1/4	Medium sand	312,000	0.0172
1/2	Coarse sand	187,000	0.0215
1	Very coarse sand	111,000	0.0316
2	Granule gravel	66,200	0.0513
4	Granule gravel	39,900	0.089

The original Straub table defines the particle size as the mean diameter but in his later study of 1954 he uses the "mean (50 percent) size of the sediment to represent the mixture". It is thus not clear what he intends, especially since in the 1954 work he also plots the 1935 values of ψ and T_O against the "mean diameter". The 1954 experimental work was not used to alter the relationship between ψ, T_O and D.

The equation for ψ is occasionally given by

$$\psi = 111{,}000/D^{3/4} \qquad \ldots 2.18$$

as derived from one of Straub's Figures. Its units are not homogeneous as the diameter is in mm whereas, from Equation 2.17, ψ would be in $lb/ft^3/sec$.

If the foregoing equation for ψ is substituted into the original Straub equation and D is expressed in ft, the formula becomes:

$$G_1 = 0.391\ T\ (T-T_O)/D^{3/4} \qquad \ldots 2.19$$

for a uniform-grain material. For mixtures, it is recommended that the mean diameter be used as the effective diameter.

2.2.3 Relative Roughness Equation

The relative roughness equation is that in which the relative roughness D/H, is used as a parameter; D and H being the grain diameter and the depth of flow respectively. An example of a relative roughness equation is the Rottner (1959) formula.

2.2.3.1 Rottner (1959) Equation

By diligent application of the least squares method to obtain linear correlations between his parameters, Rottner develops this equation, expressed in the CGS system:

$$(G_1/\rho_s\ (((\rho_s - \rho)/\rho)H^3)^{1/2})^{1/3}$$
$$= (0.06715(D/H)^{2/3} + 0.01405)V/\ (((\rho_s - \rho)-\rho)/H)^{1/2} - 2.45(D/H)^{2/3}$$

$$\ldots 2.20$$

To render the G and V parameters dimensionless, Rottner transformed the above into:

$$G_1/\rho_s \quad (((\rho_s - \rho)/\rho)H^3)^{1/2}$$

$$= ((0.667(D/H)^{2/3} + 0.14)V/ \quad (((\rho_s - \rho)/\rho)gH)^{1/2} - 0.778(D/H)^{2/3})^3$$

...2.21

In both forms, G_1 is the bed load in grams/sec/cm; ρ_s and ρ the density of the sediment grain and water, respectively, in grams/cm^3. D is the mean diameter of the sediment mixture and H the depth, both in cm; V is the velocity in cm/sec; and g is the acceleration due to gravity.

Rottner's proposal might be called a velocity equation as he has a velocity parameter and a bed load parameter, in both of which the characteristic length is the depth. Of greater contrast is his adoption of a relative roughness, D/H.

Rottner, knowingly ignoring bed form phenomena, does not relate these to his relative roughness.

Equations 2.20 and 2.21 do not contain the slope intentionally, as Rottner avoids its use mainly for reasons of convenience and because it is often not accurately known and rapidly becomes erroneous when the flow is no longer uniform. His slope parameter is $S/((\rho_s - \rho)/\rho)$, which, although used in some of his diagrams, is not used in the above two equations.

In English units, with $Q_1 = VH$, the Rottner equation becomes,

$$G_1 = 38.5\, H^{3/2} \quad (4.3\, Q_1/H^{3/2} \quad (0.06715\, (D/H)^{2/3} - 0.01405)$$

$$- 2.45\, (D/H)^{2/3})^{\ 3} \qquad \text{...2.22}$$

with G_1 in lbs/sec/ft, Q_1 in cfs/ft, and H and D in ft. To be remembered is that Equation 2.22 is for water with a specific weight of 62.4 lbs/ft^3, and sand with a specific gravity of 2.65, as throughout the entire report.

The structure of Equation 2.22 makes a general comparison with the other equations impracticable except for selected instances or a particular site. For a constant depth H, G_1 as ordinate is plotted against Q_1 as abscissa for different values of the relative roughness D/H. Q_1 and G_1 reflect changes in width, while the D/H lines give the effect of particle size due to the constancy of H. In effect, the chart is a constant depth plot and the lines are constant diameter lines. Several H-charts should make it easy to decide on design depths and width. The slope can be brought in via the Manning formula; but, since this forces the Manning coefficient into the picture, it seems desirable to work with Q_1 as a composite measure of slope and roughness coefficient.

2.2.4 Equation Based on Statistical Considerations

An example of an equation based on statistical considerations, an equation which is still widely used in engineering calculations, is the Einstein (1950) equation. Rather than simply use of an equation, this is more correctly a procedure based on a series of equations and graphs which, in turn, are based on statistical considerations.

2.2.4.1 Einstein (1950) and Modified Einstein Procedure (1955)

The Einstein procedure is complicated and laborious. The computational procedure involves nearly fifty steps, and any study of the original U.S. Department of Agriculture Bulletin number 1026 (Einstein, 1950) is a volumental task in itself.

The computational method resting on the Einstein bed load function is a thorough and carefully reasoned analytical edifice structured with all the knowledge of the fluid mechanics of the first half of this century. Einstein offered the first and consumate analytical framework, based on the ideas of Prandtl and Von Karman, incorporating the laminar sublayer whether or not it can exist in the presence of a moving bed load layer.

There are at least two basic considerations which break with the past: (1) The definition of a critical value for the initiation of sediment motion is a difficult, if not impossible, proposition. Therefore, such a criterion was avoided. (2) It is suggested that the bed load transport is related to the fluctuations of the velocity rather than to the average value of the velocity. The beginning and the end of the particle motion have to be expressed with the concept of probability, which relates instantaneous hydrodynamic lift forces to the particle's weight.

Experimental evidence has shown that there exists an intimate relationship between the bed and the bed load:

1. A steady and intensive exchange of particles was observed to exist between the moving bed load and the bed.
2. The bed load moves slowly downstream; the motion of an individual particle is one of quick steps with comparatively long intermediate rest periods.
3. The average step made by any bed load particle appears to be independent of the flow condition, the transport rate, and the bed composition, and is always the same.
4. Different transport rates can be achieved by a change of the average time between two steps and of the thickness of the moving layer.

With these concepts Einstein (1942, 1950) developed a bed load formula that relates the rate of bed load transport with properties of the grain and of the flow causing the movement. This relationship was presented empirically in 1942 and was replaced by an analytical function in 1950.

The Einstein method of computing bed load is actually a procedure complex and lengthy, but analytically structured both logically and carefully. There is some indefiniteness in the term, "bed load function", used by Einstein in his basic and classic 1950 study. In a late condensation of his method he states,

"The bed load function is the rate at which various discharges will transport the different grain sizes of the bed material in a given channel", from which one might infer a rating curve, that is, a relationship between discharge and bed load. The same source asserts that Φ_*, defined as the intensity of bed load transport, "has been found to be a unique function of an hydraulic parameter ψ_*, known as flow intensity"; and then, "The above relationship between Φ_* and ψ_*, is given in graphic form....and represents the bed load equation". We take this graphic relationship between the dimensionless parameters, Φ_* and ψ_*, to be the bed load formula. The parameters will be defined and used below. The Einstein procedure itself, however, is a mathematical technique of some thirty steps for computing the bed load and involves the aforementioned $\Phi_* - \psi_*$ graph.

The Einstein procedure utilizes a variety of data. Needed, in general, are the usual hydraulic elements: cross-sectional area, A, hydraulic radius, R, and the wetted perimeter, p, plotted or tabulated against stage or depth. Also required are the mechanical analysis of the bed material, the slope, S, and knowledge of the roughness of the banks. Normally these roughnesses are given by the Manning n or the Strickler K. Neither is used by Einstein in the calculation of the discharge with no bank friction, but where bank friction must be included, he adopts n_w, the Manning n for the wall.

The bed load is computed from

$$i_B q_B = \Phi_* i_B \rho_s g^{3/2} D^{3/2} (S_s - 1)^{1/2} \qquad ...2.23$$

wherein i_B is the fraction of the bed load of a given grain size, q_B is the bed load in lb/sec/ft, and i_b is the fraction of grain size D. In Equation 2.23

$$\Phi_* = (i_B/i_b)\Phi \qquad ...2.24$$

wherein

$$\Phi_* = q_B/g\rho_s\,(\rho_f/(\rho_s - \rho_f))^{1/2}\,(1/gD^3)^{1/2} \qquad \ldots 2.25$$

In Equation 2.25, since $1/g\rho_s\,(1/gD^3)^{1/2}$ has the same dimension as q_B, namely lb/sec/ft, Φ may be regarded as a dimensionless bed load parameter.

The flow intensity might be written, as Einstein does more recently

$$\psi_* = \xi y(\log 10.6/\log (10.6Xx/D_{65}))^2\,((\rho_s - \rho_f)/\rho_f)\,(D/R_b^1 S_e) \qquad \ldots 2.26$$

In our terminology, for a mixture

$$\Sigma(i_B q_B) = G_1 \qquad \ldots 2.27$$

In equation 2.26, ξ is a correction factor.

The above is based on both theoretical considerations and experimental findings and requires data from a long reach of channel. This complex and laborious procedure was modified in 1955 (Colby et al, 1955) to enable computation of the total discharge of all particle sizes based on data from only a single cross-section. In the modified procedure, relationships are based as far as possible on such measurable quantities as the concentration and particle size distribution of suspended sediment and mean velocity (Colby et al, 1961). Computations were further simplified by Colby and Hubbell mainly by graphical aids, to further facilitate the determination of the total sediment discharge and the approximate size distribution of the total sediment discharge.

In describing the simplified methods for computing the sediment discharge with the modified Einstein Procedure (Colby et al, 1961) the authors state: "....use of the monographs introduces much less error than is present in either the basic data or the theories on which the computations of total sediment discharge are based. The results are nearly as accurate mathematically as those that could be obtained from the longer and more complex arithmetic and algebraic computations of the Einstein procedure".

In view of the above, and further on the basis of common usage, the simplified methods outlined by Colby and Hubbell in 1961 are attempted in Chapter 4 for purposes of comparing methodologies.

2.3 Acoustic Detection of Bed Load Transport

The theory of sound is both extensive and complex. Its applications are extremely varied and broad. Even in restricting the field to underwater acoustics, the applications are so varied that it becomes necessary to develop the theory in the context of some specific application. In this way, the theory can be more readily developed and be more relevant to the important practical use.

2.3.1 Historical Review

While the "modern age" of sonar dates back a quarter of a century to the start of World War II, one of the earliest references to the existence of underwater sound was by Leonardo de Vinci. In 1490 he wrote "If you cause your ship to stop, and place the head of a long tube in the water and place the outer extremity to your ear, you will hear ships at a great distance from you" (Urich, 1967). While extremely simple, this method of listening to underwater sounds had widespread use until as late as World War I. At about this time, by the addition of a second tube between the outer ear and a point in the sea separated from the first point, a direction could be obtained and the bearing of the target could be determined.

The first quantitative measurement of underwater sound was perhaps made by Daniel Colladon, a Swiss physicist, and Charles Sturm, a French mathmatician in 1827, who at this early date measured the velocity of sound in Lake Geneva in Switzerland (Urich, 1967). They determined the velocity of sound to a surprising degree of accuracy by timing the interval between a flash of light and the striking of a bell under water.

During the latter part of the nineteenth century and early twentieth century (prior to Word War I) a number of interesting discoveries were made: a number of physicists experimented with "transduction" - the conversion of electricity into sound and visa versa; in 1980, Jacques and Pierre Curie discovered "piezoelectricity" - the ability of certain crystals, when stressed, to develop an electric charge across certain pairs of crystal faces; James Joule in the 1840's experimented with "magnetostriction" - the counterpart of piezoelectricity, wherein a magnetic field produces a change in the shape of certain substances; these and other studies were the foundation for the telephone (A. G. Bell, 1876) and echo-ranging (L. F. Richardson, 1912).

The outbreak of World War I was the impetus for the development of a number of military applications of sonar: listening, echo ranging, depth sounding, acoustic and pressure mines, homing torpedoes, underwater telephones, sonobuoys, acoustic marine spedometers, and so on. Perhaps of greater importance than the applications was the obtaining of an understanding of the vagaries of sound propagation in water. Further development subsequent to the post war period, and one that is still taking place, is the expansion of the applications of underwater sound to peaceful purposes: improved depth sounding, acoustic navigation beacons, subbottom geologic mapping in shallow and deep water, fish finding, biological and other scientific research, and in telemetry and control applications.

While the above very briefly outlines the historical highlights of underwater acoustics, of immediate relevance are those historical events related to the application of acoustic measurement techniques for bed load transport. Tywoniuk and Warnock (Tywoniuk, et al, 1973) outlined these basically as follows.

The concept of measurement of sound resulting from inter-particle or particle-instrument collision is not new. Muhlhoffer (1933) was the first to use a sonic detector in investigations of sediment movement (Johnson et al, 1969).

Considerably later, in 1951, Bradeau (Bradeau, 1951) and other researchers modified and adpated this instrumentation by attaching the microphone component to a triangular steel baseplate. The sound of interparticle collision and particle impact on the baseplate was picked up by the microphone, amplified and transmitted to a recorder. Bradeau reported: "Les résultats furent surprenants. Au cours d'une montée de débit, on pouvait entendre le phénomène avec une précision comparable à celle de sensations purement visuelles. Chaque bruit pouvait être distingué: au début, le bruissement de l'eau, les chocs et le glissement de grain de sable isolés. Ensuite, l'arrivée progressive de cailloux de différantes grosseurs, leur roulement ou leur choc répétés sur la plague. Enfin, le débit décroissant lentement, le glissement de plus en plus fréquent des cailloux et le retour, très progressive, a l'état initial" (Bradeau, 1951).

On a similar principle, Juniet in 1952 designed an instrument for fine bed materials using a thin fork-shaped rod inserted into the streambed (Juliet, 1952). In 1963, Bedeus and Ivicsics reported having utilized an acoustic detector consisting of a microphone housed in a streamlined body which could be suspended above the moving particles. Field studies in the Upper Danube were made with this instrument but quantitative results were not reported (Bedeus et al, 1963).

More recently, in 1969, Johnson and Muir reported on laboratory experiments to investigate the relationship between bed load discharge and the intensity and frequency of the sound produced by inter-particle collision during sediment movement (Johnson et al, 1969). While quantitative results were shown, they cautioned: "Limited field experience indicates that difficulties would be experienced with mixtures of sizes and extraneous noise in rivers." Also in 1969, Solov'yev reported on results obtained by an instrument based on the principle of collision of particles with a receiving plate of the sensor placed at the bottom of a stream (Solv'yev, 1969). In 1970, Hinrich experimented with two types of acoustic

devices: a hydrophone attached to a bottom plate, and an Arnhem-type direct bed load sampler with hydrophone attachment (Hinrich, 1970). While measurements were made at various locations along the Rhine river, quantitative results were once again not reported.

In addition to the European experience reported above, there have been at least two previous attempts by Canadians to develop acoustic techniques for bed load measurement. Some experimental hydrophone work was done by Hollingshead in 1967 and 1968 on the Elbow River in Alberta (Hollingshead , 1968). This was limited to qualitative detection of location of bed load movement; hence relatively simple instrumentation was used. Following this, similar qualitative measurements were made at some 51 Alberta stream sites (AWRD, 1969) for purposes of determining competent conditions, or simply for determining if there was bed load discharge at the particular measured flow at the time the stream or river site was visited. These data were to be used in the various empirical or semi-theoretical equations for bed load discharge prediction. In each of these two cases qualitative data were reported, hence indicating relative success in the use of a hydrophone for qualitative measurement of bed load movement location.

2.3.2 Basic Acoustical Concepts

Sound may be defined as the periodic variation in pressure, particle displacement, or particle velocity in an elastic medium (Albers, 1965). Because the medium is elastic, a motion of the particles of the material communicates to adjacent particles. A sound wave is thereby propagated outward from the source with a finite velocity depending upon the compressibility and density of the medium.

The time waveform of the acoustic pressure depends largely upon its method of generation. While there are many types of waves (Rayleigh, Love, longitudinal or compressional, and transverse or shear waves), longitudinal waves are by far the most important type of wave in acoustics, in general, and this is particularly so underwater (Tucker et al, 1966).

Waves generated by a point source, or one whose dimensions are small compared with their wave length, in a homogeneous medium propagate with spherical symmetry. If the medium is bounded by two plane parallel boundaries (as is the case of the sea) waves generated by a point source spread with circular symmetry only in the horizontal plane. Thin wave fronts are cylindrical and they are known as cylindrical waves. If the source is an infinite plane surface, the resulting wavefronts are also plane, no spreading occurs and the waves are known as plane waves. Although true plane waves cannot be generated in practice, both spherical and cylindrical waves approximate to plane waves when they are sufficiently removed from their sources (Tucker et al, 1966).

In the case of sound generated at the bottom of a gravel-bed river, the assumption of plane wave propagation is made. This assumption is substantiated by the fact that there are a random number of sources over a broad area resembling an infinite plane surface, and that the sources are small. The characteristic properties of these plane waves are that the acoustic pressures, particle displacements, density charges, and so on, have common phases and amplitudes at all points on any given plane perpendicular to the direction of wave propagation.

In a plane wave of sound the pressure p is related to the velocity of the fluid particles μ by

$$p = \rho c \mu \qquad \ldots 2.28$$

in which ρ is the fluid density and c is the propagation velocity of the wave. The product ρc is often referred to as the specific acoustic resistance of the fluid. For example, $\rho c = 1.54 \times 10^5$ gm/(cm^2) (sec) for seawater at 13°C; $\rho c = 42$ gm/(cm^2) (sec) for air: and $\rho c = 1.48 \times 10^5$ gm/(cm^2) (sec) for fresh water at 20°C. When the proportionality factor (ρc) between the velocity and the pressure is complex, it is often referred to as the specific acoustic impedance of the medium containing the sound wave.

A propagating sound wave is comprised of mechanical energy in the form of the kinetic energy of the particles in motion and of potential energy of the stresses set up in the elastic medium. Because of the wave propagation, a certain amount of energy per second (power) will flow accross a unit area normal to the direction of propagation. This energy per second, or power, crossing a unit area is referred to as the intensity of the wave and is related to the acoustic pressure by

$$I = p^2/\rho c \qquad \text{...2.29}$$

Because there is always some time integration inherent in the system being used, the averaged, rather than instantaneous, intensity is of practical use. For example, in the case of fresh water with $\rho c = 1.48 \times 10^5$ gm/(cm)^2 sec, the intensity per square centimeter of a plane wave in water of rms pressure 1 dyne/cm^2 is $I = .68 \times 10^5$ ergs/(cm^2) sec.

For transient signals, or for signals distorted in propagation, it is more meaningful to refer to the energy flux density of the acoustic wave. The energy flux density is the time integral of the instantanious intensity and can be mathematically expressed as

$$E = \int_o^\infty I\,dt = (1/\rho c)\int_o^\infty p^2\,dt \qquad \text{...2.30}$$

The energy flux density is in the units of ergs per square centimeter.

In underwater sound, the basic unit of intensity is the intensity of a plane wave having an rms pressure equal to 1 dyne/cm^2, which is equivalent to 1 microbar or 0.64×10^{-12} watt/cm^2. The unit of energy flux density is the energy density of a plane wave of rms pressure equal to 1 dyne/cm^2 integrated over a time interval of 1 sec, which is equivalent to 0.64×10^{-12} watt-sec/cm^2. These units are used when a particular intensity or energy density is said to be "relative to 1 dyne/cm^2" or "re 1 dyne/cm^2", or "re 1 μb". In air acoustics, on the other hand, a reference pressure of 0.000204 dyne/cm^2 is often used as this is considered to be the threshold sensitivity of the human ear at 1,000 Hz.

The decibel is commonly used for expressing intensity and energy density because it is a convenient way to describe large changes in these variables and to permit each of the variables to be multiplied together by the more simple process of adding their decibel equivalents. Hence, the decibel is the ratio of intensities (or energy densities) expressed in logarithmic units. For example, if I_1 and I_2 are the two intensities, then the intensities are said to differ by N db as follows:

$$N = 10 \log_{10} (I_1/I_2) \qquad \ldots 2.31$$

The intensity level of a sound wave is the number of decibels by which its intensity differs from the reference intensity. Hence, if I_2 in equation 2.4 is the reference intensity equal to 1 dyne/cm^2, then a sound wave of intensity I_1 has a level equal to N db re 1 dyne/cm^2. Energy flux densities may be compared with a reference energy flux density in a similar way through a specification of energy-flux-density level.

The level of a sound wave in a frequency band 1 Hz wide is referred to as a spectrum level(SPL), provided that the sounds have a "continuous" spectrum (some sound, however small, being present in any frequency band). Similarily, the level in a frequency band greater than 1 Hz wide is referred to as a band level (BL). For a band width of W hertz, and for a flat spectrum or as an approximation for any continuous spectrum if the band width is not too wide, the band level is related to the spectrum level at the middle of the band by

$$BL = SPL + 10 \log W \qquad \ldots 2.32$$

The effect of band width can be further illustrated by considering two band levels, neither of which is the spectrum level. For all noises except those consisting of a few discrete frequencies, there will obviously be more energy in a wide pass band than there will be in a narrow pass band. Therefore, in presentation of results, it is necessary to say what pass-band the sound pressures were measured

in. Occasionally, it is desirable to transfer results obtained in one set of pass-bands to another set. This conversion is made as follows:

$$BL_1 = BL_2 + 10 \log (W_1/W_2) \qquad \ldots 2.33$$

In equation 2.33, W_1 is the band width to which it is desired to convert the results and W_2 is the band width used for the measurements. BL_1 and BL_2 are respectively the desired and measured band levels. For example, assuming BL_2 = 40 dB and was measured in a 1/3 octave band (W_2 = 1/3), and that it is desired to convert to an octave band (W_1 = 1), then BL_1 = 40 + 10 log (1/(1/3)) = 45 dB.

In the addition of two random noises, it is the intensities and not the pressures that must be added. For example, if two equal noises are added, the intensity will double but, as the pressure is proportional to the square root of the intensity, the pressure will go up by a factor of 2. Thus if two band levels in decibels are added, the increase is10 log 2 or 3 dB (from Equation 2.31).

2.3.3 Theorectical Feasibility Analysis

The most recent thorough theoretical feasibility study was perhaps that of C.K. Jonys as reported in a preliminary report in 1975 (Jonys, 1975). Jonys developed an analytical model relating the rate of bed load transport with some acoustic parameters measurable in a natural stream and a theoretical transfer function relating the sound pressure levels generated by the collisions of rolling bed particles and the rate of bed load movement. The remainder of this section, 2.3.3, summarizes Jonys' theoretical development illustrating, in figure 2.2, a slightly modified hydrophone/weight configuration than that used by Jonys but which is consistent with the hydrophone system used in the field research program. This modification does not influence the theoretical results.

2.3.3.1 Modelling Concepts

In modelling experiments an attempt is made to represent as realistically as possible the real conditions. Inevitably, however, idealizations are required

to keep the model simple and readily comprehensible. Figure 2.2 illustrates the physical model developed to formulate the relationship between the rate of bed load transport, the position of the hydrophone and the positions of the sound producing river bed pebbles.

All particles were assumed to be spherical and to have a diameter D_s. The pebble arrangement locations relative to the center of the hydrophone and the symbols representing the distances are shown in Figure 2.2.

The average velocity of the moving particles was represented by $\bar{V}_p$. The particles were assumed to move by rolling or by jumping over an integral number N_j of stationary bed pebbles. For movement by rolling, N_j equals one; for movement by jumping N_j is greater than one. A moving particle collides with an individual stationary particle in its path only once so that when the motion is by rolling, collisions occur with all consecutive particles. If jumping occurs, collisions take place on the average with every N_j th bed particle. The pebbles were assumed to move in a layer one diameter deep.

Other assumptions related to pebble sound were as follows:

1. Sound is generated because of collision of moving particles with stationary particles only. It is considered that collisions between moving pebbles do not occur.
2. The location of a collision source is at the stationary bed particle.
3. All collisions generate equal acoustic power.
4. Collision generated acoustic power is a non-linear function of the average particle transport velocity.
5. The receiving hydrophone has omnidirectional characteristics.
6. The receiving hydrophone is located in the free field part of the acoustic far field.
7. Collision generated sound has continuous frequency spectrum characteristics.

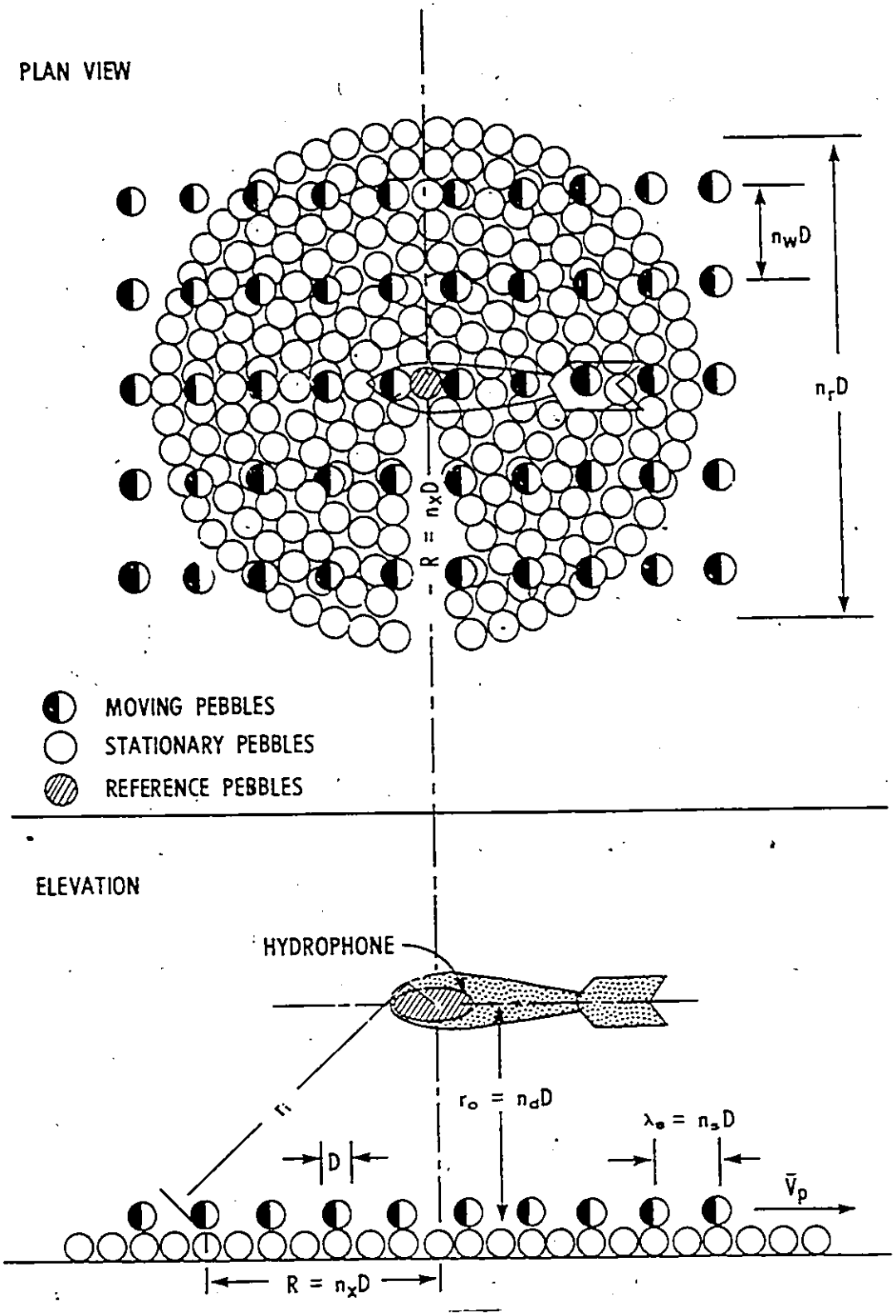

FIGURE 2.2 Physical Model for Theoretical Feasibility Analysis

8. Sound attenuation between source and receiver is due to non-directional wave divergence and negligible because of turbulence, velocity gradients and temperature variations, etc.
9. Multiple collision source sound pressure levels are additive in the same way as continuous sources if the frequency of collisions exceeds 50 Hz.
10. Background noise levels do not mask pebble generated sound.
11. Moving and stationary pebbles are of identical size.

Assumptions 1, 4, 6, 7 and 9 were supported by earlier laboratory experiments. Assumptions are further discussed in Section 2.3.3.4.

2.3.3.2 Acoustic Bed Load Transport Function

The bed load transport rate can be defined by the parameters describing the frequency at which particles pass a reference point and their mass.

Bed particles were considered to move downstream in rows separated by a distance λ_w, or by $\lambda_w = N_w D$ where N_w was the distance between the rows. The rate of bed load transport in the width λ_w was therefore $g_{ws} = fm$ in which f was the frequency at which particles passed a reference line and m was the mass of one particle or $m = \rho_s \pi D^3/6$. The passage frequency f was dependent on the average velocity, $\bar{V}_p$, and the spacing between particles, λ_s; or $f = \bar{V}_p/\lambda s$. From these relationships, the rate of bed load transport per unit width of channel was shown to be

$$g_s = fm/\lambda_w \qquad ...2.34$$

The bed load transport rate was also defined as a function of particle collision frequency. The frequency of collision with the specific reference particle depended not only on the frequency of particle passage but also upon the occurrance of impact. The occurance of impact depended upon the length of the jump which the moving particles experience between collisions. The jump length between collisions is $\lambda_j = n_j D$ where n_j is the length of jump in particle diameters. The average frequency of collision, f_c^1, with a reference bed particle in the path of

a moving row of particles is estimated from $f_c^1 = f/n_j$ for a row of moving particles in a width λ_w of the channel. The frequency of collision with any one of the stationary particles in the reference row perpendicular to the direction of motion is $f_c = f/n_w n_j$. The relationship between the rate of bed load transport per unit width of channel and the frequency of collisions with any one stationary bed particle is thus determined to be

$$g_s = f_c n_j m/D \qquad ...2.35$$

The next step was to express the relationship between the number of collisions and the total sound pressure level at a point above the bed. A concentric arrangement of the stationary bed particles in rings around the vertical axis passing through the observation point was employed. The total number of pebbles in any circular ring i located at a radius of N pebble diameters from the centre, can be estimated from $N_i = 2\pi N$. When the width of the stream of moving particles is $n_r D$ extending equal distances to both sides of the ring, and N is greater than $n_r/2$ the number of pebbles in the two segments of a ring i can be determined from

$$N_i = 2\pi N (1 - (2 \cos^{-1}(n_r/2N))/\pi) \qquad ...2.36$$

The total number of collisions per unit time in any ring or ring segment i can then be estimated from $F_i = f_c N_i$.

It has been demonstrated experimentally by Jonys (1975) that if the frequency of sound producing collisions exceeds 50 Hz and all collisions occur at the same distance from the hydrophone, that it is possible to define an equivalent sound pressure level SPL_{eq} due to one collision per second. It can be determined from the theoretical relationship $SPL_{eq} = SPL^1 - 10 \log F^1$, where SPL^1 = the observed sound pressure level generated by all collisions at a fixed range from the observation point, and F^1 is the frequency of noise contributing collisions.

Assuming that SPL_{eq} is a function of the average velocity of particles only, and hence, a constant in a given flow situation, the sound pressure level contribution SPL_i at hydrophone location due to all collisions in a ring i at range r can be calculated from

$$SPL_i = SPL_{eq} + 10 \log F_i - 20 \log(r_i/r_o) \qquad ...2.37$$

where r_o is the distance between the hydrophone and the river bed and is used as the reference range. The term $20 \log (r_i/r_o)$ represents the SPL attentuation due to wave divergence. Equation 2.37 can also be expressed in terms of f_c and N_i

$$SPL_i/10 = SPL_{eq}/10 + 2 \log r_o + \log (f_c N_i/r_i^2) \qquad ...2.38$$

The total SPL at hydrophone location can be determined by addition of the square of the rms pressures due to contributions from each of the pebble rings. Since $SPL_i = 20 \log (p_i/p_o) = 10 \log (p_i^2/p_o^2)$ it follows, therefore that p_i^2/p_o^2 = antilog $(SPL_i/10) = 10$ to the power $SPL_i/10_x$ where p_i = rms sound pressure due to collisions in ring r_i, and p_o = reference pressure of 1μbar. An expression for the total sound pressure can then be obtained from

$$p_T^2/p_o^2 = \sum_{i=1}^{k} p_i^2/p_o^2 = \sum_{i=1}^{k} 10^{SPL_i/10} \qquad ...2.39$$

or in terms of SPL by

$$SPL = 10 \log (p_T^2/p_o^2) = 10 \log \sum_{i=1}^{k} 10^{SPL_i/10} \qquad ...2.40$$

where k is the number of noise contributing pebble rings.

In deriving equations 2.37, 2.41 and 242, Jonys does not provide any explanations for the apparent lack of homogeniety of units.

Substituting SPL_i from equation 2.38 into equation 2.40, an expression for the frequency of collisions with any one stationary bed pebble is obtained as follows:

$$f_c = 10^{SPL/10}/r_o^2 \; (10^{SPL_{eq}/10}) \sum_{i=1}^{k} (N_i/r_i^2) \qquad ...2.41$$

The transfer function between the observed SPL and the rate of bed load transport is obtained by substituting equation 2.41 into equation 2.35

$$g_s = (m10^{SPL/10}/r_o^2 D) \; (n_j/10^{SPL_{eq}/10} \sum_{i=1}^{k} (N_i/r_i^2)) \qquad ...2.42$$

2.3.3.3 Numerical Simulation Results

Equation 2.42 was programmed for numerical simulation by Jonys (Jonys, 1975) to determine how the various factors affect the SPL resulting from pebble movement. The factors investigated were the distance between the hydrophone and the river bed, the aerial concentration of moving pebbles, the effect of particle saltation and the influence of the average particle velocity.

The effect of the distance of the moving bed from an omni-directional hydrophone upon the observed SPL is illustrated in Figure. 2.3. The curves represent the computed SPL values due to all collisions contained in an area of river bed defined by a radius of N pebble diameters. The rates of bed load transport g_s are the same for all curves and were calculated assuming identical SPL_{eq}, and identical n_j, n_s and n_w which were equal to one. The range of the hydrophone to the bed for the B curves was four times greater than for the A curves.

Curves A and B represent the variation of SPL due to collisions up to a radius of N = 400D, for a total width of the moving strip of bed load of 800D. Curves A^I and B^I, diverging from A and B at N = 20D, represent calculated SPL when the moving strip of bed load is only 40D wide.

When N = D, the difference in SPL between the two curves for ranges r_A and $r_B = 4r_A$ is 12 dB. However, as SPL increases with N, the difference between the calculated SPL decreases and at N = 400D is reduced to approximately 2 dB. This is because, relative to the SPL produced by the pebble directly below

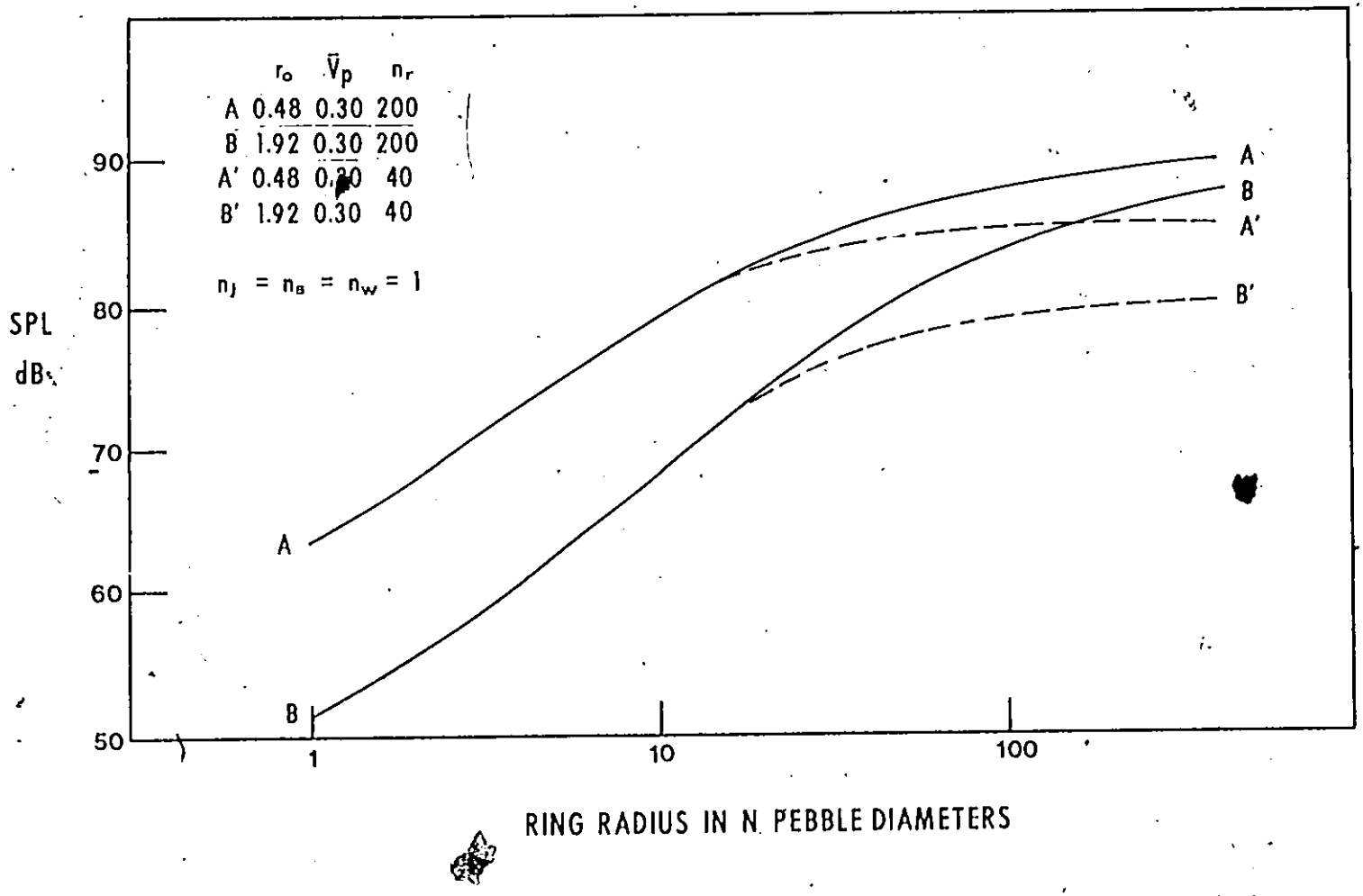

FIGURE 2.3 SPL Versus Distance of Hydrophone from the Bed, and Width of moving bed. (from Jonys, 1975)

the hydrophone, the same pebble ring contributes more sound to the hydrophone further away from the riverbed. If the hydrophones are at r_A and at $r_B = 4r_A$ from the bed and if the ranges of the hydrophones to a ring i of radius N_iD are r_A^1 and r_B^1 respectively, the ratio r_A^1/r_A will always be greater than r_B^1/r_B. Because sound attenuation due to divergence from the source is determined by this ratio, relatively more sound will be attenuated to the lower hydrophone location. This result is of practical significance because the placement of omnidirectional hydrophones at different distances from the river bed for identification of near bed noise may not be useful for large widths of moving pebbles.

For a limited strip width of moving particles, represented in Figure 2.3 by curves A^1 and B^1, the SPL contributions from the distant ring segments become negligible by a combined effect of distance attenuation and a constant number of collisions as the ring radius increases. Hence, the SPL rapidly approach saturation values. However, the difference of 5dB between the two curves A^1 and B^1, shown in Figure 2.3, represents a specific case and would vary depending upon the width of the moving gravel strip.

Figure 2.4 illustrates the influence of the aerial concentration of the moving particles, represented by values n_s and n_w, and the effects of the length of particle jump n_j. Theoretical prediction of SPL was made for four different n_j, and four aerial concentrations ranging from 1 when the lateral and transverse distances between the pebbles is zero or $n_s = n_w = 1$, to an aerial concentration of 1/64 when $n_s = n_w = 8$. SPL_{eq} for all calculations was assumed to be constant and the width of the moving stream of particle was chosen to be 40D. The results show that for any constant n_j, doubling of the rate of transport g_s corresponds to an increase of 3 dB in SPL. Similarly, when the particles begin to saltate, any doubling of the jump length decreases the SPL by 3 dB for the same rate of transport.

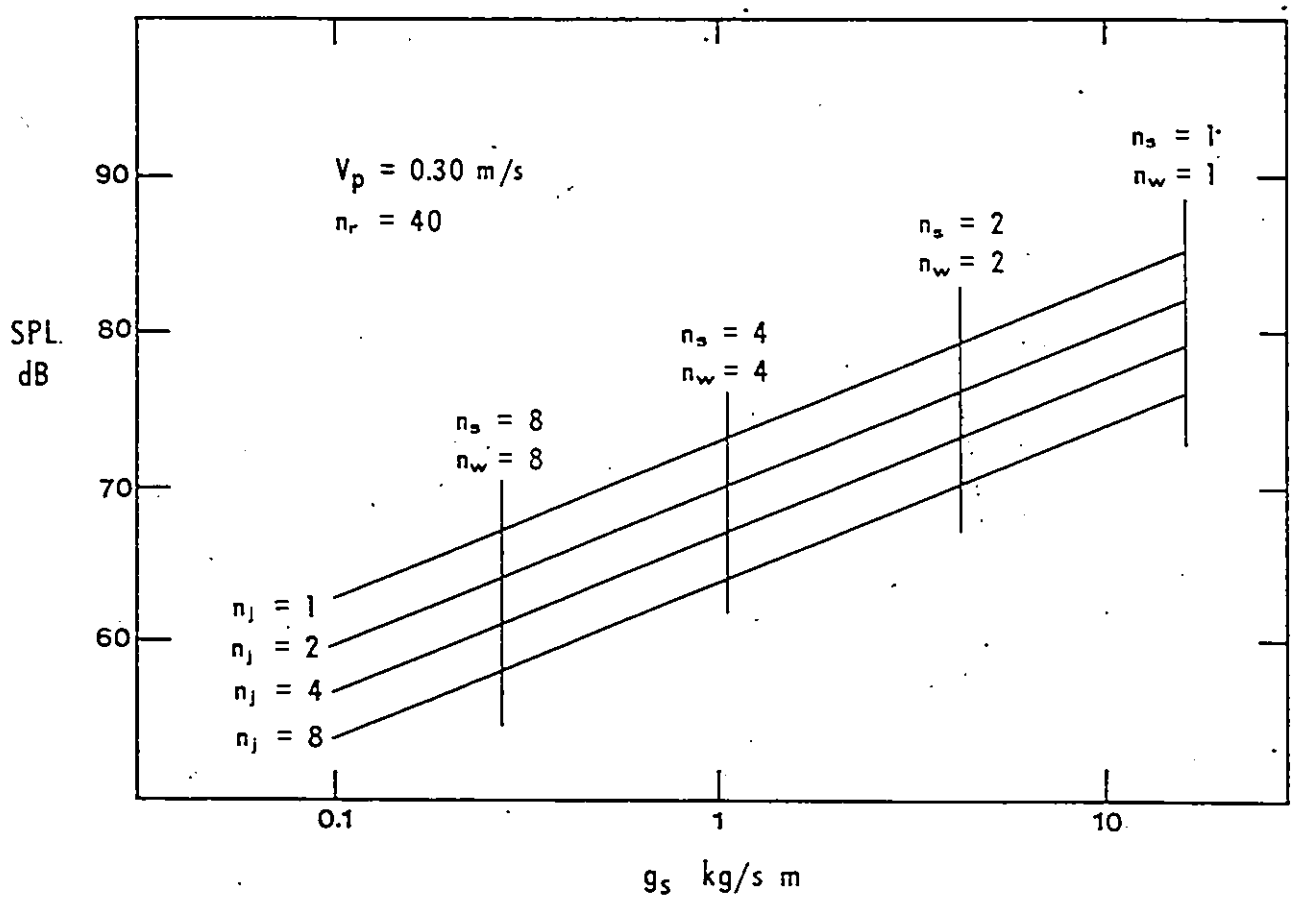

FIGURE 2.4 SPL Versus g_s for Different Pebble Jump Lengths and Different Aerial Concentrations. (from Jonys, 1975)

Figure 2.5 illustrates the effects of the force of interparticle collision and of aerial concentration of the moving particles, for movement without saltation ($n_j = 1$). On the basis of physical arguments and experimental evidence presented by Jonys (1975) it was assumed that the equivalent one collision sound pressure level is a nonlinear function of the average particle velocity $\bar{V}_p$ which can be represented by the following equation:

$$SPL_{eq} = C_1 - C_2 (\log \bar{V}_p + C_3)^2 \qquad ...2.43$$

The function is a logarithmic parabola, which depending upon the values of the constants C_1, C_2 and C_3, gives a rapid increase in SPL_{eq} at low $\bar{V}_p$ followed by a gradual decrease in SPL_{eq} as $\bar{V}_p$ increases. For the numerical simulation, the values of the constants were obtained from experimental data with 40 mm diameter ceramic spheres ($C_1 = 50$, $C_2 = 0.85$, and $C_3 = 36$) yielding $SPL_{eq} = 0$ at $\bar{V}_p = 0.01$ m/s and a maximum $SPL_{eq} = 50$ for $\bar{V}_p = 0.141$ m/s.

The simulation results, presented in Figure 2.5, illustrate that a wide range of SPL values can be obtained for the same rate of transport depending upon the values of $\bar{V}_p$. Similarly, they illustrate that large errors in estimation of g_s would be incurred from SPL observations if no consideration is given to the SPL_{eq}.

2.3.3.4 General Observations

The theoretical feasibility analysis, while based almost entirely on the work done by C. K. Jonys (Jonys, 1975), provides a detailed insight on the parameters involved in the relationship of bed load transport and the resulting sounds or acoustics. The relationship shows that the rate of bed load transport is a function of at least seven independent variables which, in addition to the measured SPL, are the size and mass of the bed pebbles, the position of the hydrophone relative to the river bed, a measure of particle saltation, the aerial extent of the moving bed, and the average acoustic power generated by a single collision between a moving and a stationary particle. In addition to this, in a field situation the bed

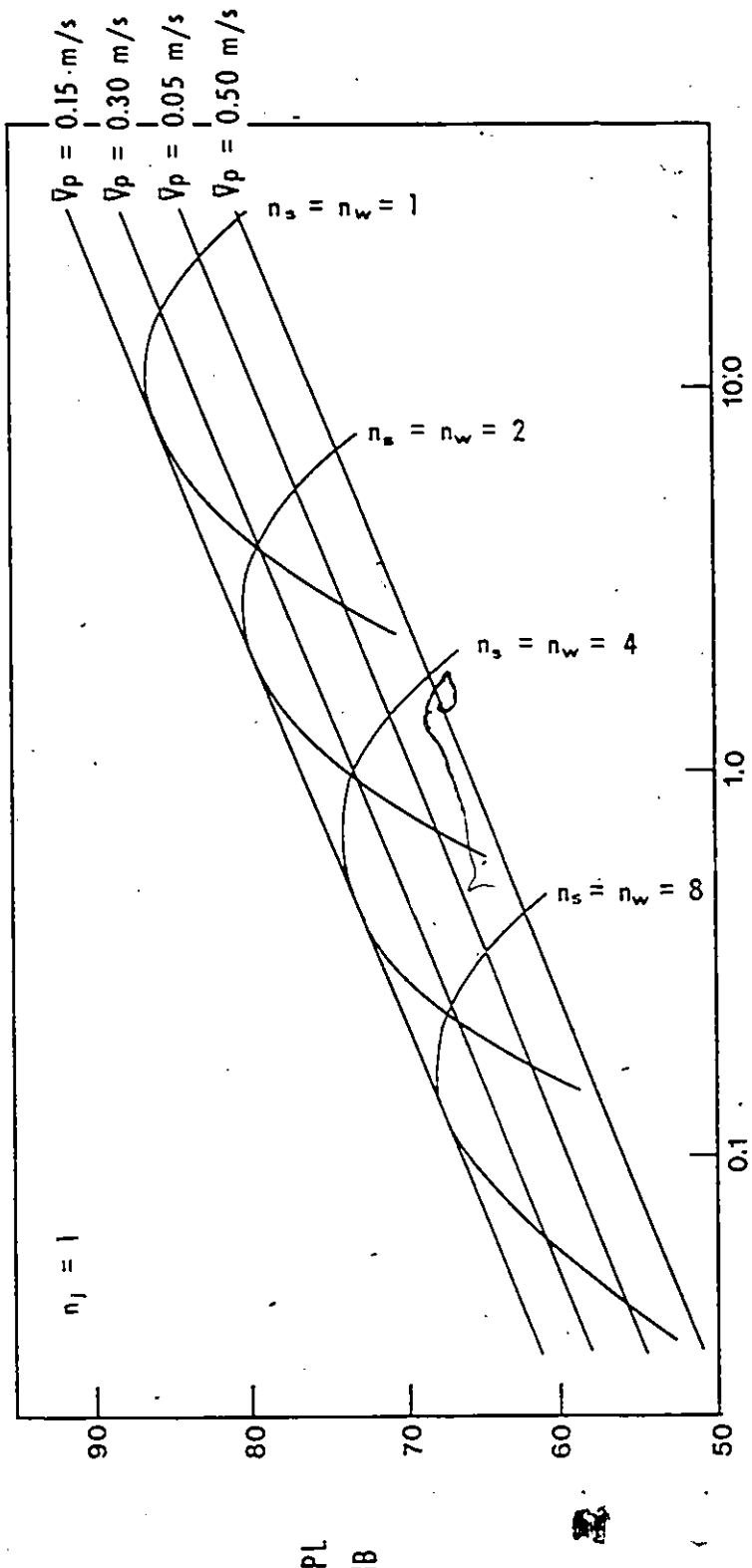

FIGURE 2.5 SPL Versus g_a for Different Pebble Velocities and Aerial Concentrations. (from Jonys, 1975)

particle characteristics and their distribution on the river bed are highly variable. Not all of the seven independent variables can be measured or controlled. Among the controllable variables are SPL and the position of the hydrophone from the river bed, and bed material samples can be obtained to measure the mass and the characteristic dimensions of the pebbles. Among the variables which cannot be readily determined are the extent of saltation or jump length, the aerial extent of the moving stream of bed load (index k of equation 2.15), and the level of sound generated by a collision SPL_{eq} which basicially provides a measure of the acoustic power emitted by a pebble. A reduction in the number of variables may be possible in some situations. For example, if particle movement is observed to be by rolling only, then $N_j = 1$; it might also be possible to determine the average velocity of the moving pebbles $\bar{V}_p$ and then to reproduce the movement in a laboratory to establish the characteristic level of collision sound SPL_{eq}. The use of a directional hydrophone may make it possible to observe pebble collision sound originating from a finite area and thereby to eliminate the unknown index k. Finally, it may be possible to measure the bed load transport rate under field or laboratory conditions and hence to "calibrate" the model (equation) for specific conditions.

It should be noted that the field observations have provided a further understanding of the acoustics/bed load relationships, and hence, of the limitations of the assumptions used in model development. Among these limitations the most significant is perharps that which implies that bed forms are not present (figure 2.2), hence the application would be limited to flat-bed, sheet-flow cases and gravel size materials. Similarily, and this relates to assumption eight, it was found that water turbulence effects were significant. Because of these limitations the value of the model is essentially that it provides at least some theoretical understanding of the inter-relationships among the variables affecting the acoustics near river beds.

CHAPTER 3

EXPERIMENTAL PROCEDURES

3.1 Hydrophone System

3.1.1 General Design Concepts

The hydrophone system was designed for use for two main purposes: firstly, to enable qualitative determination of location and relative intensity of bed load discharge; and, secondly, for more detailed study of continuous bed load transport variability, pulsation patterns and so on. The instrument developed is a wideband, portable hydrophone system capable of acquisition, conditioning and recording of underwater acoustical information. Primary features include a low-noise signal pickup, a variable electronic filter adjustable in one-third octave steps, a true logarithmic post amplifier which provides both a normalized audio output signal and a logarithmic output whose level is proportional to the input signal in decibel-volts, and a single-channel, solid-state, servo recorder. Also inclusive are rechargeable, nickel-cadmium battery packs for both the signal conditioning electronics and the recorder, thus making the system truly portable.

Physically, the hydrophone system is comprised of three sections: the hydrophone or data acquisition, the signal conditioning and the recording sections. The signal conditioning system is comprised of a variable bandpass filter, a logarithmic voltage controlled amplifier, a monitor panel, a rechargeable power supply and a portable case encompassing and interconnecting these components. The system is schematically illustrated in Figure 2.5 and is further illustrated by means of photographs in Appendix C.

The data acquisition section of the hydrophone system could not be readily used in the laboratory and field experiments as it was only several pounds in weight. The hydrophone component was therefore placed inside a 150 pound,

streamlined, Columbus-type weight frequently used for discharge measurements. This weight (encompassing the hydrophone) was then suspended by means of a reel-line and provided relatively good stability at the measurement points within the flowing water.

The system was designed so that the recording section produced a continuous reading of sound intensity on a linear scale and in terms readily convertable to decibels. An earphone output was also available to assist the observer in the data collection and in the subsequent interpretation of the data.

The above text very generally describes the components comprising the hydrophone system. The technical details or specifications of these components are quite lengthy and are therefore shown in Appendix A.

3.1.2 Operational Details

Additionally to the schematic of the hydrophone system as illustrated in Figure 3.1, it is useful to describe the operational features in terms of sound pressures, voltages at the inputs and outputs of the various components, and other acoustical parameters. Figure 3.2 diagrammatically illustrates these. With this basis, it is possible to define mathematically the operational details.

With reference to the symbols defined in Figure 3.2, the following relationships result

$$d = e_2 S_c \qquad \ldots 3.1$$

$$e_2 = \log (e_1/e_{ref}) \qquad \ldots 3.2$$

and

$$e_1 = P_{rms} S_h \qquad \ldots 3.3$$

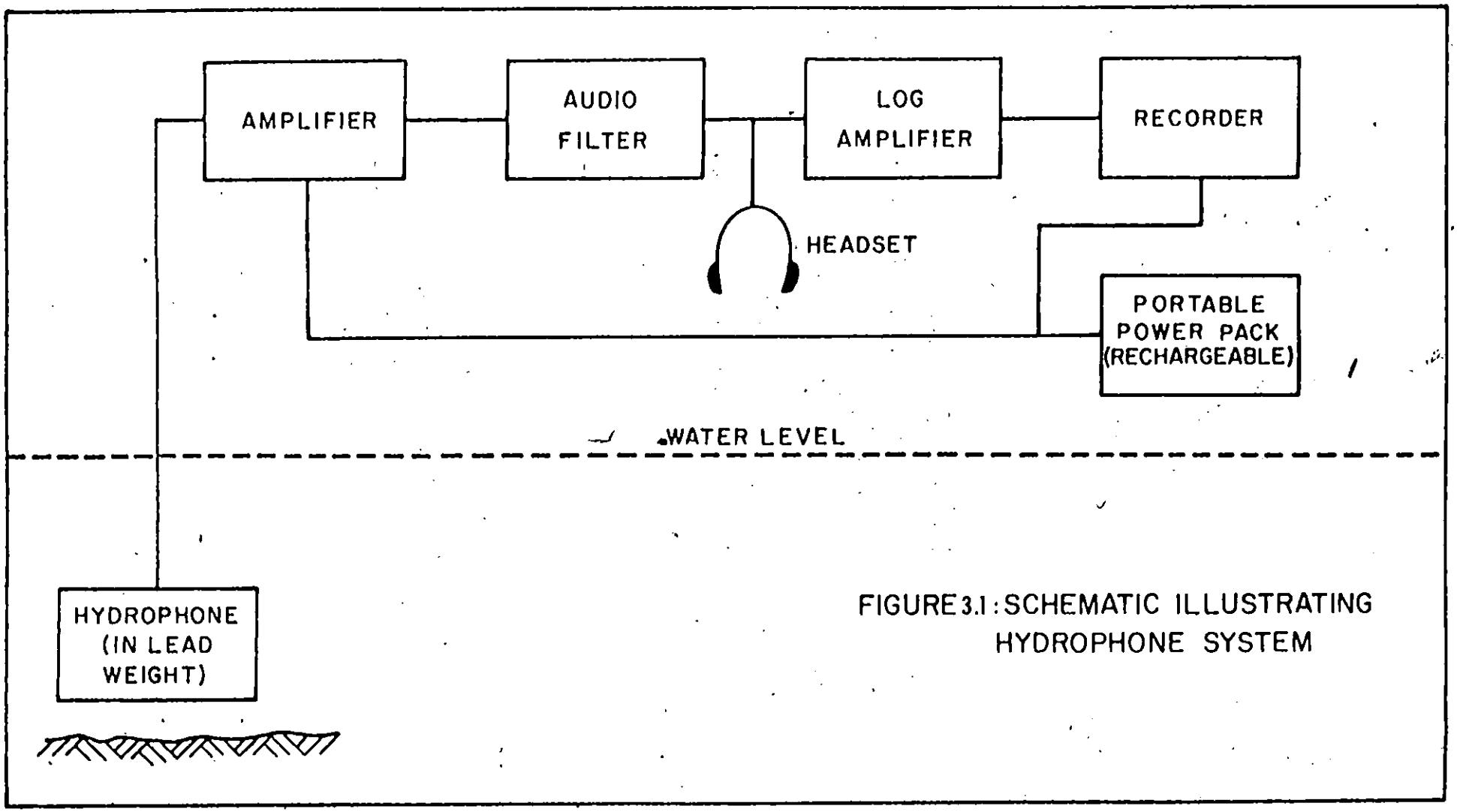

FIGURE 3.1 : SCHEMATIC ILLUSTRATING HYDROPHONE SYSTEM

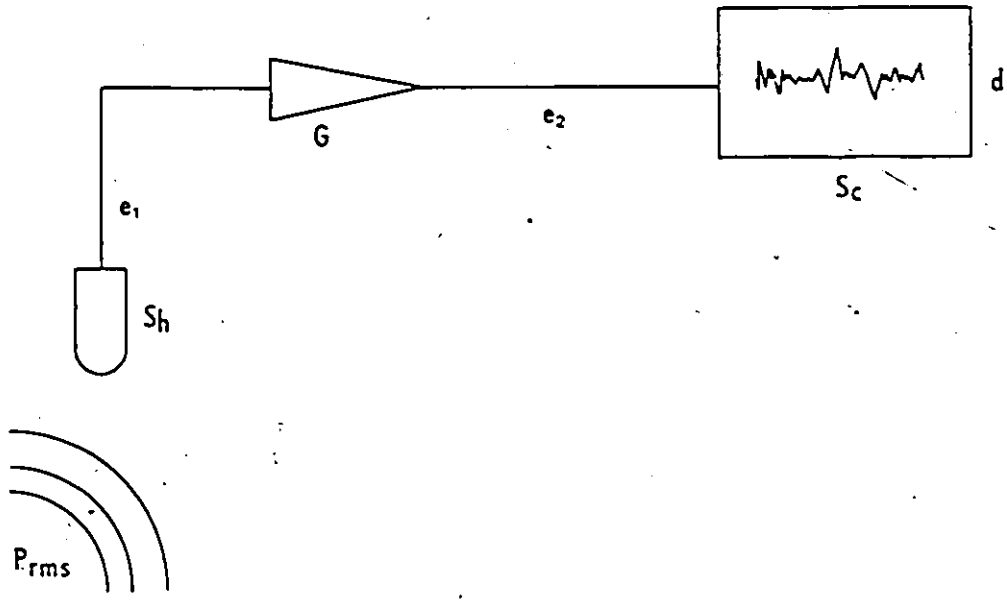

LEGEND

S_h = hydrophone sensitivity, microvolts/microbar

e_1 = hydrophone voltage output, microvolts

G = gain

e_2 = gain voltage output (chart recorder input), volts

d = chart division, in divisions from a reference

S_c = recorder sensitivity, divisions/volt

P_{rms} = rms sound pressure (at hydrophone), in microbars

FIGURE 3.2 Schematic Illustrating Acoustical Parameters

Using the above three equations, the chart reading d can be related to the rms pressure at the transducer by another equation

$$d = S_c \log (P_{rms} S_h / e_{ref}) \qquad \ldots 3.4$$

In terms of numerical values as applicable to the hydrophone system, the constants in the above equations, S_c, S_h and e_{ref} could be defined. For example, the recorder sensitivity, S_c, is equal to 10 divisions/volt. From Section A.4.3 of Appendix A, e_{ref} = 50 µbar. (Note: $N = -64 = 20 \log (S_h/S_{ref})$; $S_h = 10^{-64/20} = .000633$). These constants can be used in equation 3.4 if it is desired to relate the chart reading to the rms pressure at the transducer. The new equation becomes

$$P_{rms} = 0.079 \times 10^{d/10} \qquad \ldots 3.5$$

where P_{rms} is in µbars and d in divisions from a reference (full range of d is 80 divisions).

3.1.3 Laboratory Calibration

Additionally to ensuring that the hydrophone system instrumentation was appropriately calibrated (as described in Appendix A), it was felt desirable to at least attempt to calibrate the system for background noise due to velocity turbulence in the vicinity of the hyrophone weight. The "calibration" described in this section refers, therefore, not to the calibration required to insure appropriate functioning of the equipment, but to the determination of background noise levels resulting from turbulence and from other sound sources. Tests were made in September, 1971, and February, 1972, the results of which follow.

3.1.3.1 September, 1971, Calibration

The first series of tests or calibrations were made in the Water Survey of Canada current-meter rating tank in Calgary, Alberta. This facility was about

six feet by six feet by 300 feet long with an electrically driven rating car which drove along a longitudinal track at speeds controlled by a rheostat device.

The tests were made primarily to determine the effects of turbulence in the vicinity of the hydrophone weight. Additionally, however, some experimentation was done to determine the effects of the rating car itself on the output and to determine the possible effects of surface waves. The latter was done by varying the distance between the hydrophone weight in the water and the surface of the water in the tank.

A summary of the tests made and an illustration of their results are shown in Table 3.1 and Figure 3.3 respectively. It should be noted that for all these tests, the hydrophone was mounted "vertically" in the 150-C lead sounding weight. Consequently, it is possible that the horizontal plane of the sensor was somewhat shielded by the lead walls of the weight. The results are nevertheless useful, and having experimented with this series of tests enabled the setting up of a somewhat better later series.

Some interpretation of the results shown in Figure 3.3 is warranted: Figure 3.3 (b) illustrates the effect of depth of hydrophone on recorded output. The slightly higher output for the shallower depth, 22 inches, as compared to 48 inches depth, is probably the result of surface noise (powerline noise and surface waves) contributing more to the shallow depth test. The effect of interference from the power line used to drive the rating car is illustrated in Figure 3.3 (g) and 3.3 (h). The curves in these figures logically illustrate that the power and electric motor used to drive the rating car contribute to the background noise. Figures 3.3 (a), 3.3 (b) and 3.3 (c) further illustrate the effect of the rating car noise itself. For these tests the hydrophone was suspended immediately above the water surface and essentially monitored the noise level at the water surface.

TABLE 3.1 Summary of Calibration Tests, September 1971

Rating Number	Frequency Range (KHz)	Remarks
1-9	0.1-25	
19-21	0.1-25	Pushing rating car (motor off)
10-18	5-25	
22-24	5-25	Pushing rating car (motor off)
25-34	0.1-5	
35-44	5-10	
105-108	5-10	Weight out of water
45-53	10-16	
54-62	16-20	
63-71	20-25	
72-75	20-25	X10 for recording only
76-79	10-20	X5 for recording only
80-88	0.1-2.5	
109-112	0.1-2.5	Weight out of water
89-97	2.5-5	
98-100	2.5-5	Weight at 48" depth
101-104	2.5-5	Weight out of water
113-114	10-25	Weight out of water

Notes:

1. Water surface to bottom of tank = 60".
2. Rating 1-97 inclusive, water surface to top of weight = 22".
3. Rating 98-100 inclusive, water surface to top of weight = 48".
4. Rating 101-114 inclusive, weight out of water (just above water surface.
5. Slew rate was maximum allowable and varied with frequency range setting.
6. Hydrophone's longitudinal axis was normal to the horizontal plane.

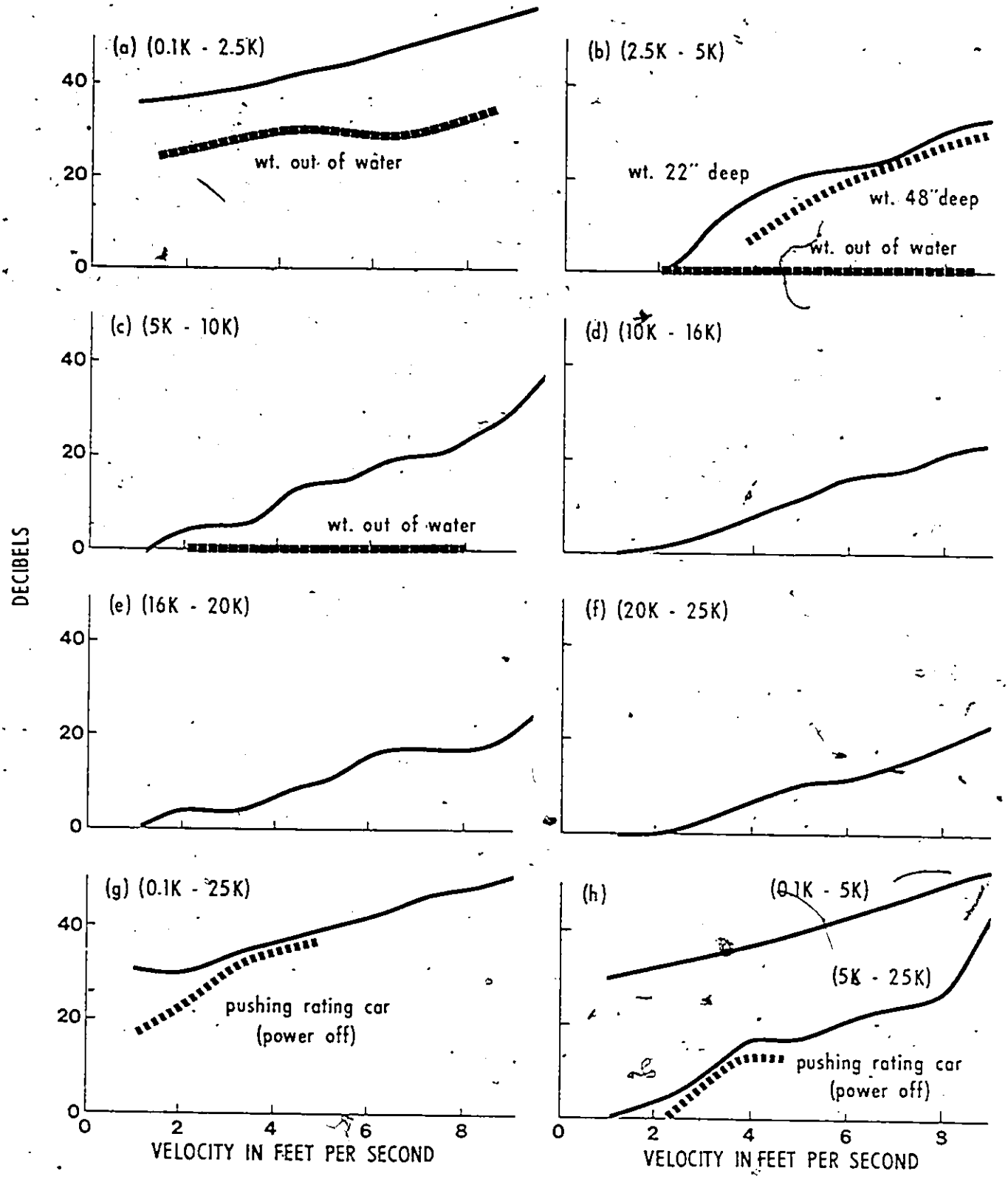

FIGURE 3.3 Recorded Output in Decibels Versus Velocity for Shown Frequency Ranges. (Data from Sept. 1971, Calibration tests)

As a result of this first series of tests, it was decided that the hydrophone should be placed "horizontally" to the horizontal axis of the encompassing weight. It was anticipated that this would prevent possible directivity problems (particularly at the higher frequency ranges at which the hydrophone sensor is omnidirectional in the horizontal plane as compared to spherical directivity at very low frequency) and that this new arrangement would make the data acquisition portion of the hydrophone system considerably more streamlined. (In the "vertically" mounted arrangement, the top part of the hydrophone was sticking out from the weight, adding considerably to the drag of the weight, hence possibly to turbulence effects.) Similarily, following the experience from these first tests, it was learned that more appropriate frequency intervals could be chosen for subsequent tests.

3.1.3.2 February, 1972, Calibration

The results of this series of tests are illustrated in Table 3.2 and Figures 3.4 and 3.5. These calibrations were made using the same facility as those described in Section 3.1.3.1.

Basically, these data illustrate the same type of results as part of the first series results: the levels of background noise resulting from turbulence and from other sound sources. The results of the first and second series of calibrations are not readily comparable because the latter series utilized somewhat improved frequency intervals and because of the different positions of the hydrophone relative to the horizontal plane. A very cursory-type comparison of the two sets of data, however, indicates that the discrepancies between the two sets of results are not significant, that is, the results are of the same order of magnitude.

TABLE 3.2 Summary of Calibration Tests, February, 1972

Rating Number	Frequency Range (KHz)	Remarks
1-9	0.1-0.2	
10-18	0.2-0.4	
19-27	0.4-0.8	
28-36	0.8-1.6	
37-46	1.6-3.15	
47-56	3.15-6.3	
57-65	6.3-12.5	
66-74	12.5-25.0	See note 5
75-83	12.5-25.0	
84-92	25.0-50.0	
1-9	0.1-0.4	
10-18	0.4-1.6	
19-27	1.6-6.3	
28-36	6.3-25.0	
37-45	25.0-50.0	

Notes:
1. Water surface to bottom of tank = 60"
2. For all calibrations, water surface to top of weight = 22"
3. Slew rate was maximum allowable and varied with frequency range setting
4. Hydrophone's logitudinal axis was parallel to the horizontal plane.
5. Data from rating numbers 66 to 74 inclusive are not good due to equipment malfunction.

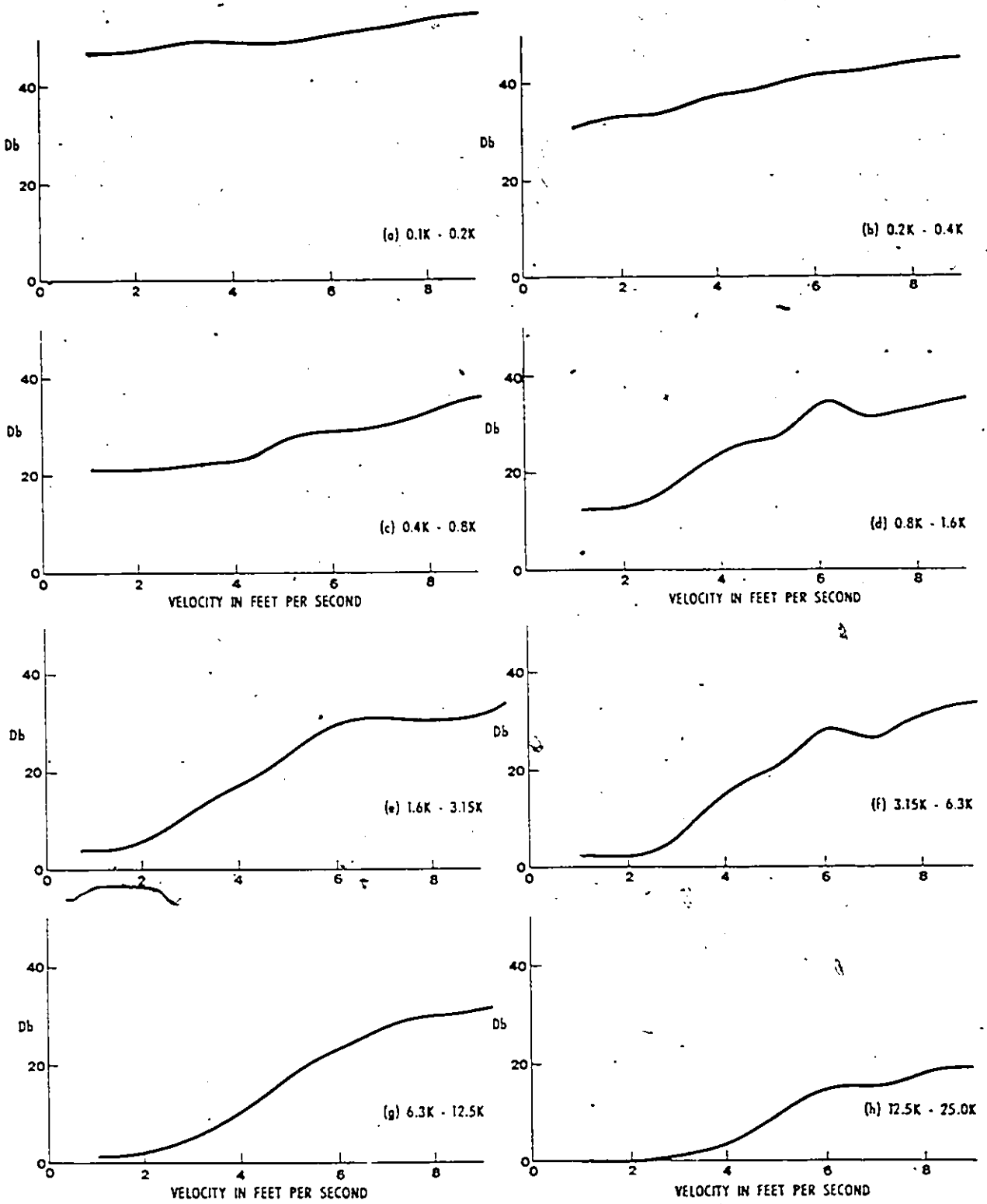

FIGURE 3.4a Recorded Output in Db Versus Velocity for Shown Frequency Ranges (Data from Feb. 1972 calibration tests).

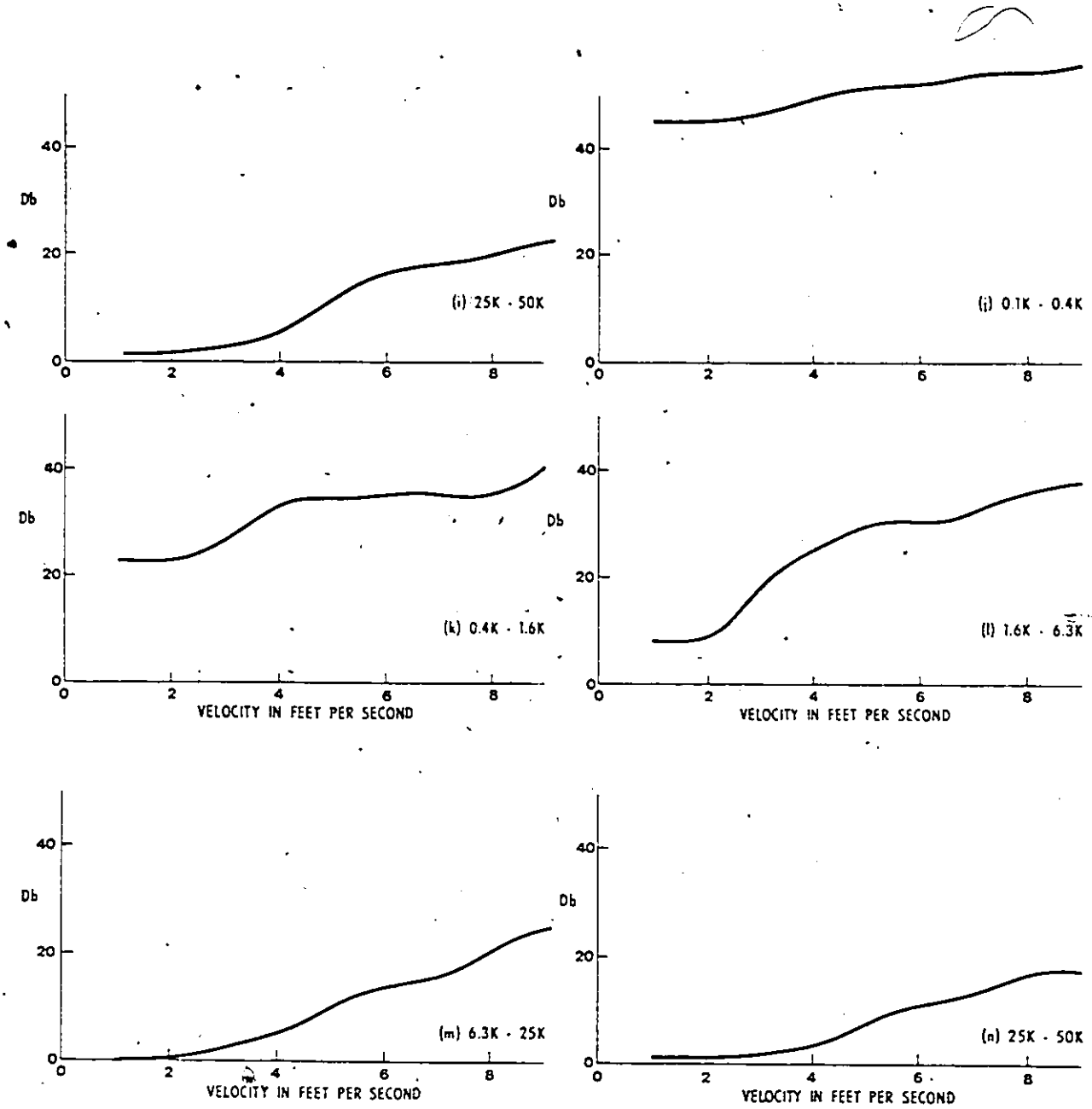

FIGURE 3.4b Recorded Output in Db Versus Velocity for Shown Frequency Ranges (Data from Feb 1972 calibration tests).

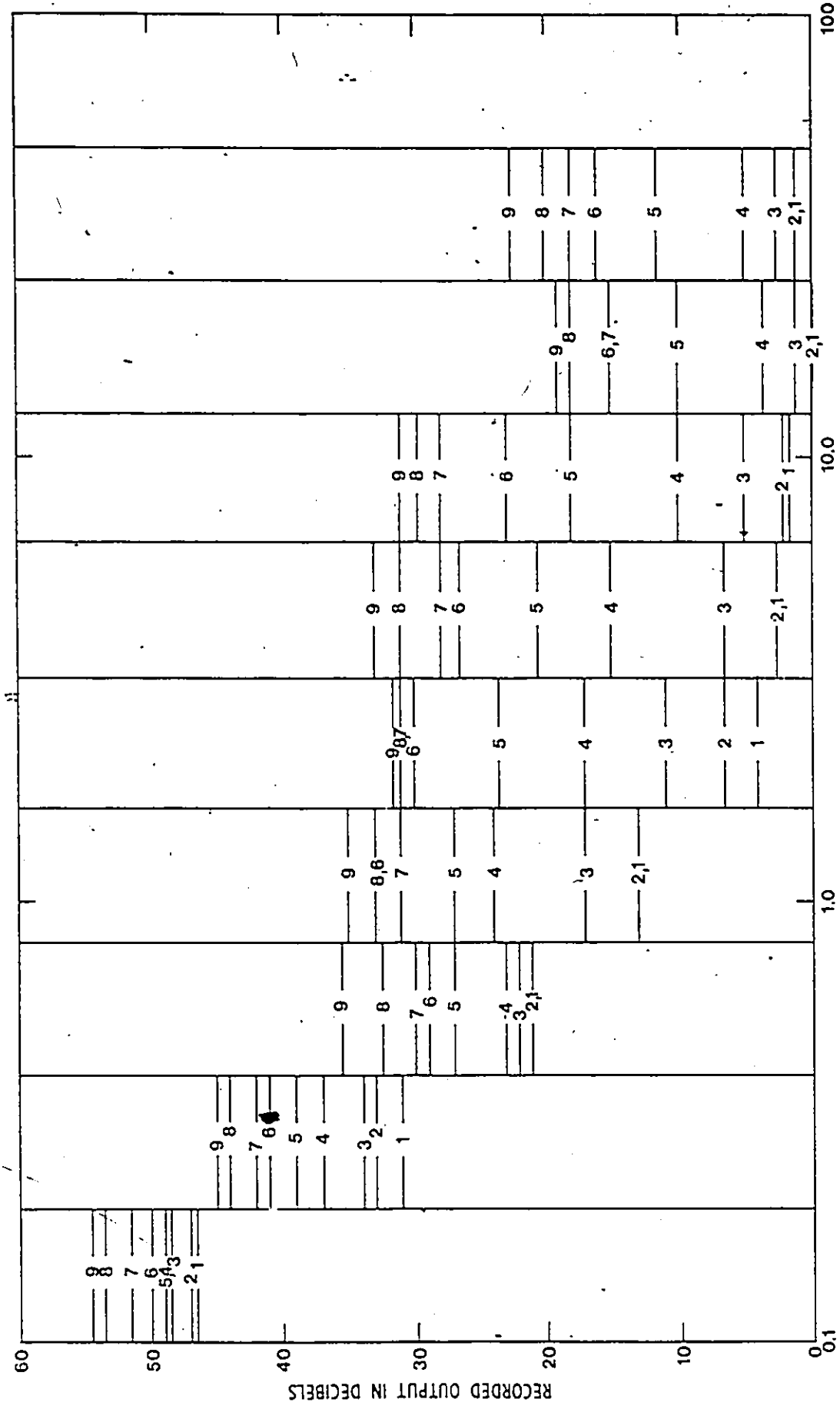

FIGURE 3.5a Recorded Output in Db Versus Frequency for Shown Velocities (Data from Feb. 1972, Calibration tests)

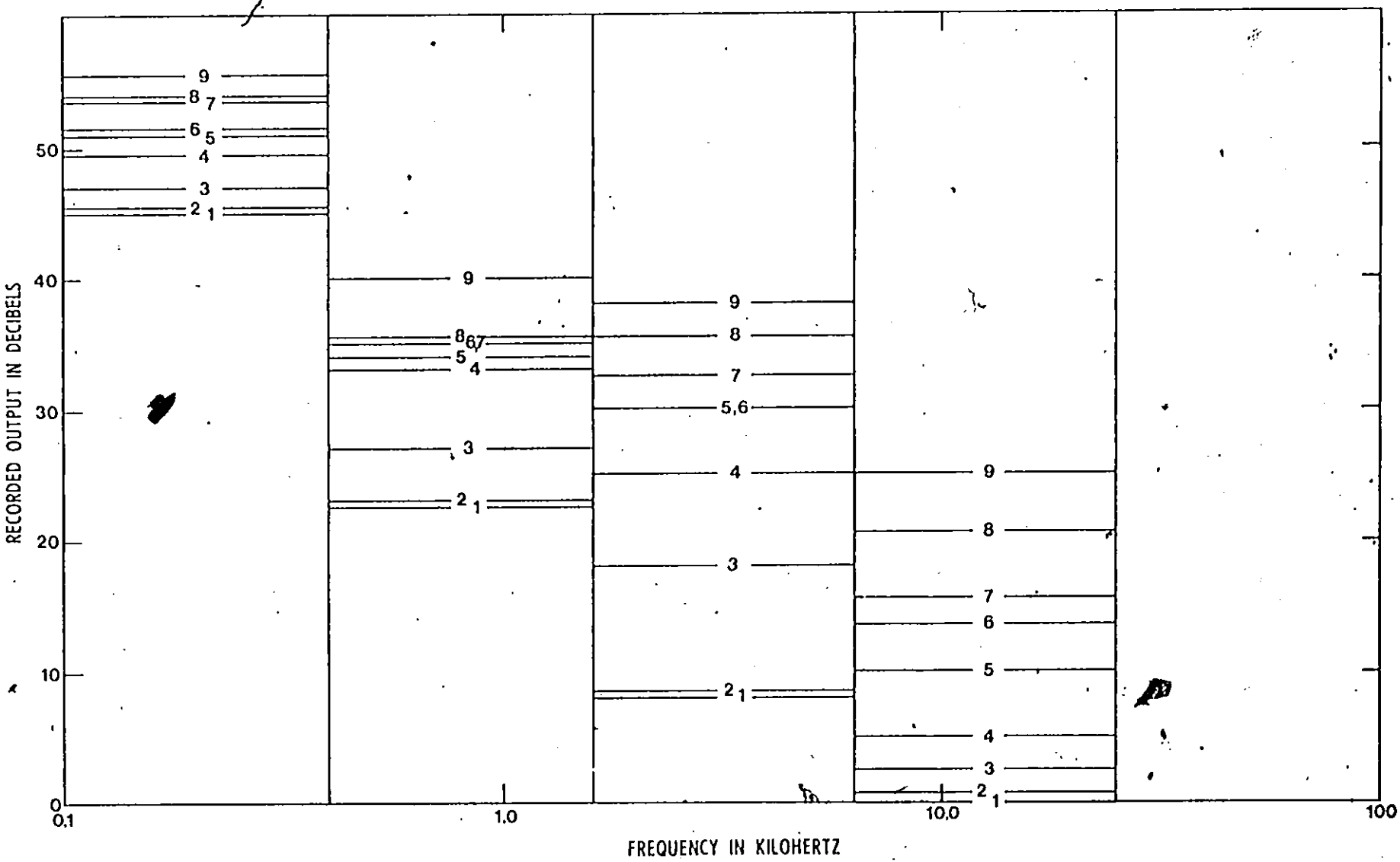

FIGURE 3.5b Recorded Output in Db Versus Frequency for Shown Velocities (Data from Feb. 1972, Calibration tests)

3.1.4 Field Procedures

The hydrophone observations were carried out at numerous verticals within a cross-section of the river. The field experiments were conducted during May and June 1972. The hydrophone observations were part of a more detailed sediment investigation consisting of the collection and analysis of hydrometric, suspended sediment, bed load, bed material and channel geometry data. The study reach of about six miles in length is illustrated in Figure 1.1. The Vedder River near Yarrow, the location where hydrophone experiments were conducted, coincides with cross-section six of the site plan.

At each point of observation, the station, total depth, depth of hydrophone, time of day, filter frequency range setting, chart recorder details and other remarks were noted: the sound data during two or three minute time intervals were recorded. Although observations were not all repeated at exactly the same locations in the vertical in all instances, they were, however, referenced in a consistent manner so that the cross-sectional data could be readily compared. An attempt was made to obtain observations at those locations within the cross-section which would best contribute towards the definition of the cross-sectional distribution of the sediment transport. It was essential also to ensure that at least some observations were taken at locations where there was no sediment transport so as to provide data for the entire cross-section. Additionally to recording the sound data, ear phones were available to enable the observer to listen to the data being recorded, hence to facilitate the observer in the data interpretation. The hydrophone observation data are detailed in Appendix B.

Initially, in the development of a routine methodology, experimental data were obtained both at various depths and verticals within the cross-section and at various frequency ranges of the audible sound spectrum. Some effort was made to ensure that the operator could distinguish between unwanted sounds and those sounds created by particle movement.

The results of the field hydrophone measurements are described and illustrated in Section 5.1.

3.2 Field Measurements (Direct)

3.2.1 Instrumentation

The basic instrumentation requirements for the field program were those for collection of hydrometric, channel geometry and sediment data. Sediment data included suspended sediment, bed load and bed material data; channel geometry included both channel configuration and slope data; hydrometric data included velocity and flow data.

3.2.1.1 Hydrometric Instrumentation

Prior to the 1971 field season there was only one standard hydrometric station in the study area: the Chilliwack River at Vedder Crossing station. The location of this station is designated by cross-section one in Figure 1.1.

The Chilliwack River at Vedder Crossing station was operational on a continuous basis for the periods November, 1911, to September, 1915; October, 1916 to May, 1931; and May 1951 to date. These hydrometric data were particularily useful, therefore, because they were long term and represented the inflow or the upper boundary condition for the study area.

The instrumentation at this station included a cableway and hand-propelled cable-car, a staff gauge, a wire-weight gauge located on the bridge, and an analog stage recorder (Stevens Type A35).

At a location about 1000 feet upstream from cross-section six (see Figure 1.1), there was another hydrometric station referred to as the Vedder River near Yarrow station. It was not a standard station, however, since it was instrumented with a staff gauge only and was periodically operated for stage recording purposes only, primarily during the summer months. The station provided useful data, however, since it was at approximately the middle of the study area and was near cross-section six where most of the sediment data were collected.

One other hydrometric station, which was of some use even though it was located outside of the study area, was the Sumas River near Sardis station. The station was located near the mouth of the Sumas River, hence near the mouth of the Vedder Canal. These two streams join just prior to discharging into the Fraser River, about two miles downstream from cross-section eleven shown on Figure 1.1. This station was instrumented with a Stevens Type A35 recorder and was operational primarily for stage purposes because of considerable influence of backwater from the Fraser River.

3.2.1.2 Bed Load Sampling Equipment

For purposes of bed load sampling, two types of sampling equipment were provided: the half size VUV and the full size basket samplers. This sampling equipment is illustrated by photographs in Appendix C.

The VUV, or VUV Hungarian sampler as it is sometimes called, is a pressure-difference type sampler and is recommended for particle sizes from one to one hundred millimeters in diameter. It has an overall field sampling efficiency of 70 percent with a hydraulic efficiency of 101 percent (Novak, 1957). The half-size VUV sampler has a mouth width of 8 1/2 inches and height of 4 1/4 inches, (inside measurements) with a total length of 41 inches. Its weight is about 95 pounds. For purposes of sampling at cross-section six, additional weight had to be provided to improve sampler stability at the river bottom. This was done by the addition of an Arnhem "frame", a Y-shaped bar with side weights and a stabilizing rear fin, for providing approximately 270 additional pounds..

The other type of bed load sampler used was the basket sampler. This sampler is essentially a large rectangular frame with a rear tail or fin section which encompasses a basket with one open end. The basket dimensions were as

follows: 30 inches long, 24 inches wide and 10 inches deep. The sampler weight is about 240 pounds. The basket portion was made from heavy gauge wire mesh with mesh sizes of 3/4 inch for the top, 1/2 inch for the sides and back and 1/4 inch for the bottom.

The average efficiency of basket type samplers is reported at about 45 percent. Recent laboratory studies indicate efficiencies varying linearly from 30 percent for a bed load transport rate of 20 lb/min/ft width to 50 percent for a transport rate of 120 lb/min/ft width (Gibbs et al, 1972).

3.2.1.3 Suspended Sediment Sampling Equipment

Standard depth-integrating samplers were used for the collection of suspended sediment data. These included the USDH-48 (4 1/2 pounds), USDH-59 (24 pounds) and US-D 49 (62 pounds), depending on the flow conditions.

3.2.1.4 Other Instrumentation Requirements

Because of the nature of the research program developed, it was essential to provide some instrumentation additionally to that in place prior to 1971. Basically, this additional instrumentation included:

(a) a new cableway at cross-section six,

(b) two, two-man, stand-up type cable cars (one for cross-section one, and one for cross-section six); each were motorized and equipped with a power reel,

(c) a 1000-pound capacity hydroscale for weighing bed load samples on site,

(d) additional hydrometric and sediment sampling equipment,

(e) bench marks, tellurometers and other survey equipment, and,

(f) a hydrophone system..

3.2.2 Field Procedures

The following paragraphs give a brief description of the field methods used throughout the study. In planning the research, one basic criteria was established: the most current field techniques would be used to the extent possible and the minimum data collected would be those data normally obtained using standard procedures. It should be noted that some of the techniques used were the result of many years of development or improvement; others were quite new because of only very recent development and experience and because of recent significant improvements in equipment and experimentation.

3.2.2.1 Hydrometric Procedures

Standard techniques were used throughout with the exception that considerably more data were collected, particularly at cross-section six. These additional data were velocity and flow data; the first to provide sufficient cross-sectional detail, and the latter to enable the construction of an appropriate stage-discharge curve.

3.2.2.2 Bed Load Sampling Procedures

The procedures used in bed load sampling were only very recently developed, that is, within the last six or eight years. Some laboratory experiments conducted as recently as 1972 (Gibbs et al, 1972) added to knowledge relating to methodology of bed load sampling. Improvements to equipment, particularly motorization of reels, added significantly to the sampling procedures. Also of significance was experience gained as a result of field testing of the sampling equipment under a variety of field conditions. This experience aided in equipment design as well as in sampling methodology and in subsequent interpretation of results.

As with hydrophone observations, the bed load samples were not always repeatedly taken at exactly the same verticals within the cross-section but were referrenced in a consistent manner. An attempt was made to concentrate the sampling at those locations within the cross-section which would best define the bed load transport at the time of sampling.

It should also be noted that the two bed-load samplers were used in a consistent manner: the basket sampler during high flows (coarse material), the VUV sampler for low flows (fine material) and both for the intermediate range. Similarily, because of the variability in the rate of bed load transport, an attempt was made to take two or three bed load samples at each sampling vertical so that the average could be used in the calculations. The obtaining of even more samples at each vertical would have been preferable, however, even with the significantly improved instrumentation, such procedures were found to be impractical.

3.2.3 Complementary Data

3.2.3.1 Cross-Section Profiles

In 1971, the 11 cross-sections shown in Figure 1.1 were surveyed for purposes of defining or obtaining channel geometry data. The cross-section locations were selected on the basis of air photo interpretation.

In order to establish a good horizontal and vertical control for the cross-section surveys, a system of bench marks was established. The elevations relative to GSC datum were determined for each of the bench marks by levelling. The horizontal distances between bench marks were obtained by means of tellurometer in the summer and autumn of 1971.

During 1972, the 11 cross-sections were profiled both prior to and subsequent to the spring runoff period for purposes of providing data for determining the changes in channel geometry. The 1972 profile data were obtained

by tag line and level for cross-sections 2 through 11. Because the location of cross-section one coincides with the hydrometric cross-section for the Chilliwack River at Vedder Crossing gauging station, it was proposed that the cross-section one profiles could be obtained from hydrometric measurement results. It was learned subsequent to the cross-section surveys that no fixed relation exists between the water level at the gauge recorder and that at the hydrometric cross-section which is located approximately 1,000 feet downstream from the gauge. Therefore the 1972 profiles for cross-section one had to be reconstructed from existing discharge notes and slope data.

In an attempt to establish good horizontal and vertical control for the cross-section surveys, a system of bench marks was established prior to the 1971 survey. The GSC elevations of the bench marks were determined by levelling and the horizontal distances between bench marks were obtained by means of tellurometer during the summer and autumn of 1971. It was found during the 1972 surveys that many of the bench marks had been moved and in some cases removed due to general instability in the area along the river. Consequently a vertical control survey was repeated for both 1972 surveys in order to re-establish correct bench mark elevations.

The cross-section profile surveys continued beyond 1972; such surveys were conducted during spring and fall of each year.

3.2.3.2 **Slope Data**

As a result of the 1971 control survey, it was possible to compute the thalweg or river distances between cross-sections. The longitudinal water surface profile could also be computed from 1971 survey results.

3.2.3.3 Particle Size Data

Particle size data were obtained for some suspended sediment, for bed load and for bed material samples. Standard laboratory techniques were used in their analysis: hydrometer and bottom withdrawal techniques for suspended sediment particle-size determination, and sieve analyses for bed load and bed material particle-size determination.

CHAPTER 4

COMPUTATIONS PROCEDURES

4.1 Hydrology

Preparatory to undertaking computations using the equations outlined in Section 2.2, it is desirable to describe the hydrology of the river basin and to define the various physical and hydraulic parameters used in the equations. In particular, the latter should include the definition of channel geometry and data related to the river hydraulics.

The drainage basin area for the station Chilliwack River at Vedder Crossing (shown as cross-section one in Figure 1.1) is recorded as 484 square miles. The topographic relief is almost entirely mountainous, varying from about 100 feet GSC datum to more than 6000 feet at some of the mountain peaks. The study reach is 32 thousand feet in length and varies in elevation from 100 feet at cross-section one to about 15 feet at cross-section 11.

The most upstream end of the study reach coincides with cross-section one. This is also the location of the hydrometric station: Chilliwack River at Vedder Crossing. This proved to be a particularly useful boundary condition because of the availability of the historical hydrometric data; the station was operational on a continuous basis for the periods November, 1911, to September, 1915; October, 1916, to May, 1931; and May, 1951, to date. According to the 1967 Sediment Data for Canadian Rivers publication, some historical hydrometric data are as follows: maximum daily discharge, 27,000 cfs on December 29, 1917; minimum daily discharge, 280 cfs on November 30, 1952; mean discharge, 2360 cfs (based on 32 years data). A flow duration curve based on mean daily discharges for the Chilliwack River at Vedder Crossing station for the period January 1, 1959, to December 31, 1968 is shown in Figure 4.1

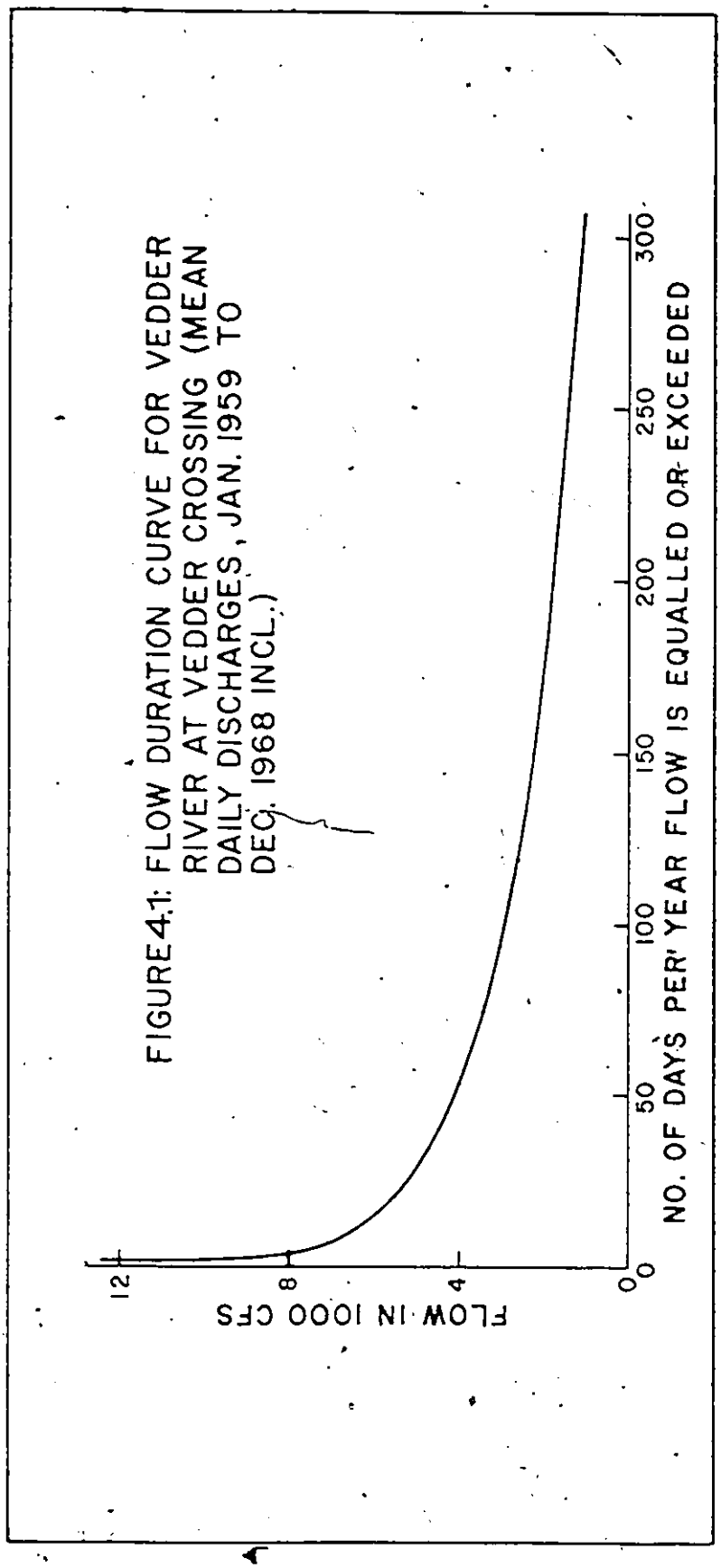

FIGURE 4.1: FLOW DURATION CURVE FOR VEDDER RIVER AT VEDDER CROSSING (MEAN DAILY DISCHARGES, JAN. 1959 TO DEC. 1968 INCL.)

From examination of discharge hydrographs for the Chilliwack River at Vedder Crossing, it is evident that the flows at this station are quite erratic throughout the year. Flows in excess of 5,000 cfs (this flow range being that of significant bed load discharge) generally occur in May, June and July of each year. From the flow duration curve, Figure 4.1, it is apparent that the number of days per year that a flow of 5,000 cfs is equalled or exceeded is in the order of 30 days. Some flows of this magnitude, however, also occur during the fall and winter months resulting from relatively large amounts of precipitation in the form of snow and rain.

The general regime conditions of the river, particularly the study reach, are also known to some extent. From the observation of air photographs of the Chilliwack River, it appears that relatively large amounts of erosion occur along the river channel upstream from approximately cross-section one of the study reach. Deposition appears to occur at points downstream, primarily throughout the six mile study reach. Variations from year to year undoubtedly occur. It was the deposition within the study reach which was of primary concern because excessive deposition in the reach creates upgrading of the river channel. Such river upgrading reduces the effectiveness of the dykes in the area and increases the possibility of overtopping and flooding.

4.2 Channel Geometry

The procedures used to obtain the channel geometry data have already been outlined in Section 3.2.3. Some of the results, particularly those parameters required in the computation of bed load are outlined herein.

For purposes of bed load measurement, the reference cross-section for which channel geometry data were required was that shown as cross-section six in Figure 1.1. This was where the sediment sampling operations were concentrated. The area-width-discharge relationships were therefore developed for this cross-section. The discharge measurement data for 1971 and 1972, which are summarized in Appendix B were used for this purpose. Hence Figure 4.2 illustrates discharge versus area, Figure 4.3 illustrates discharge versus surface breadth, Figure 4.4 illustrates discharge versus mean velocity and Figure 4.5 illustrates discharge versus depth; all of these are for cross-section six of the Vedder River.

In addition to cross-sectional geometry, it was essential to obtain longitudinal profile data. Section 3.2.3 describes the field procedures used to obtain the slope data. The longitudinal profile of the water surface for April 1, 1971, is shown in Figure 4.6. From this figure, the slope of the water surface for cross-section six was then determined to be 0.0020 ft/ft. Backwater effects from the Fraser River were unlikely during the study period as is illustrated by the relevant stage hydrographs in figure 4.7a and 4.7b. It should be noted that the stage of the Sumas River near Sardis represents the stage 20,000 feet downstream from cross-section six.

4.3 Hydraulics Data

Area-depth-discharge relationships for cross-section six are illustrated in Figures 4.2 to 4.5 inclusive. These relationships are somewhat different for 1971 than for 1972. The differences in the river hydraulics are further exemplified on the stage-discharge curves developed for 1971 and 1972 as shown in Appendix B.

The velocity distribution with respect to depth and distance across a section are illustrated in Appendix B for cross-section six. The distributions are shown for the various discharges and were developed using the field discharge measurement data. The velocity distribution data illustrates a relatively uniform

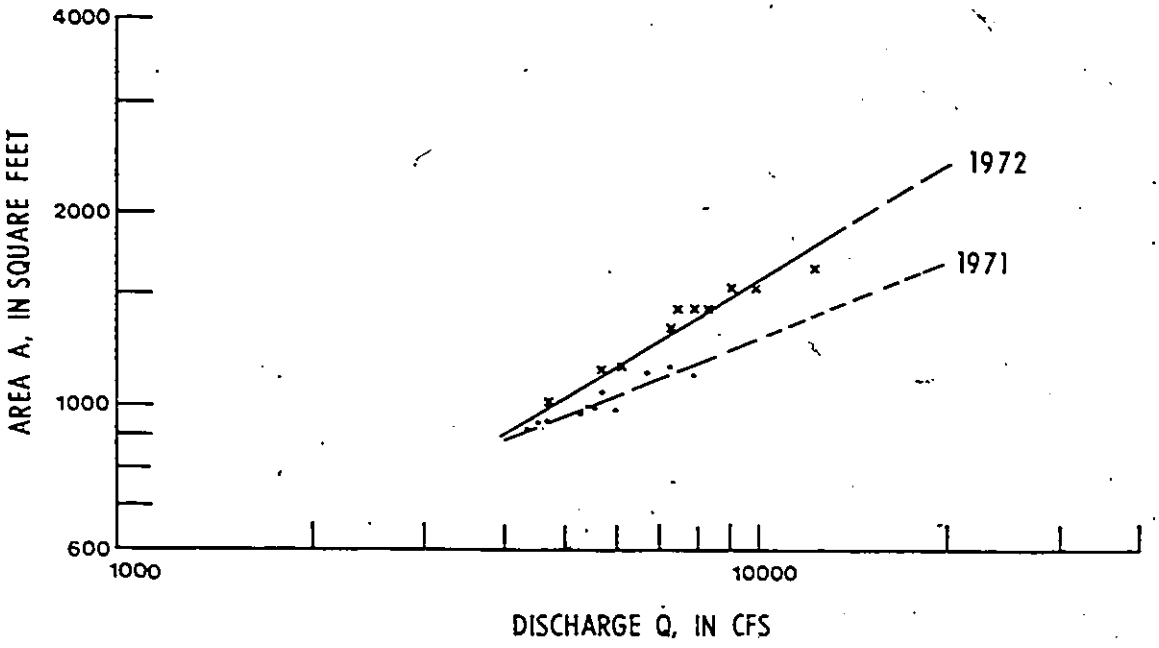

FIGURE 4.2 Discharge Versus Area for Cross-section 6

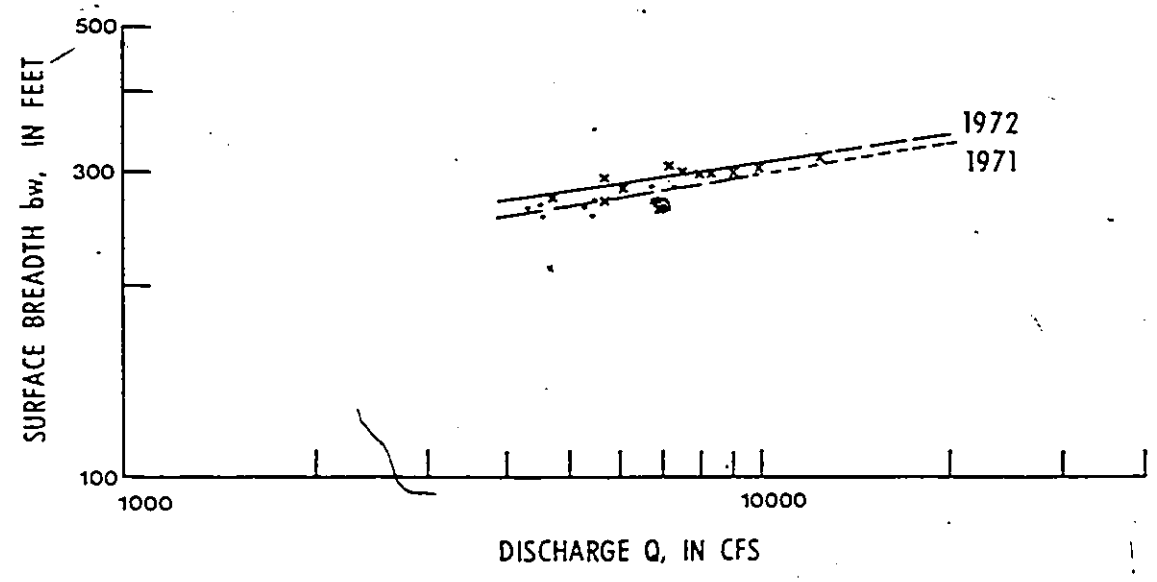

FIGURE 4.3 Discharge Versus Surface Breadth for Cross-section 6

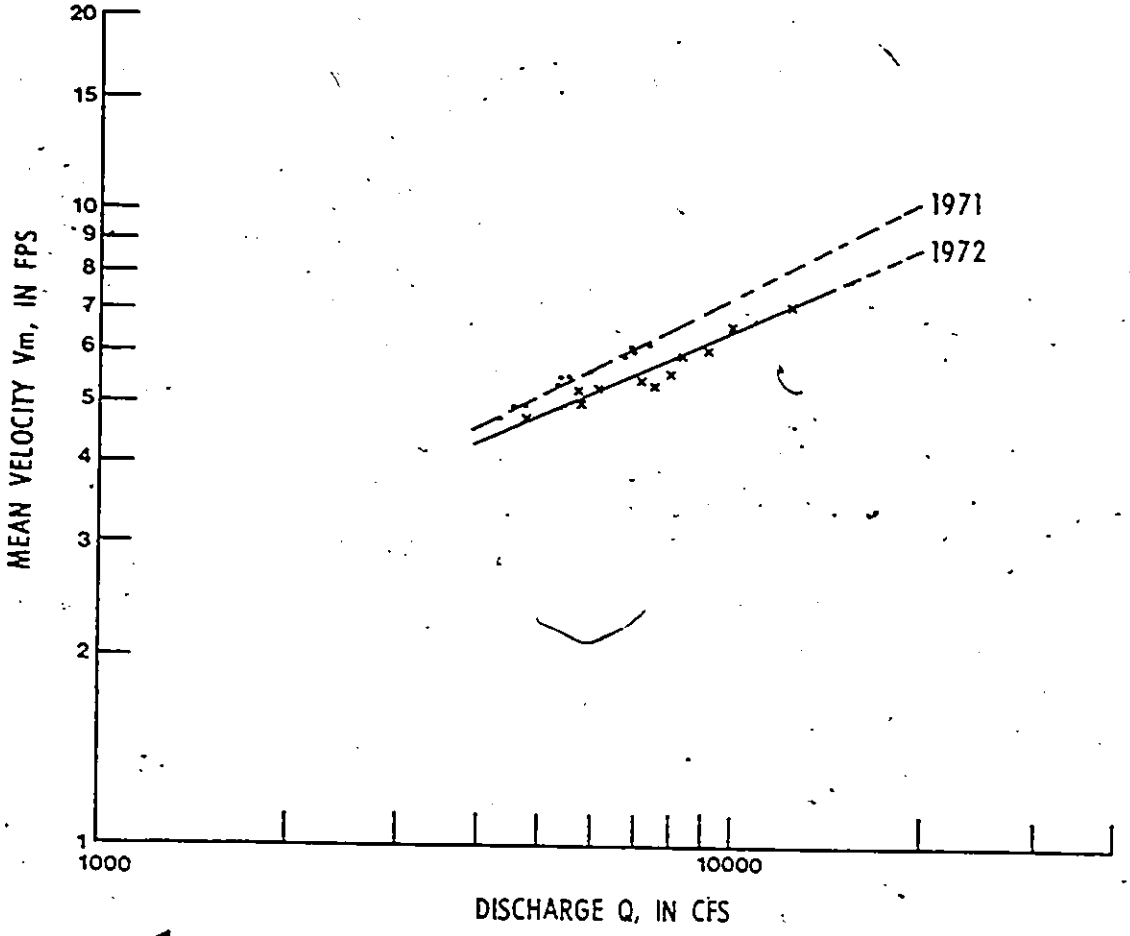

FIGURE 4.4 Discharge Versus Mean Velocity for Cross-section 6

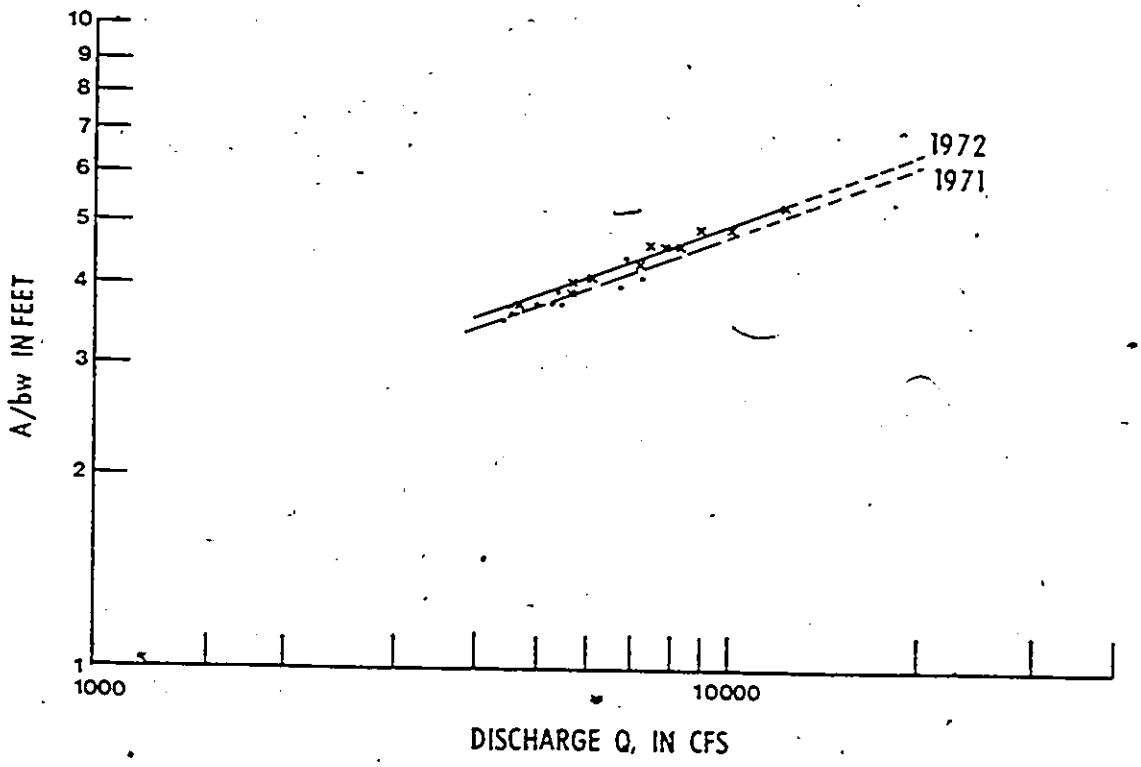

FIGURE 4.5 Discharge Versos Depth for Cross-section 6

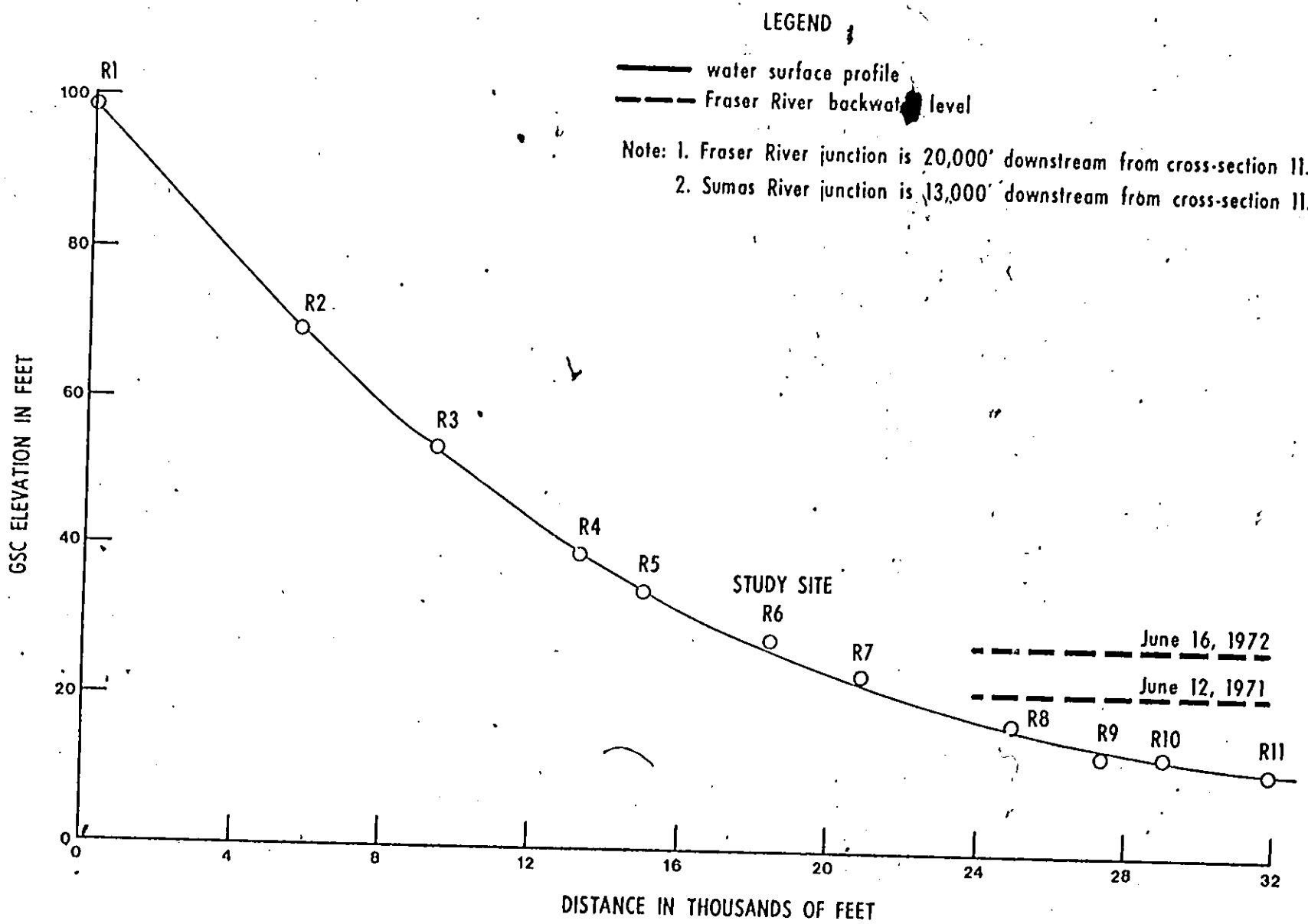

FIGURE 4.6 Longitudinal Profile of the Vedder River Study Reach (April 1, 1971. Water surface)

velocity along any horizontal line in the cross-section and quite varied velocities in the vertical with a very rapid change vertically in the vicinity of the river bottom. This velocity distribution is typical of wide, shallow gravel bed rivers. Hollingshead (Hollingshead, 1968), in experimenting with velocity fluctuations, concluded that these are quite significant in gravel bed rivers with a d/D ratio generally less than 50. He observed a range of 1.31 feet per second for velocities determined from short counts (about 5 or 6 seconds) and a range of 0.90 feet per second from long counts (50 to 60 seconds). The average velocities were 8.66 and 8.25 feet per second respectively. It has been evident that these velocity fluctuations are largest at points near the bed, while velocities at 0.2 d remain relatively constant.

4.3.1 Bed Material and Bed Load Data

The types of bed material and bed load samples taken are discussed in Sections 3.2.1.2 and 3.2.2.2. The results of the size analysis of some of the samples taken are given in Tables 4.1, 4.2 and 4.3. In all cases, these samples were analysed for particle size utilizing standard sieve analysis techniques.

The 1970 bed material samples were taken to illustrate the variation in particle sizes along the length of the river. The differences or variations are indeed very pronounced as is illustrated in Table 4.1. Bed load particle size data (Tables 4.2 and 4.3) illustrate the variations with time, and hence with the changing flow conditions, and also the variations with distance along the cross-section.

The rationale for using the 1970 bed material data in computions is provided in section 5.2.4.

4.3.2 Suspended Sediment Data

Suspended sediment data were also obtained during the course of the study. These were required in calculations of total load for the study reach. These data are not directly required in the study of bed load transport and are therefore not recorded herein.

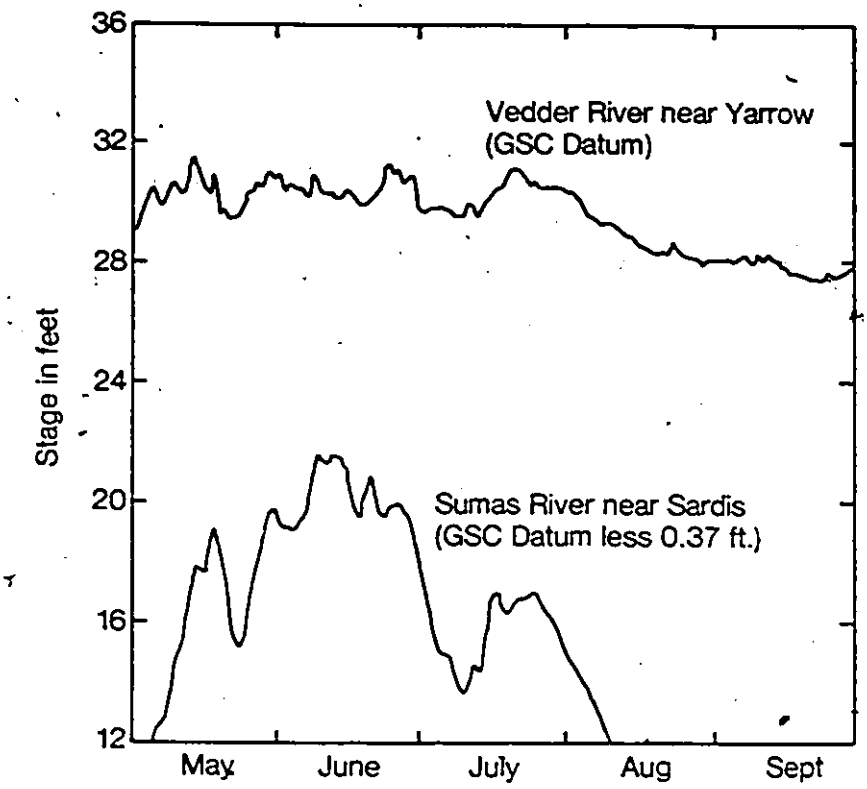

Figure 4.7 a Hydrographs for 1971

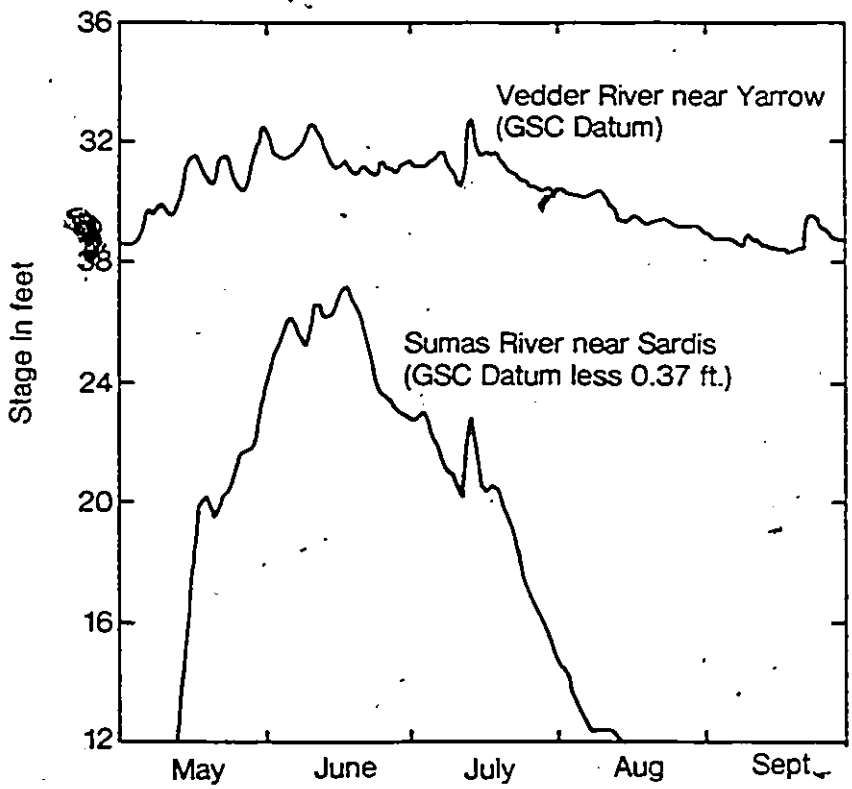

Figure 4.7 b Hydrographs for 1972.

TABLE 4.1 Bed Material Analysis Data, Vedder and Chilliwack Rivers, May 1970

Date	Time	Sampler type	Sample location	Percent finer than indicated size, in millimeters											
				128.0	64.0	32.0	16.0	8.0	4.0	2.0	1.0	0.5	0.25	0.125	0.062
12[illegible]	10:00	Lane	1*					100	98.5	93.5	75.0	29.0	1.0	0.5	0.0
	10:20	Shovel	2		100	61.0	41.0	30.0	24.0	18.0	10.5	5.5	0.5	0.0	0.0
"	11:00	Shovel	3	100	78.0	55.0	40.0	31.0	23.0	17.5	12.5	6.0	1.5	0.5	0.0

1. Vedder River (canal) at Highway 1 Bridge

2. Vedder River near Sumas Prairie Road (about 1000 feet downstream from BCHPA bridge)

3. Chilliwack River at Vedder Crossing

TABLE 4.2 Bed Load Particle Size Analysis Data, Cross-section six, June, 1971

Date	Time	Sampler type	Sample location	Percent finer than indicated size, in millimeters											
				128.0	64.0	32.0	16.0	8.0	4.0	2.0	1.0	0.5	0.25	0.125	0.062
22	1330	VUV	50							100	96.5	75.0	11.0	0.5	0.0
	1355		100			100	95.0	93.0	90.5	87.0	67.5	24.0	2.0	0.0	
	1400		125					100	99.0	96.0	71.0	25.0	2.0	0.0	
	1415		150			100	87.0	79.0	68.0	47.0	17.0	6.5	0.5	0.0	
23	0935	VUV	50								100	91.0	21.0	1.0	0.0
	0955		100				100	91.0	85.0	77.5	52.5	19.0	2.0	0.0	
	1000		120					100	98.5	93.0	65.0	23.0	3.0	0.0	
	1005		140		100	91.5	59.5	39.5	26.5	16.5	7.0	3.0	0.5	0.0	
	1015		160		100	90.5	21.5	4.8	2.1	1.8	1.5	1.0	0.0		
	1030		150		100	89.5	51.5	25.0	12.0	7.0	3.5	0.0			
	1040		130		100	94.0	56.0	49.5	47.5	42.0	23.5	6.0	0.5	0.0	
	1050		170		100	98.0	62.0	21.5	13.5	10.0	7.0	4.5	1.0	0.0	
	1100		140	100	88.5	56.5	28.0	9.5	2.0	0.5	0.0				
	1110		140	100	90.0	59.0	36.0	11.5	2.5	1.0	0.5	0.0			
24	1145	VUV	100					100	97.0	95.0	83.0	42.0	2.5	0.0	
	1155		120						100	98.0	81.0	31.0	1.5	0.0	
	1210		140					100	96.5	90.0	67.0	36.5	4.0	0.5	0.0
	1300		90							100	96.5	70.5	9.0	0.5	0.0
	1305		100					100	99.0	97.5	85.0	40.0	2.5	0.5	0.0
	1315		110					100	99.5	97.5	83.0	33.0	2.0	0.0	
	1320		120							100	97.5	78.0	11.5	1.0	0.0
	1330		130							100	96.5	75.0	11.0	0.5	0.0
	1335		140				100	98.0	92.5	79.0	53.0	25.0	2.5	0.5	0.0
25	0850	VUV	50							100	98.0	85.0	15.0	1.0	0.0
	0915		100						100	98.0	82.5	31.0	2.0	0.0	
	0925		110			100	95.5	95.0	94.0	92.5	81.0	26.0	1.0	0.0	
	0930		120					100	99.5	97.5	78.0	25.0	1.0	0.0	
	0940		130			100	89.5	83.0	78.0	66.0	34.5	10.0	1.0	0.0	
	1025		100				100	99.5	98.5	97.0	82.5	32.5	1.5	0.0	
	1035		120						100	97.5	76.5	22.5	1.5	0.0	

TABLE 4.3 Bed Load Analysis Data, Cross-Section six, May 1972

Date	Time	Sampler type	Sample location	Percent finer than indicated size, in millimeters											
				128.0	64.0	32.0	16.0	8.0	4.0	2.0	1.0	0.5	0.25	0.125	0.062
29	15:52	Basket	125	98.0	80.0	29.0	7.5	3.0	1.0	0.5	0.0				
"	16:16	Basket	112	93.5	67.5	27.0	10.0	6.0	4.0	2.5	1.0	0.0			
"	16:38	Basket	137			100	83.5	30.0	6.0	0.5	0.0				
30	14:00	Basket	200	95.0	65.0	29.0	12.5	5.5	2.0	0.5	0.0				
"	15:00	Basket	137	97.5	77.0	53.0	34.0	17.0	5.0	0.0					
"	15:26	Basket	100	100	90.5	19.0	6.5	1.0	0.5	0.0					

4.4 Discharge Equations

4.4.1 Schoklitsch (1934) Equation

The Schoklitsch equation is described in detail in Section 2.2.1.1. For purposes of computation utilizing this theory, equations 2.4 and 2.5, that is, the formula in English units, is used.

The first step in the computations involves determining the critical discharge, Q_{01}. For this purpose, a slope, S, of 0.0020 ft/ft, as determined in Section 4.2, was used. The effective diameter, D_E, was calculated utilizing the bed material data obtained in 1970 for cross-section six (as shown in Table 4.1) and further utilizing equation 4.1 below.

$$D_E = (\Sigma D \Delta p)/100 \qquad \ldots 4.1$$

From equation 2.5, Q_{01} is determined to be 21.22 cfs/ft. The bed load discharge was computed for a range of values of flow, namely 4, 6, 8, 10, 15, and 20 thousand cfs. Surface breadth values were determined using the 1971 data illustrated in Figure 4.3, and hence the value of Q_1 for each discharge was obtained by dividing the flow (cfs) by the surface breadth (feet). These values were then substituted in equation 2.4 to obtain the values for G_1, the bed load in lb/sec/ft. The details are tabulated in Table 4.5.

4.4.2 Meyer-Peter (1934) Equation

The primary assumption which one must make in utilizing the Meyer-Peter (1934) equation for the computation of gravel-size bed load is that the equation, developed for sand sizes, is applicable. The applicability, or validity of this cannot readily be determined since the experimental work resulting in the equation, was done utilizing only sand sizes. In reality, therefore, the applicability is not present. In practice, however, the equation is occasionally used outside of the range of it's development; the computational results are hence presented here, although, admittedly, with reservation.

The equivalent grain diameter for a mixture is D_{35}, that is, 35 percent of the mixture is finer than D_{35}. From a plot of the bed material sample analysis, the value of D_{35} was determined to be 11.5 mm or 0.0377 ft.

The computations are then carried out utilizing equation 2.8. The computational details are shown in Table 4.6.

4.5 Tractive Force Equations

4.5.1 Meyer-Peter and Muller (1948) Equation

The depth to width ratio for the Vedder River at cross-section six is very small, as could be readily discerned from Figures 4.3 and 4.5. Consequently, Q closely approximates Q_B so that $Q_B/Q = 1$.

A further simplification of the equation can be made with respect to form roughness. It was observed during the field experimental work that, for the most part, the bed load transport occurred as sheet flow and that the bed forms were not pronounced. As a result, the simplification can be made with respect to the terms K_B and K_G; that is, $K_B = K_G$ and the ratio of K_B/K_G becomes one. As a result Q_K also becomes equal to one. K_B is the Strickler roughness coefficient for the bed and K_G the so-called particle or grain roughness.

With these simplifications, therefore, the Meyer-Peter and Muller equation 2.16 can be utilized for the bed load transport calculations.

In equation 2.16, the effective diameter, D_E, of the bed material particle size is calculated utilizing equation 4.1. Table 4.4 illustrates this computation and the resulting value of the effective diameter, $D_E = 0.0838$ ft.

The results of the computation using the Meyer-Peter and Muller equation are illustrated in Table 4.7.

TABLE 4.4 Sample Calculation of Effective Diameter

Size Range mm	Δp %	D mm	DΔp	D ft
64.000 - 32.000	39.0	48.0	1870	0.157
32.000 - 16.000	20.0	24.0	480	.0787
16.000 - 8.000	11.0	12.0	132	.0394
8.000 - 4.000	6.0	6.0	36.0	.0197
4.000 - 2.000	6.0	3.0	18.0	.00984
2.000 - 1.000	7.5	1.50	11.3	.00492
1.000 - 0.500	5.0	0.750	3.75	.00246
0.500 - 0.250	5.0	0.375	1.88	.00123
0.250 - 0.125	0.5	0.188	0.094	.000615
	100.0		2555.	

Notes:
1. The effective diameter, D_E = 2555/100 = 25.55 mm = 0.0838 ft.
2. From the particle size curve, 52.5 percent of the material was indicated to be finer than 0.0838 ft.
3. The mean diameter, D_{50}, as determined from a plot of the data shown in table 4.2 is 23.5 mm or 0.0771 ft.
4. Other values, D_{35} = 0.0377 ft. and D_{65} = 0.1148 ft.

TABLE 4.5 Bed Load Calculation Results, Schoklitsch (1934) Equation

Q cfs	b_w feet	Q_1 cfs/ft	G_1 lb/sec/ft.
4000	255	15.7	(-.635)
6000	273	22.0	.0862
8000	287	27.9	.764
10000	298	33.6	1.42
15000	315	47.6	3.03
20000	330	60.6	4.53

TABLE 4.6 Bed Load Calculation Results, Meyer-Peter (1934) Equation.

Q cfs	Q_{B1} cfs/ft	G_1 16/sec/ft.
4,000	15.7	.0405
6,000	22.0	.119
8,000	27.9	.205
10,000	33.6	.295
15,000	47.6	.534
20,000	60.6	.767

4.5.2 Straub (1935) Equation

As with the other equations, a number of constants and relationships must first be determined for computations by the Straub equation. In these calculations, equation 2.19 as expressed in Section 2.2.2.2 is utilized.

In equation 2.19, the tractive force T is considered to be equal to γHS; this, of course, is acceptable for this purpose as the river is considered to be a wide shallow river.

The calculation of T_o, the critical tractive force, for this case is more difficult since the tabulated values for T_o (Table 2.1) are not provided for the range of particle sizes encountered at cross-section six.

The "sediment characteristic", ψ, can be determined from equation 2.18 in which the effective diameter, D, is considered to be the mean diameter. D_{50} as determined from a plot of the data shown in Table 4.1 is 23.5 mm or 0.0771 feet. ψ is calculated to be 10,400 from equation 2.18 and using a value of 23.5 mm for D_{50}.

Since the tabulated critical tractive force values for the Straub equation were outside of the range of conditions encountered on the Vedder River, it became necessary to calculate the value of T_o by some other means. It was felt that the work of Shields would be reasonably applicable since the work of Shields also fell into the general category of "tractive force equations". Hence, Figure 4.8 illustrates the comparison of critical tractive force for a wide range of effective particle size diameters. It should be noted that the T_o for D = 0.5 mm was calculated from $T_o = 0.315D^{.663}$; for D = 1, 2 and 4, from $T_o = 16.8D^{1.262}$; and for D = 10, 15 and 23,5 mm, from $T_o = 6.18D$. These relationships represent

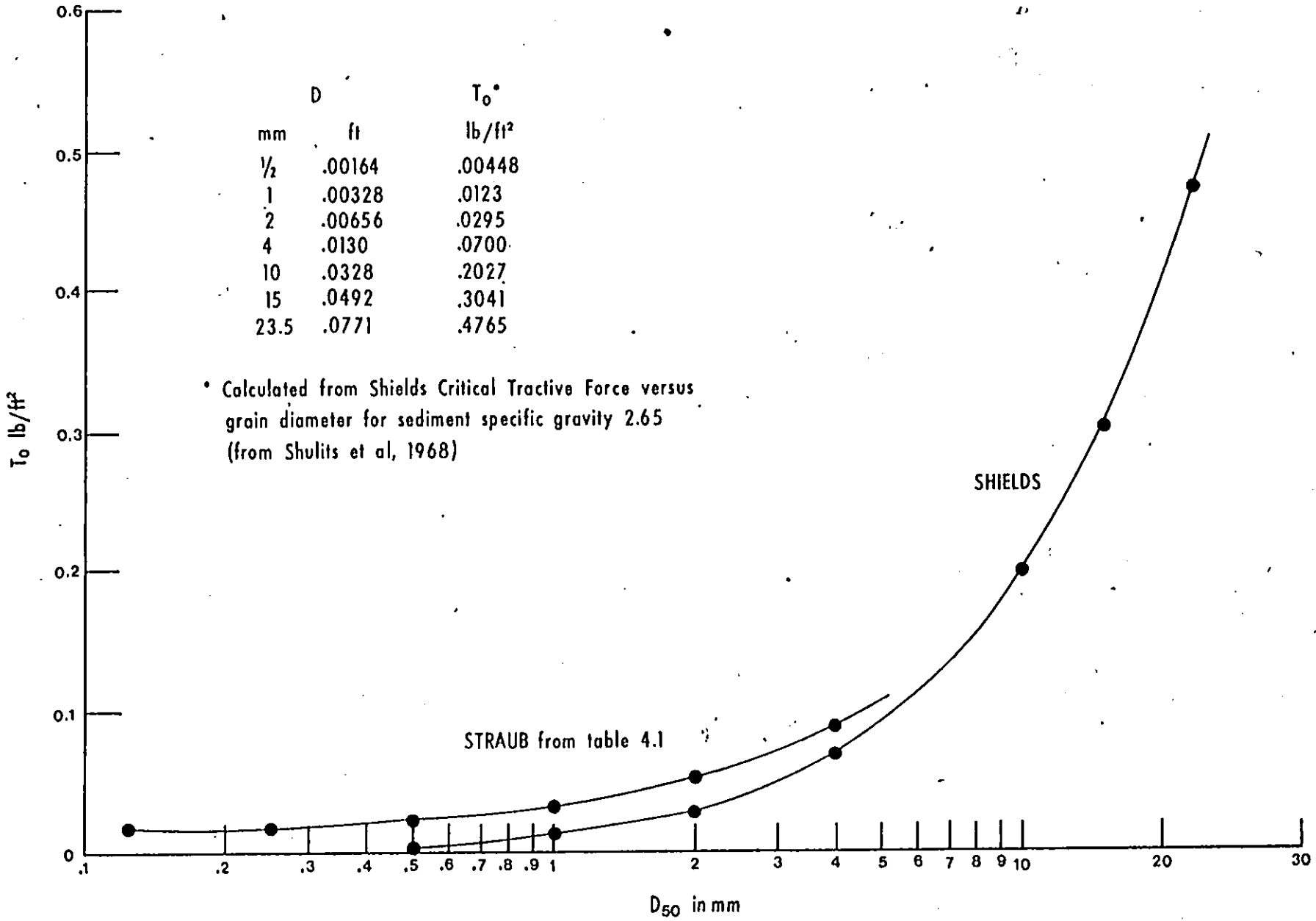

D		T_o*
mm	ft	lb/ft²
½	.00164	.00448
1	.00328	.0123
2	.00656	.0295
4	.0130	.0700
10	.0328	.2027
15	.0492	.3041
23.5	.0771	.4765

* Calculated from Shields Critical Tractive Force versus grain diameter for sediment specific gravity 2.65 (from Shulits et al, 1968)

FIGURE 4.8 Comparison of Critical Tractive Force Derivations

approximations of the Shields diagram as outlined by Shulits and Hill in 1968. The result of this procedure is that an estimate of T_o = 0.476 lb/ft^2 is obtained for use in the Straub equation.

Utilizing the above parameters, therefore, computations were performed with equation 2.19; the results of which are illustrated in Table 4.8.

4.6 Relative Roughness Equations

In the relative roughness equations, the parameter D/H, or grain diameter/depth of flow, is utilized. The ratio D/H is, of course, the designation for relative roughness.

4.6.1 Rottner (1959) Equation

Equation 2.22 is utilized for computing the bed load, the equation being that of Rottner. The theoretical discussion with respect to this equation is presented in Section 2.2.3.1. The results are shown in Table 4.9 below. For these purposes D is the mean diameter of the sediment mixture, previously shown to be 0.0771 ft.

4.7 Equation Based on Statistical Considerations

Section 2.2.4 describes very briefly the Einstein (1950) equation and the Modified Einstein procedure (1955). These descriptions are indeed so brief that they should not be used without consultation of the references indicated; the brief treatment is shown in Section 2.2.4 primarily to illustrate the complexity of the procedures.

4.7.1 Modified Einstein Procedure (1955)

The simplified methods "...can be applied without an extensive knowledge of the developments leading to the modified Einstein procedure and the assumptions involved in the procedure..." (Colby, et al, 1961).

TABLE 4.7 Bed Load Calculation Results, Meyer-Peter and Muller (1948) Equation.

Q cfs	H ft.	G_1 lb/sec/ft.
4,000	3.40	.610
6,000	3.95	.855
8,000	4.40	1.08
10,000	4.75	1.26
15,000	5.50	1.68
20,000	6.10	2.05

TABLE 4.8 Bed Load Calculation Results, Straub (1935) Equation.

Q cfs	H ft.	G_1 lb/sec/ft.
4,000	3.40	1.95
6,000	3.95	2.90
8,000	4.40	3.81
10,000	4,75	4.60
15,000	5.50	6.53
20,000	6.10	8.31

TABLE 4.9 Bed Load Calculation Results, Rottner (1959) Equation.

Q cfs	H ft.	Q cfs/ft	G_i lbs/sec/ft
4,000	3.40	15.7	.0005
6,000	3.95	22.0	.0516
8,000	4.40	27.9	.156
10,000	4.75	33.6	.385
15,000	5.50	47.6	1.44
20,000	6.10	60.6	3.01

In spite of these assurances, however, the simplified methods as outlined by Colby and Hubbell could not be readily applied. The magnitude of some of the measured parameters used in the calculations (for example, particle size) were well outside of the range of the monogram scales developed for this purpose. As a result, it was necessary to resort to the lengthy and laborious procedures of Einstein (1950).

4.7.2 Einstein (1950) Equation

Shulits and Hill, 1968, provided an explanation or clarification of each of the some 30 steps in the Einstein procedure. The work of Hollingshead (1968) was also found to be of particular assistance in the organization and performance of the computations shown below.

Steps one to six of the Einstein procedure involve the hydraulic calculations for channels in general.

The effective slope, as determined in Section 4.2, is taken as 0.0020. The average values of the channel geometry for the study reach were readily obtained from Figures 4.2 to 4.5 inclusive. Although the methods used in determining values of slope and hydrualic geometry are different than those of Einstein, the results are of no appreciable difference.

For purpose of comparison of computational techniques, the grain size composition of the bed is considered to be as outlined in Table 4.4. The particle size which enters the equation of transport, D_{35} = 0.0377 ft, and the size characteristic for friction is D_{65} = 0.115 ft.

In performing the hydraulic calculations for a channel without bank friction, values of the hydraulic radius with respect to the grain are first assumed. These are given in column one of Table 4.10. The friction velocities, shown in

TABLE 4.10 Hydraulic Calculations for a Channel without Bank Friction

(1)	(2)	(3)	(4)	(5)	(6)	(7)	(8)	(9)	(10)	(11)
R_b^I ft	V_*^I ft/sec	V_m ft/sec	Ψ_1	V_m/V_*^{II}	V_*^{II} ft/sec	R_b^{II} ft	R_b ft	A ft	b_w ft	Q cfs
1.2	.278	3.37	25.8	5.94	.567	4.99	6.19	690	231	2200
1.6	.321	4.12	19.3	6.61	.623	6.03	7.63	810	248	3300
2.0	.359	4.81	15.5	7.25	.663	6.83	8.83	920	260	4430
2.5	.401	5.59	12.4	7.94	.704	7.70	10.2	1030	272	5990
3.0	.439	6.32	10.3	8.55	.739	8.48	11.5	1140	283	7550
3.5	.475	7.03	8.83	9.12	.771	9.23	12.7	1270	295	9500
4.0	.508	7.68	7.73	9.59	.801	9.96	14.0	1330	303	11200
4.5	.538	8.29	6.87	10.1	.821	10.5	15.0	1410	310	12900
5.0	.567	8.89	6.18	10.6	.839	10.9	15.9	1480	317	14800
5.5	.595	9.47	5.62	11.1	.853	11.3	16.8	1530	322	16900
6.0	.622	10.0	5.15	11.5	.870	11.8	17.8	1630	329	18600

column two of this table are calculated using

$$V_*^I = (SR_b^I g)^{1/2} \qquad ...4.2$$

in which S = 0.0020 and g = 32.2 ft/sec^2.

The next steps require the determination of the thickness of the laminar sublayer $\delta = 11.6\omega/V_*$ in order to obtain a correction allowing for boundary conditions and thereby to calculate the apparent roughness. Since $k_s = D_{65} = 0.115$ ft., the values of k/δ are large and this makes x = 1.0 in all cases. The apparent roughness $\Delta = k_s/x$ is therefore constant and is equal to 0.115 ft.

The average flow velocity, V_m, is calculated using

$$V_m/V_*^I = 5.75 \log_{10} (12.27\ R_b^I\ x/k_s) \qquad ...4.3$$

The values of columns one and two (Table 4.10) are used and the result is given in column three.

For the determination of the friction contribution of the channel irregularities, the parameters ψ' is calculated from

$$\psi' = (s_s - 1)D_{35}/R_b^I S \qquad ...4.4$$

For this calculation, D_{35} = 0.0377 ft., S = 0.0020 and s_s = 2.64. The results of equation 4.4 are shown in column four of Table 4.10. When values of ψ' are known, values of Vm/V_*'' are then obtained from Einstein's figure 5 (friction V_*'' due to channel irregularities). These results are shown in column five. The value for V_*'', as shown in column six, is then calculated from columns three and five.

In column seven, R_b^{II} is calculated from

$$R_b^{II} = V_*''^2 /Sg \qquad ...4.5$$

in which S = .0020 and g = 32.2 ft/sec. The two components R_b^I and R_b^{II} are usually the only components of the hydraulic radius R_b pertaining to the bed and are

therefore added directly and entered in column eight. For the values of V_m, the cross-sectional area, A, the channel width, b_w, and the discharge, Q are then determined from Figures 4.2, 4.3 and 4.4, and entered in columns nine, ten and eleven. The average section rating curve need not necessarily be constructed and was therefore not used.

Additional calculations for bank friction were not made since the channel was relatively wide and further since it was considered that the banks consisted of similar material to the bed.

Table 4.11 shows the further step by step calculations for determining bed load discharge. In this table, the representative grain sizes, which are the geometric mean of each size range as found in Table 4.4, are presented in column (1). The fraction by weight for each range, of the total of the bed material samples i_b is given in column (2). The values of R_b^1 from 1.2 to 6.0 are given in column (3); these values correspond to calculated discharges ranging from 2200 to 18600 cfs.

With this basis, therefore, we get to step 25 of the procedure. This step involves the calculation of intensity of shear, ψ; this is performed utilizing the following equation;

$$\psi = (s_s - 1)\, D/R_b^1\, S \qquad \ldots 4.6$$

In this case $s_s = 2.64$, $S = 0.0020$ and D and R_b^1 are obtained from columns (1) and (3) of Table 4.11. Values of ψ are entered in column (4).

The reference grain size X is the smallest of the grain sizes in a given bed which is fully affected by the turbulent flow. For rough beds, $\Delta > 1.80\delta$, $X = 0.77\Delta$ and for smooth beds $\Delta > 1.80\delta$, $X = 1.39\delta$, where $S = D_{65}/x$ and $\Delta = 11.6/V_*^1$ and further where x is the parameter for transition smooth-rough, determined from Einstein's Figure 4. In this case, the $\Delta/\delta \gg 1.80$, therefore $X = 0.77 \times 0.115 = 0.0886$. (Note Δ was calculated for use in equation 4.3). The values for D/X could

therefore be calculated and entered in column (5). Then, from Einstein's figure 7 of ξ vs D/X, values of ξ are obtained and entered in column (6). For purposes of extrapolating for values of D/X that were less than 0.1, it was assumed that the D/X vs ξ relation was logarithmically linear for values of D/X< 0.1. The relationship obtained was log D/X = -2.2303 log ξ - 0.4285.

From Einstein's figure 8, a plot of y vs k_s/δ it is noted that for values of $k_s/\delta>4$, y is constant at a value of 0.53. Since this case k_s/δ is large, y = 0.53 in all cases. The next parameter β_x is calculated from

$$\beta_x = \log_{10}(10.6\ x/\delta) \qquad ...4.7$$

and is 0.912 with x = 0.0886 and $\Delta = D_{65}$ = 0.115 feet. The parameter $\beta = \log_{10}$ (10.6) = 1.025 is divided by β_x = 0.912 and squared to give β/β_x = 1.26. The parameter ψ_* is calculated from

$$\psi = \xi y(\beta/\beta_x)^2\psi \qquad ...4.8$$

and the values are given in column (7). Equation 4.8 is simplified to $\psi_* \simeq$ 0.668 $\xi\psi$ for these calculations.

From Einstein's figure 10, essentially a graph of ψ_* vs ϕ_*, values of ϕ_* were then determined and entered in column eight.

The bed load rate $i_B g_s$ is calculated from:

$$i_B g_s = \phi_* i_b \rho_s g^{3/2} (s_s - 1)^{1/2} D^{3/2} \qquad ...4.9$$

in which ρ_s = 2.64 x 1.94 = 5.12, $g^{3/2}$ = 185 and $(s_s - 1)^{1/2}$ = 1.28 with ϕ_*, i_b and D from columns (8), (2) and (1) of Table 4.11

Steps 35 to 42 of the Einstein procedure involve the calculation of the suspended load of the particle sizes for which the bedload function exists. Since the results being computed and compared are those of bed load discharge only, it was not necessary to go through the computation of these steps.

TABLE 4.11 Calculations for Determining Bed Load Discharge (Einstein, 1950)

(1) D ft	(2) i_b o/o	(3) R'_b ft	(4) ψ	(5) D/X	(6) ξ	(7) ψ_*	(8) ϕ_*	(9) $i_b g_s$ lbs/ft/sec
0.157	39.0	1.2	107.283	1.77	1.00	71.665	—	—
		1.6	80.462			53.749	—	—
		2.0	64.370			42.999	—	—
		2.5	51.496			34.399	—	—
		3.0	42.913			28.666	—	—
		3.5	36.783			24.571	.00036	.011
		4.0	32.185			21.500	.00125	.037
		4.5	28.609			19.111	.00320	.094
		5.0	25.748			17.200	.00700	.206
		5.5	23.407			15.636	.0135	.397
		6.0	21.457			14.333	.0220	.647
0.0787	20.0	1.2	53.778	0.888	1.22	43.827	—	—
		1.6	40.334			32.871	—	—
		2.0	32.267			26.296	.00014	.007
		2.5	25.814			21.037	.00150	.008
		3.0	21.511			17.531	.00640	.034
		3.5	18.438			15.026	.0170	.091
		4.0	16.133			13.148	.0340	.182
		4.5	14.341			11.687	.0540	.289
		5.0	12.907			10.519	.0740	.396
		5.5	11.733			9.562	.0950	.508
		6.0	10.756			8.766	.120	.642
0.0394	11.0	1.2	26.923	0.445	5.40	97.117	—	—
		1.6	20.192			67.441	—	—
		2.0	16.154			58.271	—	—
		2.5	12.923			46.616	—	—
		3.0	10.769			38.846	—	—
		3.5	9.231			33.298	—	—
		4.0	8.077			29.135	—	—
		4.5	7.180			25.900	.00020	.000209
		5.0	6.462			23.310	.00058	.000605
		5.5	5.874			21.189	.00140	.00146
		6.0	5.385			19.425	.00300	.00312

TABLE 4.11 continued...

(1) D ft	(2) i_b o/o	(3) R_b^1 ft	(4) Ψ	(5) D/X	(6) ξ	(7) Ψ_*	(8) ϕ_*	(9) $i_b q_s$ lbs/ft/sec
0.0197	6.0	1.2	13.462	0.222	26.0	233.808	—	—
		1.6	10.096			175.347	—	—
		2.0	8.077			140.281	—	—
		2.5	6.462			112.232	—	—
		3.0	5.385			93.527	—	—
		3.5	4.615			80.153	—	—
		4.0	4.038			70.132	—	—
		4.5	3.590			62.351	—	—
		5.0	3.231			56.116	—	—
		5.5	2.937			51.010	—	—
		6.0	2.692			46.755	—	—
0.0984	6.0	1.2	6.724	0.111	122	547.979	—	—
		1.6	5.043			410.984	—	—
		2.0	4.034			328.755	—	—
		2.5	3.228			263.069	—	—
		3.0	2.690			219.224	—	—
		3.5	2.305			187.848	—	—
		4.0	2.017			164.377	—	—
		4.5	1.793			146.122	—	—
		5.0	1.614			131.535	—	—
		5.5	1.467			119.555	—	—
		6.0	1.335			108.797	—	—
0.00492	7.5	1.2	3.362	0.0555	572	1284.607	—	—
		1.6	2.521			963.264	—	—
		2.0	2.017			770.688	—	—
		2.5	1.614			616.703	—	—
		3.0	1.345			513.919	—	—
		3.5	1.153			440.557	—	—
		4.0	1.009			385.535	—	—
		4.5	.897			342.740	—	—
		5.0	.807			308.351	—	—
		5.5	.734			280.458	—	—
		6.0	.672			256.769	—	—

The values of $i_{B}g_{s}$ found in Table 4.11 were therefore summed for each stage and the results presented in Table 4.12.

TABLE 4.12 Bed Load Discharge by Einstein Method

R_b^1 ft	R_b ft	Q cfs	$\Sigma i_b G_s = G_1$ lbs/ft/sec	b_w ft
1.2	6.19	2200	—	231
1.6	7.63	3300	—	248
2.0	8.83	4430	.00014	260
2.5	10.2	5990	.00150	272
3.0	11.5	7550	.00640	283
3.5	12.7	9500	.01736	295
4.0	14.0	11200	.03525	303
4.5	15.0	12900	.05740	310
5.0	15.9	14800	.08158	317
5.5	16.8	16900	.10990	322
6.0	17.8	18600	.14500	329

CHAPTER 5

DATA ANALYSIS AND RESULTS

5.1 Hydrophone Measurements

The extent of hydrophone observations and other field observations made in 1971 and 1972 are illustrated in a data summary in figure 5.1.

The field procedures developed for hydrophone observations are outlined in Section 3.1.4. Initially, it was intended to do field measurements in both 1971 and 1972. The hydrophone instrumentation, however, was not available in time for the 1971 field season.

As noted in Section 3.1.4, initial experimental data were obtained both at various depths and verticals within the cross-section and at various frequency ranges of the audible sound spectrum. An effort was also made to ensure that the operator could distinguish between unwanted sounds and those sounds created by particle movement.

Some hydrophone observations and analyses of observations for the Vedder River were first reported in May 1973, at the Nineth Canadian Hydrology Symposium (Tywoniuk and Warnock, 1973). Although quite a lot of acoustical information was obtained in 1972 (274 data points), only part of these data were then illustrated. These data are further illustrated herein and additional data and analyses for 1972 are summarized in Appendix B. Table 5.1 summarizes the hydrophone measurements obtained at cross-section six in 1972.

The cross-sectional sound intensities (detailed) for May 31, 1972 are illustrated in Figure 5.2. Data for other dates are similarily illustrated in Appendix B. The sound frequency intervals illustrated are 100 to 200, 200-400, 400-800 and 800-1600 cycles per second. For each of these intervals and for 10 seconds

TABLE 5.1 1972 Hydrophone Measurements at Cross-section Six

Date	Time	Number of Sampling Points	Stage (GSC)	Flow* (cfs)
May 26	8:20- 9:30	17	30.30	5,500
May 29	13:20-14:30	13	31.70	12,000
May 31	8:35-11:15	45	32.11	11,600
June 2	8:45-10:00	29	31.54	8,280
June 7	13:25-14:25	22	31.98	10,300
June 8	13:45-15:00	20	32.02	10,300
June 12	16:30-17:50	72	31.90	8,620
June 15	9:50-10:45	56	31.20	6,300

* Flow recorded at Vedder Crossing Station and adjusted by a one hour time lag.

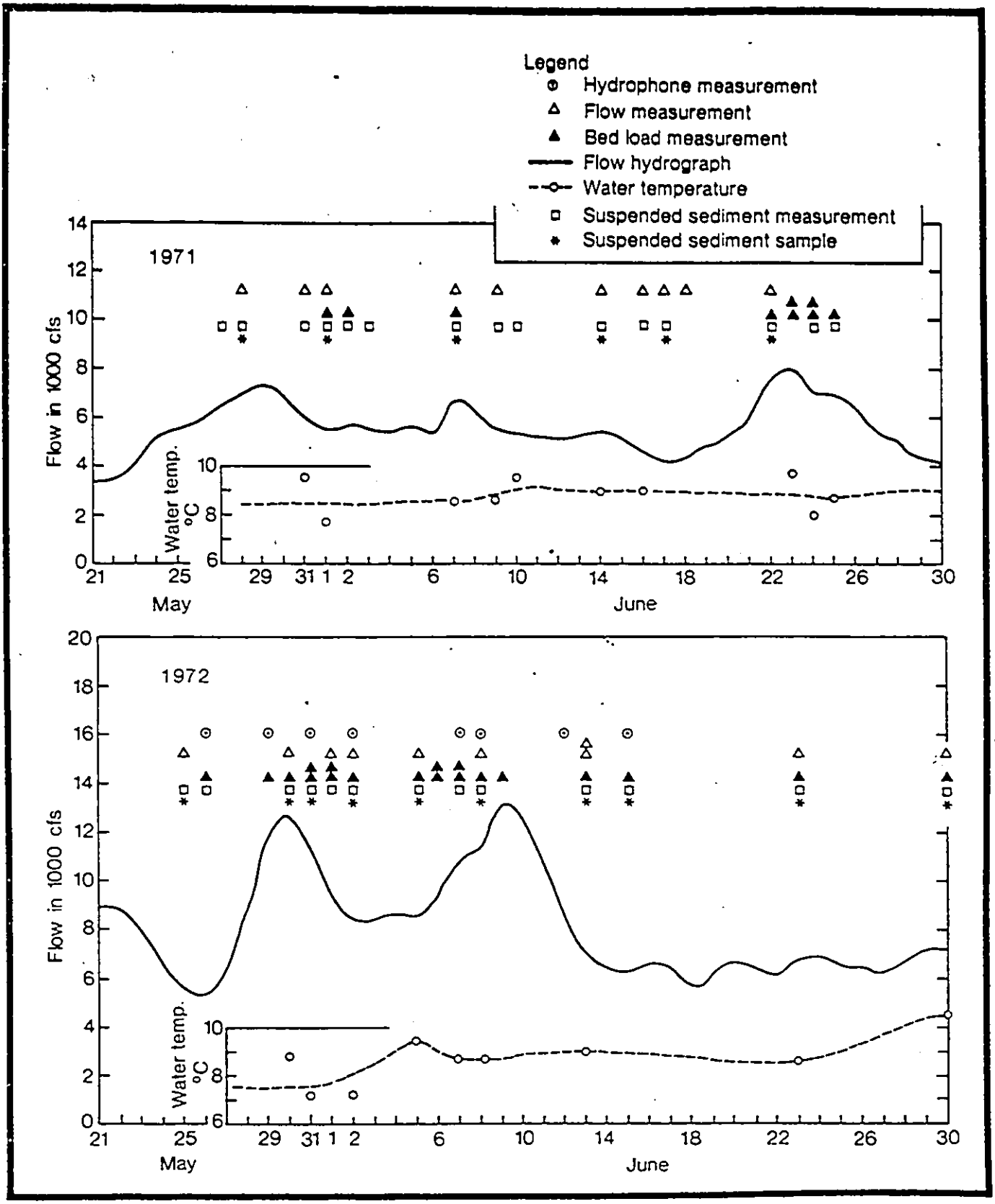

Figure 5.1 1971 and 1972 Data summary (cross-section six).

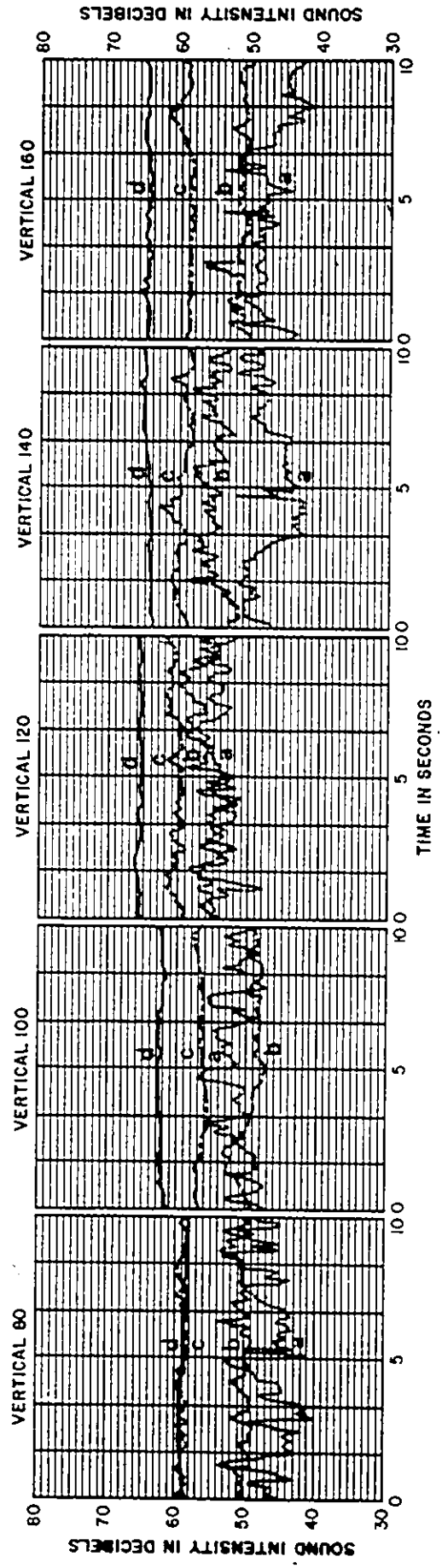

FIGURE 6.2 CROSS-SECTIONAL SOUND INTENSITIES (DETAILED), MAY 31, 1972

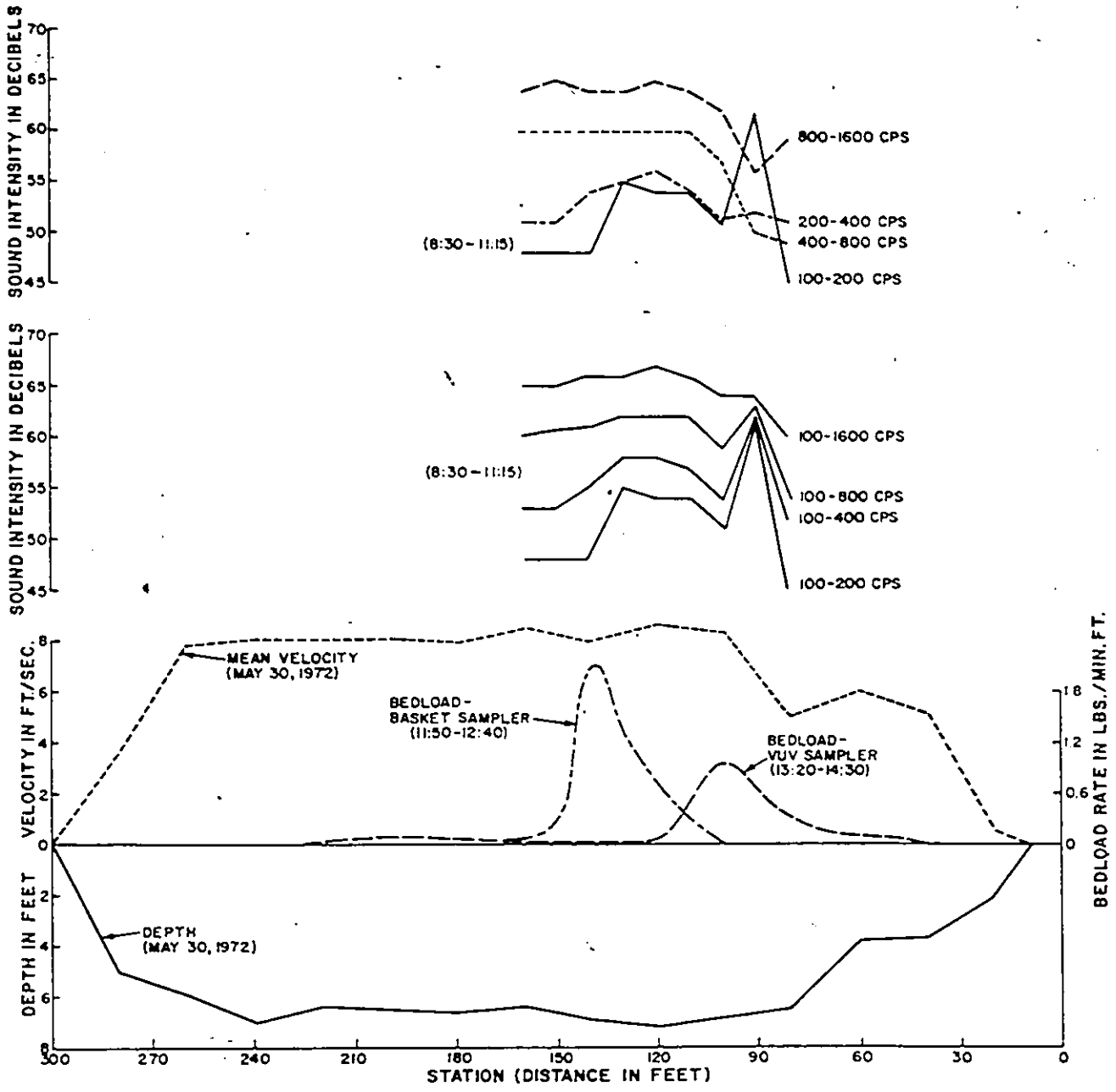

FIGURE 5.3 CROSS-SECTIONAL SOUND INTENSITIES, BEDLOAD RATES, VELOCITIES AND DEPTHS, MAY 30 AND 31, 1972.

ALL DATA ARE FOR MAY 31, 1972, EXCEPT AS SHOWN

duration, data are reported for verticals 80, 100, 120, 140 and 160 of the cross-section which is illustrated in Figure 5.3. It should be noted that the low frequency interval sounds exhibit the greatest variations. The higher frequency ranges, 800-1600 cycles per second, exhibit the least variations.

Additional information on cross-sectional intensities (averaged) as related to bed load rates, velocities and depths is shown in Figure 5.3. This figure illustrates the difficulties involved in obtaining erratic type field data. For example, the bed load rate data were obtained approximately two hours apart, the first time with the basket sampler and subsequently with a half-size VUV sampler. The figure illustrates that there was considerable change in magnitude as well as in location within the cross-section of the bed load rate. The sound intensity data reflect this erratic nature to some extent as well. This is particularly well shown for sound intensities for the ranges 100-200, 200-400, 400-800 and 800-1600 cycles per second, shown at the top of the figure. It is apparent that part of the variability in sound intensity must be the result of the variability in the bed load movement. The other sound intensity data as shown in the middle of the figure, illustrate the same data shown on top of the page except accumulated so as to be representative of 100-200, 100-400, 100-800 and 100-1600 cycles per second. Other bed load data obtained at this cross section illustrated that the bed load moves in a relatively narrow strip between about verticals 70 and 150.

Additional depth/velocity/sound intensity relations are shown in Figure 5.4 for verticals 125 and 225 for June 12, 1972 and June 15, 1972. It should be noted that while the velocity profiles are not particularly different between the two days, the sound intensity profiles do vary considerably. The June 15, 1972 sound intensity data are readily explainable; the relatively high sound intensity at

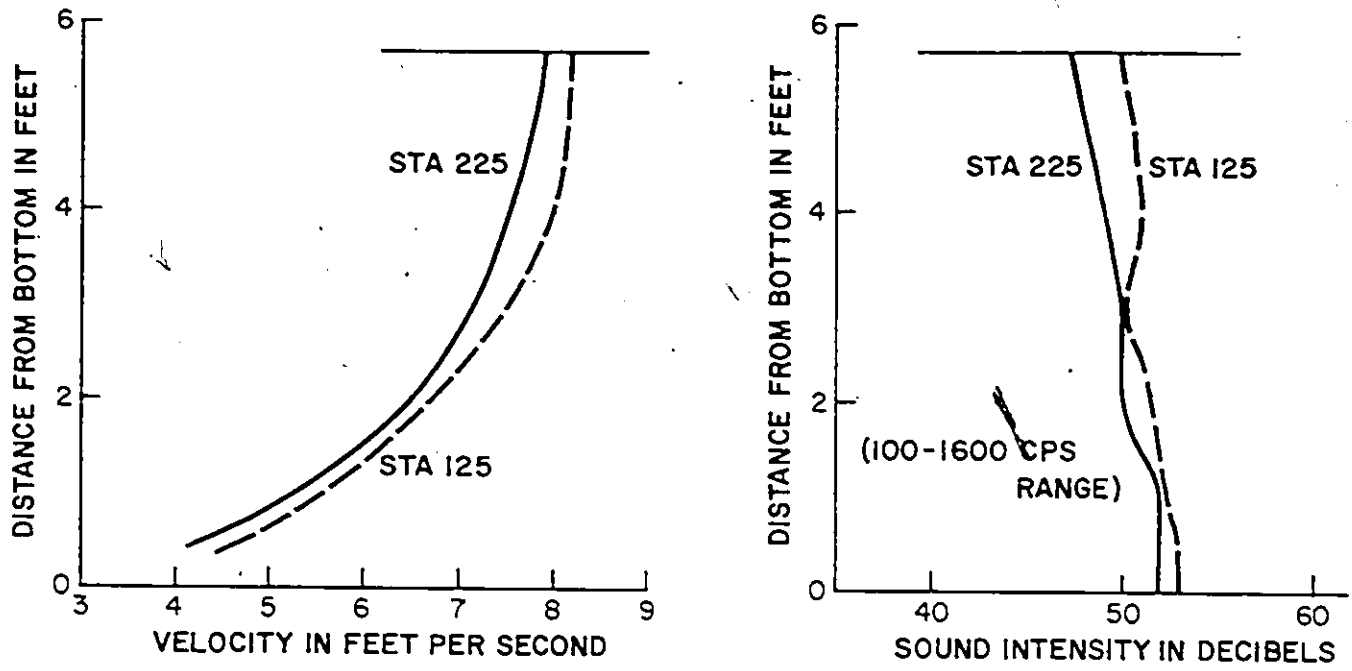

FIGURE 5.4a DEPTH-VELOCITY-SOUND INTENSITY RELATIONS
JUNE 12, 1972 (FLOW = 8,500 CFS)

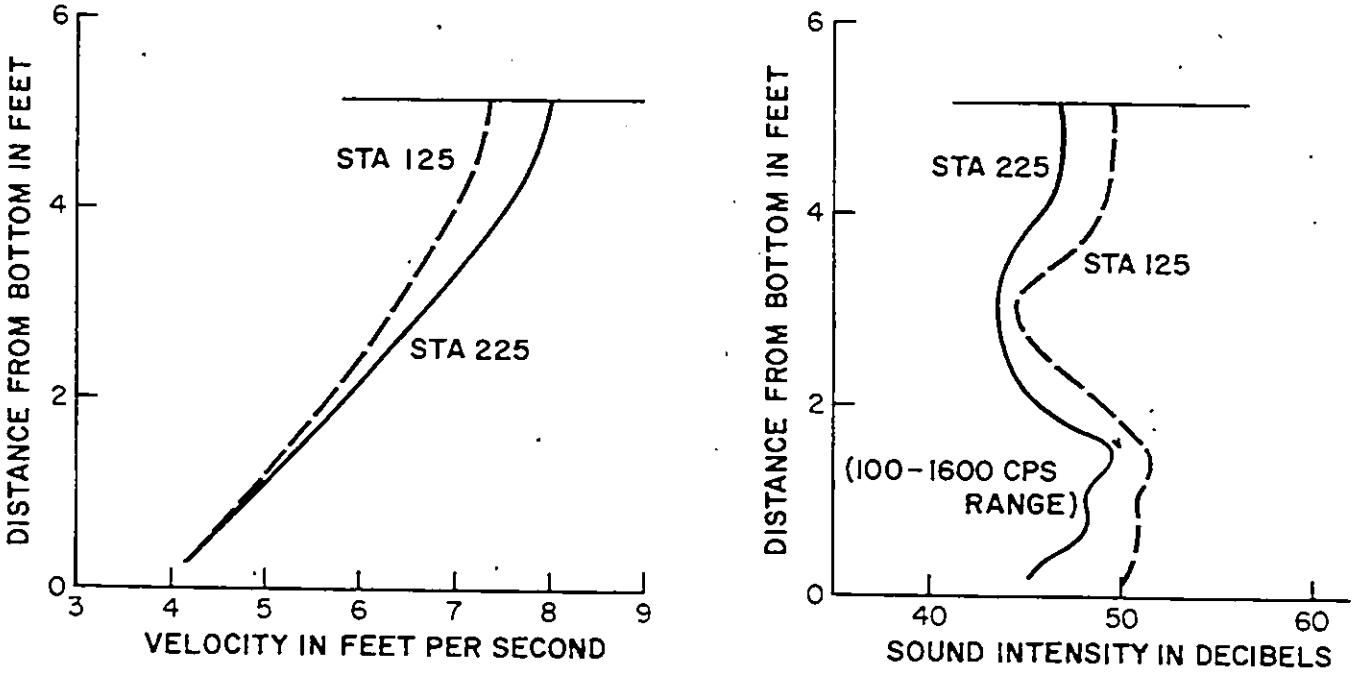

FIGURE 5.4b DEPTH-VELOCITY-SOUND INTENSITY RELATIONS
JUNE 15, 1972 (FLOW = 6,380 CFS)

station 125 is likely indicative of bed load movement at the station. Station 225 would be roughly the same if one assumed that the sound intensity was directly related to bed load movement. However, because direct sampling results indicated that little bed load movement occurs at station 225 even at high flows, these data illustrate that there are parameters other than bed load discharge which have made the sound intensity at station 225 approximately equal to that at station 125.

Hydrophone data, in the form obtained in the field for various stations and for various depths are further shown in Appendix B. These are being included to further illustrate the type of sound data that were obtained. It is readily evident from this data and from Figures 5.2 and 5.3 that, while the data are quantifiable, there is not an obvious direct relationship between sound level intensity (decibels) and bed load transport.

To further illustrate the relationships among sound intensity levels, bed-load discharge and velocity, and the cross-sectional variance of these parameters, these data are further summarized in Appendix B. A tabular summary is shown, followed by graphical illustrations of bed load data versus sound intensity, (for field and adjusted data), and of bottom velocity versus sound intensity. The designation "field" refers to the hydrophone data obtained directly from field observations; "background" refers to laboratory data shown 3.4 and is meant to represent the "velocity" component of sound; "adjusted" refers to the difference between field and background as calculated utilizing equation 2.31. The graphical illustrations further illustrate the lack of correlation and that the velocity effects around the hydrophone can be significant.

The instrumentation developed had a number of very useful features. The sound intensity could be continuously recorded and the instrumentation was designed to enable the observer to listen to the acoustical information being

collected. The system was readily portable and provided for data acquisition in terms of decibels, a universally accepted unit for sound intensity measurement, instead of in microamperes, volts, etc., which are electronic rather than sound parameters, and which have been used in the past by some researchers.

The hydrophone has been proven to be useful in the qualitative assessment sense; in the use to determine when and where the bed load is moving. This qualitative assessment can be particularly useful as it provides a means of determining the "critical" discharge information required in many theoretical and semi-theoretical equations for prediction of bed load discharge.

5.2 Direct Measurement Results

The sampling of bed load is carried out by means of bed load samplers with the assistance of a motorized reel in a cable car. The details of the bed load sampling equipment are outlined in Section 3.2.1.2. Additionally to utilizing samplers, the volumetric measurement methods are also often considered to be a direct measurement technique. The results of both are discussed herein.

5.2.1 Bed Load Discharge Results

Only a small number of bed load measurements were obtained in 1971. This was due to two factors: a considerable effort was made to set up the facilities and to get them operational and, secondly, May and June was a relatively low flow period. In spite of these drawbacks, a total of 94 bed load samples were obtained, a number of which were of the "little or no recovery" type.

In May and June, 1972, 158 bed load samples were obtained at cross-section six. The freshet flows were comparatively higher in 1972 with the result that more bed load was moving and a greater number of measurements was possible.

During both years, it was observed that the Vedder River exhibited flat-bed, sheet-type transport. As a result it was not necessary to take into account the possible effects of bed forms on bed load measurement results.

The bed load sampling procedures are outlined in section 3.2.2.2. In computing the bed load discharge, the sample data (ordinate) was plotted against location (abscissa). Cross-sectional interpolation was then done graphically (using the mean value of bed load discharge at those verticals where several samples were obtained) to define the cross-sectional discharge. The area outlined by the curve was then obtained and this area was multiplied by the appropriate factors to give led load discharge in tons per day, and subsequently lb/sec/ft. Finally, these values were multiplied by three, an adjustment to account for sampler efficiency and for material passing through the sampler. The data and computational details are illustrated in tabular and graphical form in Appendix B.

The bed load measurement results for 1971 and 1972 are summarized in Table 5.2. As noted in the table, the bed load sampling was conducted with the half size VUV and full basket samplers with the latter proving to be more suitable for the high flow conditions. The measured bed load discharges were correlated to flow with the following results: for the half size VUV sampler (the bed load discharge in tons per day, Y, and the flow in 1,000 cfs, X), $Y = 0.211\ X^{2.16}$ and for the full size basket sampler, $Y = (4.43)\ 10^{-6}\ X^{6.89}$. The correlation coefficients were 68 and 33 percent respectively (Tywoniuk et al., 1973). Figure 5.5 further illustrates the relationship between flows and bed load discharges.

It should perhaps be noted that an earlier regression analysis using only the 1971 half size VUV data was performed (Tywoniuk, 1972) with the resulting relationship being $Y = (16.116)10^{-10}\ X^{2.689}$, and coefficient of correlation of 0.73. It was cautioned, however, "...that the above relationships, although based on a sound analysis technique, can only be treated as very approximate because of the small number of measurements taken for a narrow range of flows".

TABLE 5.2 Summary of Bed Load Measurements at Cross-section Six, 1971 and 1972

Date	Time	Flow cfs*	Area sq. ft.	Mean Velocity fps	Number of Samples	Sampler Type	Bed Load Tons/day**
1971							
June 1	08:45-10:20	5400	1010	5.35	5	Basket	No recovery
June 2	10:20-11:00	5690	1020	5.58	9	Basket	No recovery
June 7	12:50-13:25	6710	1140	5.89	9	Basket	No recovery
June 22	13:30-15:05	7640	1170	6.53	9	1/2 VUV	41.4
June 23	09:35-11:05	8040	1210	6.64	12	1/2 VUV	54.3
June 23	12:50-16:00	8040	1210	6.64	13	Basket	9.3
June 24	08:30-09:35	6990	1140	6.13	5	Basket	No recovery
June 24	11:40-13:35	6990	1130	6.19	17	1/2 VUV	29.1
June 25	08:50-10:45	6970	1150	6.06	17	1/2 VUV	43.5
1972							
May 26	10:05-10:50	5210	975	5.34	6	1/2 VUV	9.6
May 29	15:20-16:38	11220	1430	7.85	7	Basket	1062
May 30	12:15-15:26	12480	1660	7.52	20	Basket	453
May 31	11:50-12:37	11640	1610	7.23	8	Basket	27.9
May 31	13:20-14:32	11300	1610	7.02	7	1/2 VUV	33.9
June 1	10:07-10:40	9630	1490	6.46	6	Basket	2.7
June 1	11:30-12:37	9630	1490	6.46	6	1/2 VUV	18.3
June 2	10:21-11:10	8250	1380	5.98	6	1/2 VUV	22.5
June 5	13:56-14:35	8330	1380	6.04	6	1/2 VUV	24.6
June 6	08:12-08:41	9400	1450	6.48	6	Basket	No recovery
June 6	09:00-10:18	9350	1450	6.45	6	1/2 VUV	15.6
June 7	08:49-09:56	10800	1560	6.92	8	1/2 VUV	98.7
June 7	10:24-11:41	10800	1560	6.92	14	Basket	120
June 8	08:27-09:53	11020	1600	6.89	14	Basket	287
June 9	14:06-14:51	13120	1700	7.72	9	Basket	22.2
June 13	08:17-09:01	7400	1400	5.29	6	1/2 VUV	29.1
June 15	11:30-12:28	6200	1260	4.92	6	1/2 VUV	6.0
June 23	09:03-09:50	5860	1190	4.92	7	1/2 VUV	16.5
June 30	08:45-10:04	7360	1330	5.53	10	1/2 UVU	6.3

* As measured at Chilliwack River at Vedder Crossing (approximately three and a half miles upstream of cross-section six), using a one hour time lag.

**Adjusted to account for sampler efficiency and for material passing through sampler.

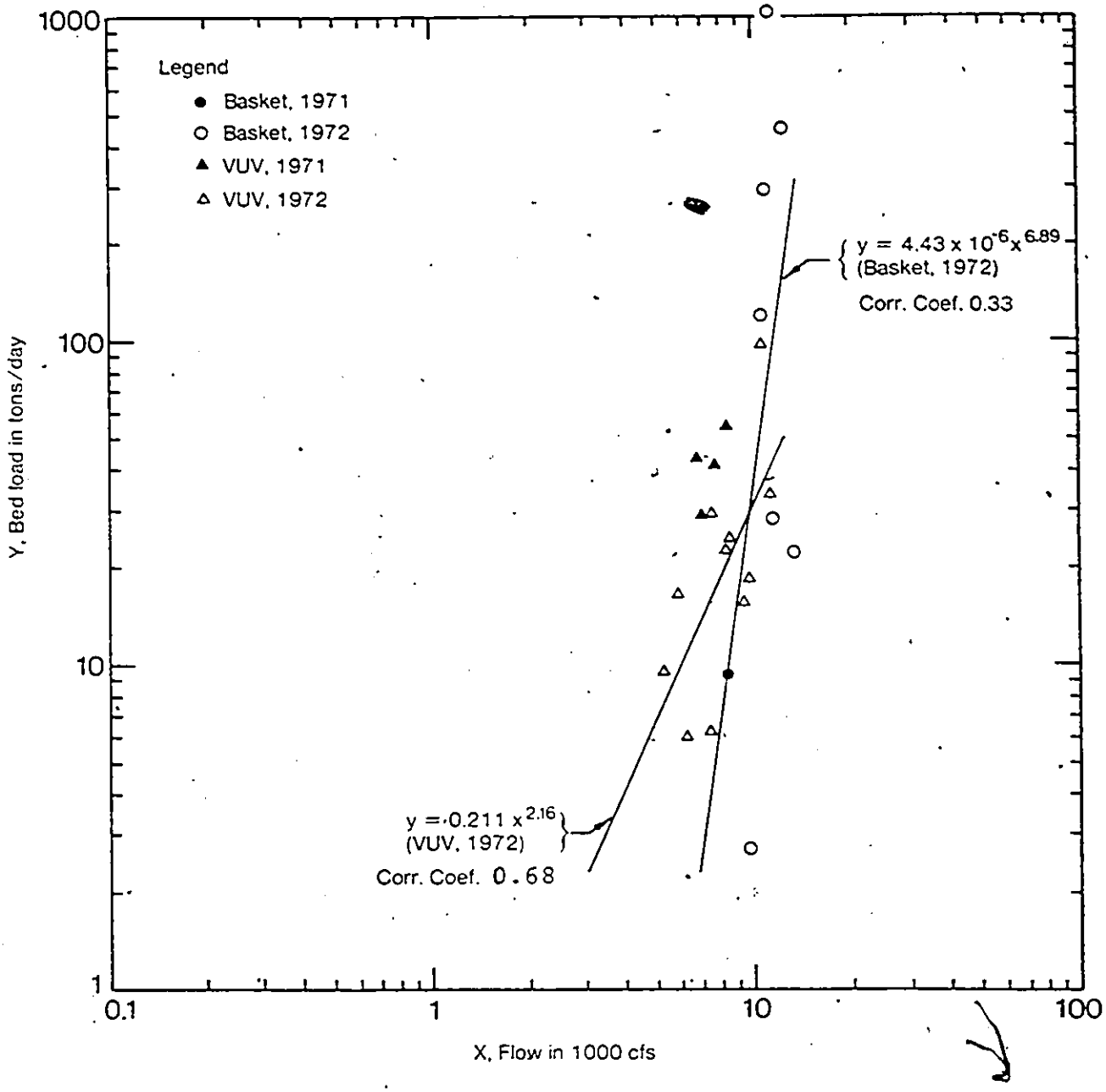

Figure 5.5 Flow versus bed load discharge, from measurements.

For purposes of comparing with computed bed load discharges the above equations (developed using 1971 and 1972 data) were used for computing the bed load discharge for various values of flow. These are summarized in Table 5.3. The results of the computations are used later in comparing with volumetric measurements.

5.2.2 Bed Load Particle Size

Some bed load particle size data are shown in Tables 4.3 and 4.4 for 1971 and 1972 respectively. The 1971 data were analysed further to show the relationships between the mean diameter, D_{50}, and the mean and bottom velocities at the vertical of sampling (Tywoniuk, 1972). The results of these analyses were reported as follows: for velocities greater than about six feet per second, $D_{50} = 10.94V_b - 57.89$ (coefficient of correlation, 0.74), and $D_{50} = 16.23V_m - 109.5$ (coefficient of correlation, 0.80). For velocities less than about six feet per second, $D_{50} = 0.1845V_b - 0.2842$ (coefficient of correlation 0.51), and $D_{50} = 0.1732V_m - 0.3527$ (coefficient of correlation 0.53). In these relationships, V_m and V_b refer to the mean velocity in the vertical and the velocity at a point about one foot from the bottom of the vertical respectively, in ft/sec; D_{50} is in units of mm.

In the D_{50}/velocity relationships, the low range of velocities represents primarily the sand transported at relatively low flows. The high range represents the relatively higher flows and the larger sand and gravel sizes transported by these flows. The dividing point of "about six feet per second" is not precise since bed load sizes at this point may be either sand or gravel, depending on a variety of other variables. It is of interest, however, to note the level of correlation for the gravel sizes.

The bed load particle size data are graphically displayed in figure 5.6. It is evident from this illustration that for the cross-section to the right of station 120, the particle size quartiles (D_{75}, D_{50} and D_{25}) represented particle diameters

less than about 2 mm. To the left of this station, particle diameters exceed 2 mm. This is logical considering that velocities, particularily bottom velocities, are lower at the left, and higher to the right as is illustrated in the velocity distribution curves in Appendix B.

The basket bed load sizes shown in figure 5.6 are generally larger than 10 mm for the quartiles chosen. This is the result of several factors: (a) a large percentage of the "fines" are not retained by the basket sampler, and (b) the data represent a high flow range (hence higher bottom velocities), and therefore larger particle sizes.

5.2.3 Suspended Sediment Data

The suspended sediment sampling and computations were done using standard field and computational techniques. It should be noted that although the sampling was done at the Vedder River near Yarrow, flow data for the Chilliwack River at Vedder Crossing were used in the computations. As a result, the data are shown under the latter station name.

Although this report concerns a study of bed load transport, the suspended sediment data are nevertheless of some interest. The data are not presented in detail herein, however, as they are published by the Water Survey of Canada. Some typical values are of interest; for example, for the dates shown for 1971 in Table 5.1, the corresponding mean daily suspended sediment discharges in tons per day were as follows: June 1, 550; June 2, 330; June 7, 1250; June 22, 1250; June 23, 2250; June 24, 1800; and June 25, 1500 (Tywoniuk, 1972). Similar data are shown for May and June 1972 in Appendix B.

5.2.4 Bed Material Sample Data

Bed material analysis data for May 1970 are shown in Table 4.1. These clearly illustrate a variation in particle size gradation with distance along the thalweg of the river.

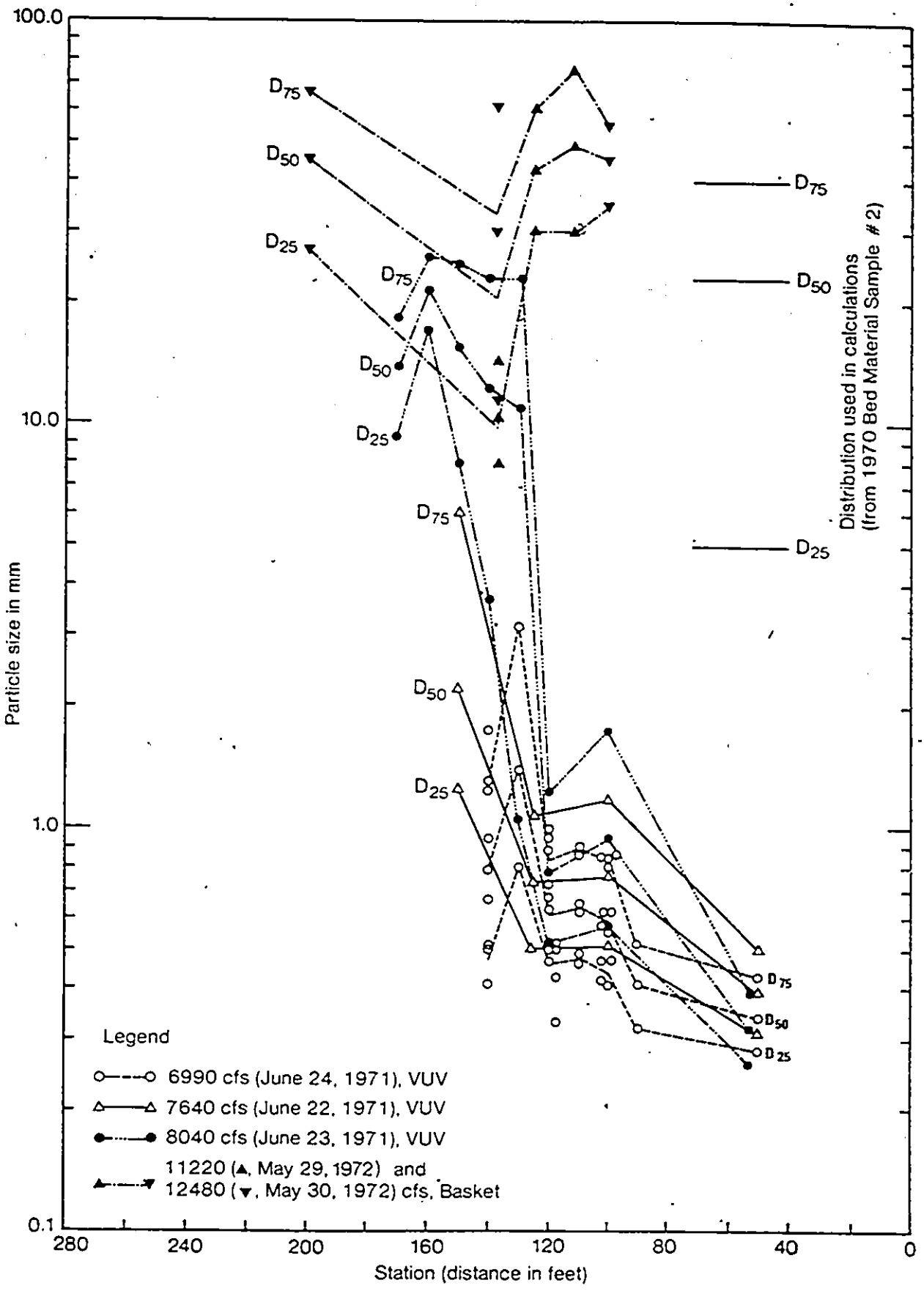

Figure 5.6 Bed load particle size distribution versus location

TABLE 5.3 Bed Load Discharge Results from Direct Measurements

Q cfs	b_w feet	Sampler Type	Bed Load tons/day	G_1 lb/sec/ft
4000	255	half VUV	4.21	0.000383
6000	273	"	10.1	0.000858
8000	287	"	18.8	0.00152
6000	273	Basket	1.02	0.000086
8000	287	"	7.39	0.000596
10000	298	"	34.4	0.00267
15000	315	"	562.	0.0413
20000	330	"	4080.	0.286

Notes: 1. For half size VUV, $G_1 = 2.11\ (Q/1000)^{2.16}/432b_w$ and for the basket, $G_1 = 44.3(10^{-6})(Q/1000)^{6.89}/432b_w$.

2. These are basically the regression equations developed using 1971 and 1972 sampling data as described in section 5.2.1 (but adjusted for G_1 to be in lb/sec/ft).

More revealing results are perhaps those of bed material sampling conducted in the spring and fall of each of 1974 and 1975 (Environment Canada, 1976). The particle size-data were displayed graphically illustrating the 25, 50 and 75 percentiles of the particle size of bed material located on the river bed at each of the 11 ranges. This information is summarized in Table 5.4 to further illustrate the variation in particle size with distance along the longitudinal axis of the river.

For the May 1970 bed material sample two, the results of which were used in the calculations, the material sizes (mm) for the corresponding percentiles were: D25 - 5 mm, D50 - 23 mm, and D75 - 40 mm. These values, in comparison with data obtained at this location at subsequent dates, illustrate that bed material does not change substantially with time. The use of the 1970 data for 1971 and 1972 calculations was, therefore, appropriate.

5.2.5 Volumetric Measurement Results

Section 3.2.3 outlines the procedures used to obtain channel geometry data; many of these data were to be used for computing, volumetrically, the deposition or erosion which occurred at the 11 ranges or locations of the study reach. The 1971 and 1972 channel geometry work was continued until fall of 1975. The results of the profiling work were reported by Environment Canada in 1976. These results are shown in Table 5.5.

It should be noted that the deposition and scour values presented in Table 5.5 are given in square feet. These are therefore not volumetric since the figures do not account for the longitudinal distance, the distance which each cross-sectional area represents.

5.3 Results of Equations

The results of computations utilizing bed load discharge equations are tabulated in Tables 4.5 to 4.9 inclusive and in Table 4.12. The values calculated for the various flow levels were plotted for graphical representation as shown in Figure 5.7.

TABLE 5.4 Bed Material Particle Size versus Distance along Study Reach

Date and Percentile	R1 (0 mi)	R2 (1.1 mi)	R3 (1.8 mi)	R4 (2.5 mi)	R5 (2.9 mi)	R6 (3.5 mi)	R7 (4.0 mi)	R8 (4.7 mi)	R9 (5.2 mi)	R10 (5.5 mi)	R11 (6.1 mi)
April/74											
D25	—	29	10	42	4	5	12	3	2	4	1
D50	—	60	26	64	21	24	26	10	10	12	1
D75	—	84	45	84	42	51	44	22	24	26	9
Sept/74											
D25	—	27	9	14	46	1	2	1	1	5	2
D50	—	66	31	26	68	15	14	1	10	17	7
D75	—	81	69	46	90	30	38	9	19	31	21
April/75											
D25	—	5	19	8	19	5	4	1	4	3	1
D50	—	16	41	30	54	16	10	2	12	11	6
D75	—	48	68	66	76	31	26	13	29	26	16
Sept/75											
D25	—	9	15	1	28	7	1	4	3	2	1
D50	—	32	44	14	39	20	1	16	12	9	6
D75	—	68	66	24	51	36	11	34	34	21	14

Notes: 1. Particle sizes shown are in millimeters.

2. Percentiles show percentage of material finer than indicated size.

TABLE 5.5 Net Sediment Deposition and Scour at Cross-sections

Cross Section	6 (1225)[1]	7 (3315)	8 (3255)	9 (1995)	10 (2290)	11 (2910)	Total (14990)
Spring 72-Fall 72	102 D [2]	53 D	217 D	20 D	34 S	56 D	--
Bed load (Vol)	10300[3]	14500	58400	3300	6440	13500	93600 D
Bed load (M)	4430[4]						
Suspended (M)	123000[5]						
Fall 72-Spring 73	44 D	131 S	56 S	7 S	138 D	18 D	--
Bed load (Vol)	4460	35900	15100	1150	26100	4330	43400 S
Bed load (M)	234						
Suspended (M)	13800						
Spring 73-Fall 73	13 D	105 D	500 S	28 D	24 S	42 D	--
Bed load (Vol)	1320	28800	135000	4620	4540	10100	40300 D
Bed oad (M)	1220						
Suspended (M)	29000						
Fall 73-Spring 74	35 D	71 D	234 D	11 S	38 S	21 D	--
Bed load (Vol)	3540	19500	63000	1810	7190	5050	82100 D
Bed load (M)	932						
Suspended (M)	36800						
Spring 74-Fall74	38 D	235 S	74 D	1 S	25 D	82 S	--
Bed load (Vol)	3850	64400	20000	165	4730	19700	55700 S
Bed load (M)	5480						
Suspended (M)	135000						
Fall 74-Spring 75	1 D	128 D	150 D	72 D	36 S	116 D	--
Bed load (Vol)	101	35100	40400	11900	6820	27900	108600 D
Bed load (M)	644						
Suspended (M)	29500						

...cont'd

TABLE 5.5 Net Sediment Deposition and Scour at Cross-sections (cont'd...)

Cross Section	6 (1225)[1]	7 (3315)	8 (3255)	9 (1995)	10 (2290)	11 (2910)	Total (14990)
Spring 75-Fall 75	113 D[2]	23 S	63 D	21 D	52 D	37 S	--
Bed load (Vol)	11400[3]	6300	17000	3460	9850	8900	26500 D
Bed load (M)	1930[4]						
Suspended (M)	45200[5]						
Total	346 D	32 S	682 D	122 D	55 D	134 D	--
Bed load (Vol)	35000	8770	184000	20100	10400	32200	252000 D
Bed load (M)	14900						
Suspended (M)	412000						

Notes: 1. Figures in brackets indicate representative distance in feet.

2. Figures represent deposit (D) or scour (S) in square feet at the cross section (data from Environment Canada 1976).

3. Figures represent computed volumetric bed load in tons (and assuming specific gravity of bed load is 2.65).

4. Figures represent bed load in tons computed in the standard way (measurements plus regression equations) for April 1 to September 30 or October 1 to March 31.

5. Figures represent measured suspended sediment in tons for same periods as in 4 above.

6. Prior to Spring, 1973, survey there was significant filling of material inside the left dyke of range 10 due to road building along the dyke. This figure was therefore not used in the calculations.

7. During 1973 there was considerable material removed from range 3 for road construction purposes. This figure was therefore not used in the calculations.

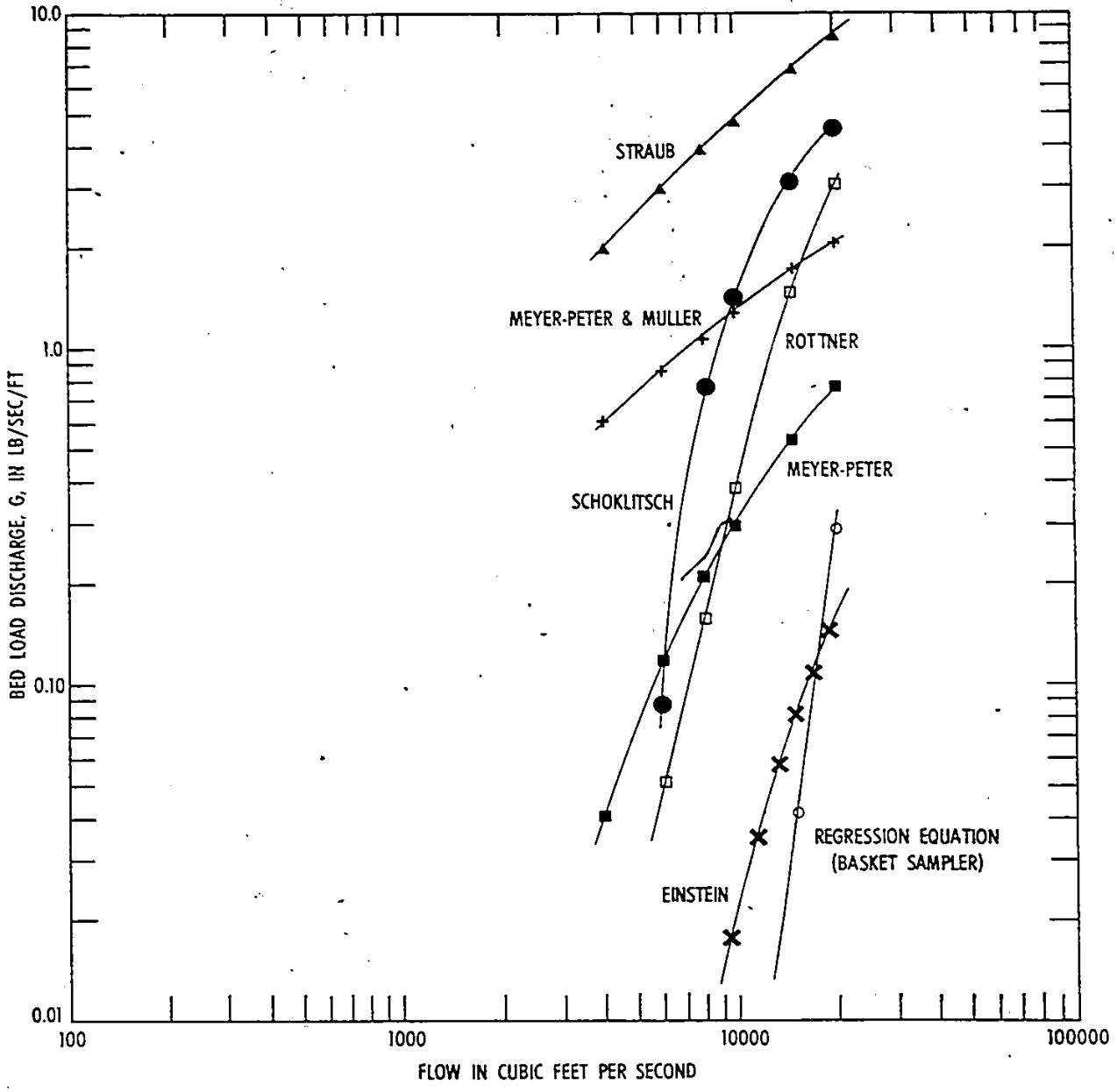

FIGURE 5.7 FLOW VERSUS BED LOAD DISCHARGE RESULTS FROM COMPUTATIONS USING BED LOAD FORMULAE.(VEDDER RIVER AT CROSS-SECTION SIX)

Upon initial observation, the differences in results among the computations for the six equations appears to be astronomical. For example, for a flow of 10,000 cfs, the range for bed load discharge varies from 0.022 lb/sec ft for the Einstein method to 4.6 lb/sec ft for the Straub equation. The other equations produced values between these two extremes.

The variations among the results from the numerous equations are in fact not too inconsistent with other researchers observations. Hollingshead found similarly large variations among computational techniques during research conducted in 1967 and 1968 on the Elbow River at Bragg Creek in Alberta. For example, at a flow of 5000 cfs, the bed load discharges in lb/min computed using the Meyer-Peter and Muller and Einstein methods were 58,000 and 5,000 respectively. Other comprehensive research such as that of Shulits and Hill, 1968, has also demonstrated that the variations in computed results such as obtained for the Vedder River are indeed to be expected. The author has also experienced results of this type for rivers having parameters which more closely resemble those for which empirical equations were developed; it is therefore not too surprising to get results which are variable when using parameters such as slope and particle size which are significantly outside of the range for which the equations were developed.

The mis-application is perhaps appropriately summarized by Shulits and Hill in their discussion of the selection of a discharge or Q-formula. They state: "The astonishing fact is that bed load formulas are being applied outside their basic experimental range. It is relevant and practical to compare the Q-formulas in the flume data range and to extend the comparison into the river data range..... , The scope of comparison is for grain sizes from 0.3 to 7.0 mm, slopes from 0.0004 to

0.30, and discharges from 0.1 to 100 cfs/ft." (Shulits et al, 1968). The one exception is that of Meyer-Peter and Muller who used grain sizes from 3.0 mm to 28.6 mm.

5.4 Comparisons of Bed Load Discharge Results

Comparisons can be made between two pairs of results: the results of bed load discharge computations utilizing empirical equations can be compared with the results obtained by sampling and the volumetric measurement results can be compared with the bed load discharges obtained by direct measurement (sampling).

5.4.1 Comparison of Equation and Sampling Bed Load Discharges

Figure 5.7 illustrates the bed load discharge results from computations using equations or bed load formulae and the results of regression analyses utilizing the sampling data. The comparison of interest is that of the regression equation developed from sampling data with the other curves resulting from the computations based on empirical equations.

Before persuing further with this comparison it is essential to note the results of Table 5.3. This table summarizes the bed load discharge results from direct measurements. Specifically, it should be noted that the bed load discharges for the low flows are indeed quite low when compared to the values obtained from calculations utilizing the empirical equation; in particular the Straub and Meyer-Peter and Muller results. Because these bed load discharges are comparatively considerably lower, they were not plotted in Figure 5.7.

From Figure 5.7 it is evident that the regression equation (basket sampler) most closely coincides with the curve obtained using the Einstein equation. The other curves correspond to considerably higher bed load discharge rates with the Straub equation results differing the most from the regression

equation. There is perhaps an exception at the lower flow level (in the 4000 to 6000 cfs range) where the curve representing the Schoklitsch equation results would intersect both the Einstein and the "regression equation" curves.

This comparison of measured and semi-theoretically computed results is of particular significance. In practice the tendency is to place greatest faith on the physically measured results particularly since alternatives, such as the six curves illustrated in Figure 5.7, utilize parameters outside of the intended range of the equations. Shulits and Hill, in discussing their selection of a discharge formula perhaps better express this significance as follows: "Again, finally and emphatically, only studies on actual rivers will give the answer. Our main point is the sensibleness and convenience of investigations with one formula, chosen logically and pragmatically, rather than confusing computations with several formulas." (Shulits et al, 1968). In the case of the Vedder River at cross-section six, the field measurement results would support the use of the Einstein equation or perhaps a modified Meyer-Peter equation. Similarly, because of the reasonable coefficient of correlation obtained for the regression equations, the regression equations could perhaps be used most reliably in the estimating the bed load discharges for periods between measurements.

5.4.2 Comparison of Volumetric and Direct (Sampling) Measurements

Table 5.5 illustrates the comparative values of volumetric and direct or sampling measurements.

The volumetric change was computed utilizing data tabulated in the 1976 progress report (Environment Canada, 1976). This report provided values of net sediment deposition and scour in square feet at the 11 cross-sections. Since bed load sampling occurred only at cross-section six it was felt that the volumetric change only downstream of Range six was of interest in the comparative analysis.

The data of direct sampling results were also taken from the various annual progress reports prepared for the study. These data were in the form of mean daily bed load discharge in tons per day. They were computed primarily on the basis of regression equations developed from sample and measurement data, and taking into account the measurement data and the flow hydrograph. The word measurement in this context refers to sampling at various verticals (often a number of samples at each vertical) within a cross-section for purposes of determining the bed load discharge at that cross-section.

Table 5.5 also illustrates the values of the suspended sediment loads (determined from measurements and computations based on measurements) for the time periods indicated. The reason for providing these summary data was to further enable a comparison since it is certain that at least some of the suspended sediment measured at cross-section six would become deposited in the downstream sections.

It is of interest to comment on some of the comparative results. In looking at the total for cross-section six, it is evident that the "volumetric" bed load is about 2 1/2 times the "measured". In both instances, the bed load tonnage is substantially less than the number of tons of suspended sediment load: only 8.5% in the case of volumetric and 3.6% in the case of measured. In the case of "volumetric" bed load for the downstream reach (252,000 tons), this represents 61.2% of the suspended sediment load or 59.0% of the total measured load at cross-section six (suspended sediment plus measured bed load). One must conclude that the difference, 41.0%, would be the suspended sediment outflow at the downstream boundary. While from experience and knowledge of the reach these analysis results appear to be "about right", the exact sediment balance of the reach could not be determined since suspended sediment at the downstream point was not measured.

The reason for it not being measured was that Range 11 was not intended to be a boundary point. Ranges one and six were initially to be the boundary points; however, problem conditions at Range one resulted in appropriate data not being obtained.

A similar type of comparative analysis could be done for each of the time periods. This has not been done, however, since the detailed data were considered to be too variable in both time and distance to provide meaningful results. The details are nevertheless provided in the event that they may be of use to others. It should perhaps be further noted that the accumulated mean daily flows, in cfs for the periods shown starting with Spring 72 - Fall 72, were as follows: 831,000; 266,000; 393,000; 396,000; 771,000; 278,000; and 547,000.

CHAPTER 6

CONCLUSIONS AND RECOMMENDATIONS

6.1 Conclusions

A number of conclusions and recommendations have already been made in the various annual progress reports. Among these were items related to the type and quantity of data needed, field operational procedures, and suggestions for improvements in instrumentation. As a result, the field research continued beyond 1972, until the fall of 1975, and improvements to instrumentation, in particular, the hydrophone were made. The end result was a much better understanding of the bed load transport process and hence a much better information base for technique comparison purposes.

A number of conclusions can be made with respect to the measurement of bed load discharge by direct sampling:

(a) From Sections 5.2 and 5.4, it is concluded that considerably greater confidence can be placed on results obtained by direct measurements than on results of theoretical or semi-theoretical computations. Volumetric measurements can add significantly to this confidence if they are conducted accurately, over a long period of time and over a suitable length of reach. The importance of appropriate boundary conditions cannot be over-emphasized.

(b) Although efficiency of field sampling has improved over the years as a result of equipment improvements, motorized winches, etc., there still remains the need to collect large numbers of samples for a useful quantitative analysis. This need remains because of the large fluctuations of bed load discharge with respect to time and location. The required sample quantities were well defined by Gibbs and Neill (Gibbs et al, 1972) as a result of laboratory studies for the purpose of defining the relationship of basket sample efficiency to bed transport rates, and the number of samples and sampling durations required

required to give acceptable estimates of bed load in various transport conditions. These results indicated that the average percent deviations of an η - sample mean from a 50 - sample mean are 36% for η = 2, 30% for η = 3, 20% for η = 6 and 10% for η = 15, for conditions where bed load transport was associated with progression of low dune-types bed forms. Since the Vedder River exibited primarily flat-bed, sheet-type transport, the laboratory results are not readily transferrable; however, the laboratory results clearly demonstrate the significance of how "many" samples at each vertical contribute to confidence in the data. Of similar significance is the need for many sampling verticals within the cross-section so that the cross-sectional variance of the bed load discharge could be well defined.

(c) The field or flow conditions may also significantly affect a direct sampling program. Direct sampling is useful at only a limited number of days per year at which the conditions are above "competent" or at which the bed load discharge is high enough to make direct sampling useful.

Some conclusions can be made with respect to the use of various equations for the computation of bed load discharges:

(a) Section 5.3 shows that the results among equations can vary by a factor of 100 or more.

(b) In the case of the Vedder River at cross-section six, Schoklitsch, Meyer-Peter and Rottner equations provide relatively consistent results, and in the intermediate range. Einstein and Straub equations provide the low and high range results respectively. Results of direct sampling compare most closely with results obtained using the Einstein equation.

A number of conclusions can be made with respect to the hydrophone data analysis and results:

(a) From Section 5.1 it was concluded that, while the hydrophone data are quantifiable, there is not an obvious direct relationship between sound level intensity (decibels) and bed load transport. This lack of correlation is further illustrated graphically in Appendix B. It is concluded that the results are not useful for purposes of application (that is, engineering and design use) because of the lack of correlation.

(b) It is apparent that factors other than bed load movement contribute to total measurable sound intensity levels, among these are turbulence effects (both around the hydrophone and at the stream bed), the extent of bed-load movement, the extent of saltation and inter-particle collision and the velocities at which particles are moving. It is further apparent that these factors are common to all the ranges of sound frequency intervals used in the observations. The results in this respect were discouraging.

(c) It was concluded that the hydrophone data were useful in the qualitative assessment sence, to determine when and where the bed load was moving. It has application as a tool, therefore, in determining competent conditions (required for some bed load discharge equations) and further in assisting field staff in direct sampling.

(d) Laboratory calibrations or tests were conducted to determine the potential for background noise due to water turbulence and other interference. It was determined that there is measurable "interference" due to both water turbulence and other factors, but later concluded that these values of background noise did not significantly assist in determining the sound levels generated by bed load transport. (Reference section 5.1 and Appendix B).

(e) The matematical model described in Chapter two has a number of limitations including i) application to flat-bed cases only, ii) the assumption that turbulence effects are insignificant, iii) the assumption that only the top bed-layer is capable of moving, and iv) the application to "spherical" particles.

Finally, further observations of sections 5.3 and 5.4 lead to conclusions with respect to the Vedder River study reach itself:

(a) Channel geometry and volumetric bed load discharge computations indicate clearly that the channel in the study area is highly unstable. The state of channel geometry is variable in both time and location with a long-term trend of net deposition or aggradation between ranges six and eleven.

In summary it can be concluded that the research conducted on the Vedder River in 1971 and 1972, and in subsequent years by other staff, greatly contributed to the knowledge of the acoustics and bed load transport within the river reach and provided an opportunity for both original and comparative research.

6.2 Recommendations

A number of recommendations logically follow from the conclusions of section 6.1.

(a) Following the 1972 field research, it was strongly recommended that hydrophone research efforts continue, perhaps with some modifications to both the equipment and procedures, and be complemented by laboratory research. Subsequently, the field program continued until the end of 1975, and substantial further hydrophone research took place. In a sense therefore, this recommendation has been implemented; however, the results of this additional work have not been promising.

(b) There is a need for research to continue in areas such instrument/particle collision measurement techniques, directional hydrophone applications, and hydrophones embedded at locations across a river cross-section. Such

research might include "remote sensing" techniques other than the hydrophone, for example, techniques based on light as the sensor.

(c) There is a need for more sophisticated analysis of acoustic data; for example, research into acoustic signal spectra by means of spectral analysis.

(d) It is recommended that further research into the bed load transport of a gravel bed river be conducted at other river sites. A new site would provide further useful information on bed load transport in gravel-bed rivers. The site should be carefully selected to ensure, among other things, that the river bed is known to be active for a large number of days each year. Future studies should have carefully defined boundary limits and suspended sediment should be measured in conjunction with bed load. This would enable a "sediment balance" evaluation and would therefore be a check on direct measurements and on results of equations. There is also a need for a more accurate direct measurement of bed load than by the use of samplers.

(e) The method of volumetric bed load measurement used for the Vedder River research is recommended for future studies. This method is superior to the previously used method of excavating a hole in the river bed, then measuring its rate of fill when bed load movement commences. The recommended method is less ecologically damaging and does not alter the river regime within the study reach. Should such volumetric studies be done, however, it is recommended that the cross-section network be considerably denser for greater accuracy, and that sediment inflow and outflow be carefully measured. Increased frequency of cross-section definition would also provide improved information. Instrumentation such as the hydrographic data acquisition system (HYDAC-100) used by the Water Survey of Canada should be utilized. This system is comprised of two dynamic distance measuring devices, an echo-sounder/digitizer, a precision electronic digital clock, a data coupler, a magnetic tape recorder, a micro-computer, and a plotter and printer. The system is coupled with a series of computer programs to process

and analyse the data.

Finally, some recommendations can be made with respect to the practical application of research results.

(f) Equations for bed load discharge calculation should be used only with the appropriate field data including direct bed load measurements. This is particularly critical in the case of gravel-bed rivers since existing equations will almost definately be "misapplied", or used outside of their intended range.

(g) Acoustic, flow, stage and other data should be used as a tool in estimating or interpolating the bed load between measurements.

(h) Bed load measurements should consist of many samples since bed load movement is erratic in space and time.

(i) In view of bed load transport being a stochastic process with highly variable rates of movement, there is a need for research into how this stochastic component could be incorporated into the regression models and the semi-theoretical equations.

(j) Studies of entire river reaches are recommended for cases requiring a more comprehensive knowledge of river regimes.

BIBLIOGRAPHY

Albers, V.M., 1965, Underwater Acoustics Handbook II. The Pennsylvania State University Press, University Park, Pennsylvania, U.S.A.

Alberta Water Resources Division (AWRD). Hydrology Branch, 1969, Hydrophone Measurements. Open file report, Alberta Department of Agriculture.

Bedeus, K. and Ivicsics, L., 1963, Observation of the Noise of Bed Load, Proceedings International Association Science Hydrology, Publication No. 65, page 384.

Braudeau, G., 1951, Quelques techniques pour l'étude et la mesure du débit solide. La Houille Blanche, Spc No. A. p. 243.

Broch, J.T., 1971, The Application of Bruel and Kjaer Measuring Systems to Acoustic Noise Measurements. Bruel and Kjaer Canada Limited, 2nd edition, January, 1971.

Chow, V.T., 1959, Open Channel Hydraulics, McGraw-Hill Book Co. Inc., New York, N.Y.

Colby, B.R. and Hubbell, D.W., 1961, Simplified Methods for Computing Total Sediment Discharge with the Modified Einstein Procedure, Geological Survey Water Supply Paper 1593, U.S. Department of the Interior, Washington, D.C., 1961.

Cooper, R.H., 1970, A Study of Bed Material Transport Based on the Analysis of Flume Experiments, Ph.D. Thesis, Department of Civil Engineering, University of Alberta, Edmonton.

Cooper, R.H., and Peterson, A.W., 1968, Analysis of Comprehensive Bed Load Transport Data from Flumes, Proceedings, ASCE Hydraulics Specialty Conference, Mass. Institute of Technology, August 21-23, 1968.

Cooper, R.H., and Peterson, A.W., 1969, A Review of Data from Sediment Transport Experiments. Report No. HY-1969-ST2. Department of Civil Engineering, University of Alberta.

Cooper, R.H., and Peterson, A.W., 1970, Discussion of "Coordination in Mobile-Bed Hydraulics" by Thomas Blench, Journal of Hydraulics Divisoin, ASCE, VOlume 96, HY9, Proc. Paper 7497, Sept. 1970, p. 1880-1888.

Einstein, H.A., 1950, The Bed Load function for Sediment Transportation in Open Channel Flows, Technical Bulletin No. 1026, U.S. Department of Agriculture, Washington, D.C. September, 1950.

Environment Canada., 1976, Data Report, Vedder River Bed Load Study, 1974-1975, Inland Waters Directorate, 1976.

Galay, V.J., 1971, Some Hydraulic Characteristics of Coarse-Bed Rivers. Ph.D. Thesis. Department of Civil Engineering, University of Alberta.

Gibbs, C.J., and Neill, C.R., 1972, Interim Report on Laboratory Study of Basket-Type Bed Load Samplers. Report No. REH/72/2. April, 1972, Research Council of Alberta.

Hinrich, H., 1970, Bedload Measuring by Means of Bottom Plates and Bed Load Samplers with Hydrophone Attachment. Proceedings, International Symposium on Hydrometry, Koblenz, Germany, September, 1970.

Hollingshead, A.B., 1968. Measurement of the Bed Load Discharge of the Elbow River, M.Sc. Thesis, Department of Civil Engineering, University of Alberta, Edmonton.

Hollingshead, A.B., 1971. Sediment Transport Measurements in a Gravel River. Journal of Hydraulics Division, A.S.C.E. Vol. 97, No. HY11, pp. 1817-1834.

Hubbell, D.W.,1964, Apparatus and Techniques for Measuring Bed Load. USGS Water Supply Paper. 1748, Washington, D.C.

Johnson, P. and Muir, T.C., 1969. Acoustic Detection of Sediment Movement. Journal of Hydraulic Research/Journal de Recherches Hydrauliques 7 (1969). No. 4, pages 519-540.

Jonys, C.K., 1975, Acoustic Measurement of Bed Load; Laboratory Experiments. Open file report, Department of the Environment, 1975.

Jonys, C.K., 1975, Acoustic Measurement of Bed Load; Theoretical Feasibility Analysis. Open file report, Department of the Environment, 1975.

Jonys, C.K., 1976, Acoustic Measurement of Sediment Transport, Scientific Series No. 66, Inland Waters Directorate, Department of the Environment, 1976.

Juniet, M., 1952, L'Arenaphone, un appareil détecteur des mouvement des sédiments fins. Grenoble, Société Hydrotechnique de France. Transport Hydraulique et Décantation des Matériaux Solides, p. 178.

Leopold, L.B., Wolman, M.G. and Millar, J.P., 1964, Fluvial Processes in Geomorphology, W.H. Feeman and Co., San Francisco.

Meyer-Peter, E. and Muller, R., 1948, Formulas for Bed Load Transport, Proceedings of the 2nd meeting of the IAHR, Slockholm, Sweden, 1948.

Novak, P., 1957, Bed Load Meters - Development of a New Type and Determination of Their Efficiency with the Aid of Scale Models, International Association of Hydraulic Research, Trans V. 1, pp. A9-1 to A9-11, 7th general meeting, Lisbon, 1957.

Peterson, E.R., 1969, Surface Water, Instrumentation and Observation Techniques. Proceedings, 7th Canadian Hydrology Symposium, Victoria, B.C., May 14 and 15, 1969.

Shulits, S., and Hill, R.D., Jr., 1968, Bed Load Formulas. Part A. A Selection of Bed Load Formulas. Part B. Program Listings for Bed Load Formulas. Penn. State University, NTIS, PB 194950, December, 1968.

Simons, D.B., and Richardson, E.V., 1963, Form of Bed Roughness in Alluvial Channels; ASCE Trans., V. 12, 1963.

Solov, yev, N. Ya, 1969, Improvement and Test of an Instrument for Recording Coarse Sediments, Transactions of the State Hydrologic Institute (Trudy GGI No. 141, 1969, pp. 158-172).

Stichling, W., 1969, Instrumentation and Techniques in Sediment Surveying. Proceedings, 7th Canadian Hydrology Symposium, Victoria, B.C., May 14 and 15, 1969.

Stichling, W., and Smith, T.F., 1968, Sediment Surveys in Canada, Inland Waters Branch, Department of Energy, Mines and Resources, Technical Bulletin No. 12.

Tucker, D.G., and Gazey, B.K., 1966, Applied Underwater Acoustics, Pergamon Press.

Tywoniuk, N., 1971, Background Interference Tests for WSC Hydrophone System. Open file report, Water Resources Branch, Department of the Environment, October, 1971.

Tywoniuk, N., 1972, Sediment Discharge Computation Procedures, Journal of the Hydraulics Division, ASCE, Vol. 98, No. HY3, March, 1972.

Tywoniuk, N., and Stichling, W., 1973, Sedimentation Phenomenon of the Lower Fraser River, Proceedings, International Symposium River Mechanics, IAHR, Bangkok, Thailand, January, 1973.

Tywoniuk, N., 1972, Progress Report, 1971, Bed Load Study, Chilliwack River, B.C. Open file report, Water Resources Branch, Department of the Environment, May 1972.

Tywoniuk, N., and Drennan, L., 1973, Progress Report, 1972 Bed Load Study, Vedder River, B.C. Open file report, Water Resources Branch, Applied Hydrology Division, Department of the Environment, March 1973.

Tywoniuk, N., and Warnock, R.G., 1973, Acoustic Detection of Bed Load Transport. Proceedings, 9th Canadian Hydrology Symposium on Fluvial Processes and Sedimentation, Edmonton, Alberta, May 8 and 9, 1973.

Urick, R.J., 1967, Principles of Underwater Sound for Engineers, McGraw-Hill Book Company.

Water Survey of Canada, Sediment Data for Canadian Rivers, Water Resources Branch, Department of the Environment, Annual Publication.

Yalin, M.S., 1972, Mechanics of Sediment Transport, Permagon Press Ltd.

APPENDIX A

Specifications and Operational Details of Hydrophone System

A.1 General Description

This Appendix describes the installation, operation and maintenance of the Hydrophone System in general terms. For precise details, reference should be made to the manufacturers manuals describing the Ithaco Model 411 filter, Ithaco Model 3161 logarithmic amplifier, Esterline Angus Model T 171B chart recorder, Ithaco Model 9120-78 hydrophone system, Ithaco Model 450R rechargeable power supply, Ithaco Model 45052 portable case, and the Ithaco Model 605 wideband hydrophone. The Hydrophone System is a wideband, portable hydrophone system designed for the acquisition, conditioning, and recording of underwater acoustical information. Primary features include a low noise signal pickup, a variable electronic filter adjustable in 1/3 octave steps, a true logarithmic post amplifier which provides both a normalized audio output signal and a logarithmic output whose level is proportional to the input signal in dbv, and a single channel, solid state, servo recorder. Also included are battery pack power supplies for both the signal conditioning electronics and the recorder, thus making the system truly portable.

Physically, the system is comprised of 3 sections: the hydrophone or data acquistion section, the signal conditioning section, and the recording section. The signal conditioning section can be further broken down into the Variable Bandpass Filter, the Logarithmic Voltage Controlled Amplifier, the Monitor Panel, the Rechargeable Power Supply, and the Portable Case.

A.2. Component Specifications:

A.2.1 Wideband Hydrophone

The Ithaco Model 605 Wideband Hydrophone is a highly sensitive, nearly omnidirectional hydrophone which includes an integral preamplifier in order to obtain optimum noise performance within its 75 KHz useable bandwidth.

The transducer and preamplifier are electrostatically shielded, and molded in void-free polyurethane. The standard hydrophone includes a nominal 5 feet of undersea electrical cable.

Additional specifications are as follows:

MIDBAND SENSITIVITY (db re 1 volt/microbar)	-64 typical at preamp output (50 ohm termination)
	-78 typical at transducer output
FREQUENCY RESPONSE	±3 db 5 Hz to 30 KHz typical
DIRECTIVITY	±1 db to 75 KHz in horizontal plane
NOISE (with hydrophone source impedance)	Less than Seastate Zero over the entire frequency band
MAXIMUM OUTPUT SIGNAL FOR LINEAR OPERATION	3-v rms into 50 ohms
PRESSURE SENSITIVITY	-2 db change at 1500 psi (3000 ft. depth maximum pressure rating)
ELECTRICAL CALIBRATION	Amplifier output nominally equal to calibration input midband
POWER SUPPLY	+15V at 20ma
DIMENSIONS	2.00" outside diameter, 12" long
CABLE LENGTH	5 feet nominal
CONNECTOR	Marsh - Marine RM Series

A.2.2. Variable Electronic Filter

The Ithaco Model 411 Variable Electronic Filter is comprised of two independently tuned active filters in cascade. Both filters are four pole (24 db/octave) Butterworth type. The passband is selectable in 1/3 octave steps in the

range 10Hz to 100KHz. Designed for maximum dynamic range, the filter has 100 microvolts of self-noise, and will handle ±10 volts of signal.

Additional specifications are as follows:

FILTER CHARACTERISTIC	Each Filter section is a four pole Butterworth (maximal flat passband, 24 db/octave stopband)
FREQUENCY RANGE	-3 db nominal at 1 Hz to 100 KHz
CORNER FREQUENCY RANGE	1.0, 1.25, 1.6, 2.0, 2.5, 3.15, 4.0, 5.0, 6.3, 8.0, 10.0 Hz Note: One control each for high and low corner
FREQUENCY RANGE MULTIPLIER	OUT, X10, X100, X1K, X10K
FREQUENCY ACCURACY	±2% of setting
PHASE MATCH	±5 degrees between any 2 units at the same frequency setting measured between 10 Hz - 50 KHz
INPUT	
Impedance	10 megohm shunted by less than 50 pf
Level	10 volt peak maximum
OUTPUT	
Impedence	100 ohm nominal
Level	10 volts peak maximum
Load	5,000 ohms minimum

GAIN	1.0 ±1% (with a decade separation between cutoffs)
LINEARITY	0.1%
NOISE AND RIPPLE	Below 100 microvolts rms at the output
CONNECTORS	BNC input and output on rear panel
Model 411M101 Configuration	Replace BNC imput by XLR with power for remote preamp
POWER	±15 v @ 130 ma
SIZE	6.75" high, 2" wide panel, 10.5" deep

A.2.3. Universal Logarithmic Amplifier

The Model 3161 Universal Logarithmic Amplifier provides a variety of ways of operating a wideband voltage controlled amplifier with a precise logarithmic gain control characteristic.

Amplifier gain can be set manually by a ten-turn front panel dial calibrated directly in decibels, or the amplifier gain can be set remotely or as part of a system by a control voltage with a gain sensitivity of 10 db/volt.

Inclusion of a precision detector to close the loop around the voltage controlled amplifier permits the automatic gain control system to operate as either a precision logarithmic converter, ±1/4db over 80db dynamic range or as a signal compressor.

When operating as a compression amplifier, the amplifier output level is a measure of the amplifier gain so that a single channel data acquisition and recovery system can be formed around a 3161 which will accept signals with 80db dynamic range and compress them to less that 20 db for recording on tape. During

playback the 3161 is operated in the gain recovery mode and the amplified gain analog is provided so that the compressed signal and the gain analog are simultaneously available. The phase information is preserved in the compressed signal and the gain correction to the signal will provide the signal amplitude.

Typical applications include high speed log conversion, computation of ratios. . (both linear and logarithmic), acquisition and recovery of wide dynamic range signals on a single tape track, and control of a number of amplifiers by a single gain command such as computerized gain.

The amplifier specifications are as follows:

GAIN		Equal to 10 (8-Ec) db ± 0.25 db where EC is the control voltage
GAIN RANGE		0 to + 80 db continuous with gain accuracy ±0.25 db
GAIN STABILITY		±.02 db/degree C maximum
INPUT	Type	Single-ended input
	Impedance	1 megohm minimum shunted by less than 100 pf
	Level	3 volts peak to peak linear, ±75 volts without damage
OUTPUT	Type	Single-ended
	Impedance	100 ohms in series with 60 microf nominal
	Load	10K ohms minimum
	Level	10 volts peak to peak maximum
MANUAL CONTROL		A ten-turn front panel dial controls the gain in manual mode. The dial is calibrated directly in db.

VOLTAGE CONTROL	Type	Single-ended, BNC input (Rear Panel)
	Impedance	10.0K ohms nominal
	Sensitivity	10 db/volt (0 v = 80 db, 8 volts = 0 db)
	Slew Rate	10^7 db/sec
	Feedthrough	Negligible at slew rates less than 10^6 db/sec
DISTORTION		1% maximum
FREQUENCY RESPONSE		$\pm$1 db, 10Hz to 100 KHz; $\pm$3 db, 5 Hz to 200 KHz
PHASE ACCURACY		$\pm$2 degrees between amplifiers from 30 Hz to 20 KHz
NOISE (Broadband)		5.5 microvolts rms maximum referred to the input at maximum gain

The logarithmic converter specifications are as follows:

DYNAMIC RANGE		80 db
ACCURACY		1/4 db
DETECTION		Average
INPUT	Range	50 microvolts in 0.5 volts rms
	Level	2 v peak maximum, $\pm$75 volts without damage
NORMALIZED OUTPUT	Level	Amplifier output is held constant regardless of input (output is held to 0.45 volt average which corresponds to 0.5 v rms sinewave)

	Crest Factor	10:1
LOGARITHMIC	Sensitivity	.1 v/db
OUTPUT	Impedance	1 ohm maximum
	Load	1,000 ohms minimum

FREQUENCY RESPONSE

Range Setting	Frequency Interval, Hz	Frequency Response
10 Hz	10 - 30	± 1 db
	30 - 30K	+ 1/4 db
	30K - 100K	+ 1 db
100 Hz	10 - 100	± 1 db
	100 - 30K	± 1/4 db
	30K - 100K	± 1 db
1 KHz	300 - 1K	± 1 db
	1K - 30K	± 1/4 db
	30K - 100K	± 1 db
10 KHz	3K - 10K	± 1 db
	10K - 30K	± 1/4 db
	30K - 100K	± 1 db

SLEW RATE

RANGE SETTING	SLEW RATE
10Hz	1 db sec
100 Hz	10 db sec
1 KHz	100 db sec
10KHz	1,000 db sec.

NOTE: The specified slew rate is the maximum slew rate for which the 3161 will track a signal with less than 1/2 db error. The 3161 will slew twice as fast with a 1 db error, or conversely half as fast for 1/4 db error.

DISTORTION		Less than 1% on each range setting (greater than 1% for frequencies below range setting)
TEMPERATURE COEFFICIENT		±0.02 db/degree C maximum

The compression amplifier specifications are as follows:

INPUT	Dynamic Range	Greater than 80 db
	Detection	Average
	Crest Factor	5:1
	Max Input	2 v peak, ±75 v without damage
OUTPUT	Dynamic Range	Less than 20 db
	Gain Envelope	.005 v/db
	Max Output	0.5 volts
CHARACTERISTIC		Amplifier Gain, db = 100 - 200Eo ±0.25 db where Eo = Output Voltage
DISTORTION		Less than 1%
FREQUENCY RESPONSE		Same as log converter above
SLEW RATE		Same as log converter above

The amplifier configuration details are as follows:

SIZE	6.75" high, 2" wide, 10.5" deep
FUNCTIONS ON FRONT PANEL	
Mode Switch	Manual — Voltage Controlled Amplifier — Logarithmic Converter — Compression Amplifier — Gain Recovery
Range Switch	10 Hz, 100 Hz, 1 KHz, 10 KHz

Manual Gain Control	10-turn dial
Connectors	Input and output BNC

FUNCTIONS ON REAR PANEL

Blue Ribbon Connector	±15 volt power, ground and control
BNC Connectors	Input, Output, Control, Log Out

A.2.4 Rechargeable Power Supply

The Ithaco model 450R power supply is essentially a D6 regulated battery pack with the capability of recharging the battery from the 117v, 60 Hz line. The regulated output is ±15v and the current capacity is about 30 channel hours, hence it is intended for use primarily with a maximum of three channels.

A.2.5 Portable Case

The Ithaco model 450 S2 case encompasses the conditioning portion of the hydrophone system. The case is a three channel portable use type with outside dimensions of about 7 inches high, 9.5 inches wide and 14 inches deep.

A.3 Component Operations

A.3.1 Inter Unit Cabling

Because of the modular nature of each of the units in the hydrophone system, all that is required prior to operation is to complete the inter-unit connections.

The cabling between units in the signal conditioning section can be left connected while shipping or storing the equipment. However, since the hydrophone and its associated cable represent a significant weight on the filter input connector, the hydrophone cable should be tied to a rigid structure prior to being connected to the filter. Failure to do so may result in loss or damage to the remainder of the system.

A.3.2 Rechargeable Power Supply

A.3.2.1 Operating Controls

The operating controls are as follows:

A. Power Switch - Front panel toggle switch which controls AC power to DC power regulators and battery charging circuits. Placing this switch in the CHG position permits AC operation of the system and battery recharging

B. Mode Switch - Front panel, 3 position rotary switch which controls the power supply mode of operation

OFF - No DC power output from power supply. Batteries may be recharged by placing POWER SWITCH in the CHG position

AC - DC power derived from AC line; batteries being recharged at the same time. POWER SWITCH must be in the CHG position

BAT - DC power derived from batteries

A.3.2.2 Operation Description

The power supply is essentially a DC regulated battery pack with the capability of recharging the battery from the 117v, 60 Hz line. Current capacity is approximately 30 channel-hours, and thus it is intended for use primarily with a maximum of 3 channels. However, it may be used to operate up to 7 channels of amplifiers with a resultant decrease in operating time. The operating time may be extended by leaving it in the recharge mode, however the battery will ultimately become discharged to the point where the amplifiers will not operate properly. This then necessitates placing the AMPL switch in the OFF position to allow the battery to recharge.

A.3.2.3 Recharge Mode Operation

To recharge the battery, connect the power supply to the 117v, 60 Hz line by means of the power cord at the rear. Place the CHG switch in the ON position and the AMPL switch in the OFF position. This permits the battery to be charged without draining current into the DC regulator or the amplifiers. No meter indication will occur in this situation. The power supply may be removed from the Rack Adapter or Portable Case for recharging.

To permit extended charging time without damage to the batteries, the charging current is set at a low level. For this reason, a discharged battery should be charged for a minimum of 16 hours.

A.3.2.4 Amplifier Operation Mode

The power supply may be used to operate any of a number of possible amplifiers. It may further be used with the CHG switch in either the ON or OFF position. The CHG switch serves to connect and disconnect the rectification and filtering circuits to the 60 Hz line. The AMPL switch connects the regulator, meter and amplifiers to the DC power lines.

When used with the CHG switch in the OFF position and the AMPL switch in the ON position, the meter and amplifiers are connected to the DC lines. The battery has a 1.2 amp-hour rating. Thus, since the regulator requires approximately 15 ma and each amplifier requires approximately 35 ma, a fully charged battery should operate 3 channels for at least 8 hours or 7 channels for at least 5 hours. When the meter drops below midscale (approximately $\pm$16.5 v) the DC regulator will not function properly, and proper amplifier operation cannot be guaranteed.

When used with the CHG switch in the ON position and the power cord connected to the AC line, the possible operating time may be extended. In this

situation, it may be possible to reach an equilibrium point for 3 channel operation in which the battery will remain partially discharged. For 7 channel operation the battery will eventually become full discharged.

A.3.2.5 Maintenance and Calibration

Access to the circuitry of the power supply is obtained by removing two side panel screws from the right side panel, and sliding the panel toward the rear. The regulator card may be removed by sliding its retaining spring, located in the upper structural member, towards the front. The card should then be lifted into the upper slot, its lower edge pulled out and down, thus freeing it from the power supply structure. The left side panel may be removed by first removing the two retaining screws at either end of the panel. Care should be taken during this operation to avoid breaking the battery connections to the front panel AMPL switch. The battery is secured by two screws to the left side panel, and may be removed from this panel by removing the two screws.

The power supply has an integral current limiting feature in each polarity which limits output current to 400 ma, and a power output diode protection which holds both polarities at ground when they are shorted together. Thus before assessing the lack of DC power to a power supply failure, the power supply output should be checked with no amplifiers connected to it.

The battery pack consists of 30 rechargeable NiCd, 1.5v cells, (Burgess CD12L or equivalent) interconnected to provide a maximum of $\pm$22V. The cells are potted to form a solid block. The user may replace individual cells or may entirely replace the battery pack.

The only calibration which may be necessary is an adjustment of the regulator output voltages. This adjustment is provided by a potentiometer for the

positive regulator and by another potentiometer for the negative regulator. Both controls are located on the regulator card.

A.3.3 Filter

The operator controls on the Ithaco Model 411M102 are as follows:

A.	Low Pass Corner Frequency	Front panel rotary switch which selects the high frequency corner of the filter
B.	Low Pass Corner Frequency Multiplier	Front panel rotary switch which selects the decade of operation for the Low Pass Corner Frequency Switch
C.	High Pass Corner Frequency	Front panel rotary switch which selects the low frequency corner of the filter
D.	High Pass Corner Frequency Multiplier	Front panel rotary switch which selects the decade of operation for the High Pass Corner Frequency Switch

A.3.4 Universal Logarithmic Amplifier

The operating controls on the Ithaco Model 3161 are as follows:

A.	GAIN	Front panel 10 turn potentiometer with turns counting, locking dial for setting amplifier gain when operated in the MAN Mode. Dial reading multiplied by 10 equals amplifier gain. Inoperative for all other modes.
B.	MODE	Front panel 5 position rotary switch for selection amplifier Mode of operation.

MAN — Manual gain mode. Amplifier gain determined by GAIN control above

VCA — Amplifier operates as a voltage controlled amplifier when a 0 to +8 volt DC level is applied through CONTROL VOLTAGE BNC or rear panel. 0V = 80db, +8V = 0db

LOG — Amplifier operates as a precision logarithmic amplifier. Amplifier output is held to a constant 0.45 volts average and a DC level on the LOG OUTPUT BNC on the rear panel indicates amplifier gain with a sensitivity of 0. 1v/db.

COMP — Amplifier operates as a compression amplifier. Signals with 80db dynamic range are compressed to less than 20db for recording on magnetic tape. Amplifier output is related to gain by gain (db) = 100 - 200 Eout.

GAIN REC — Provides a means for converting compressed signal amplitude into a DC level corresponding to amplifier gain. Used only for signals recorded

in the comp mode

C. FREQ/SLEW RATE — Front panel 4 position rotary switch used to select the low freqency cutoff and maximum gain slew rate for less than 1/2db error

A.3.5 Monitor Panel

The Ithaco Model 9120-78 provides a phone jack output and level control for monitoring the signal channel output.

A.3.6 Chart Recorder

The operating controls on the Esterline Angus T171B Chart Recorder as follows:

A. RANGE — Front panel 14 position rotary switch used to select desired full scale range. ZERO knob used to select the zero point on the chart.

B. CHART SPEED — Front panel 6 position rotary switch used to select desired chart speed. Any speed so selected can be multiplied by 2 by placing the SPEED MULTIPLIER rocker switch in the X2 position.

C. PEN LIFTER — Front panel toggle for manually raising and lowering the pen.

D. CHART TRANSFER — Front panel thumbwheel for manually advancing the chart paper

E. CHART — Front panel toggle switch for starting and stopping the chart drive motor.

F. SOURCE — Front panel toggle switch for controlling power to the recorder. NOTE: Power Source first must be selected by a 3 position slide switch located on the left side of the case.

G. GAIN ADJ — Rear panel screwdriver potentiometer for adjusting the gain of the balancing amplifier to obtain minimum deadband

H. DAMPING — Rear panel screwdriver potentiometer for controlling the damping (overshoot) of the pen

I. SPAN ADJ — Rear panel srewdriver potentiometer for adjusting full scale span. Used only during calibration in conjunction with an external DC standard.

A.4 System Operation

A.4.1 General

It is firstly necessary to complete the inter-unit cabling as described in A.3.1. Following this basic requirement, the operational steps are as follows:

A. Insure that an adequate supply of ink is loaded into the recorder, and, if battery operation is anticipated, that the recorder batteries are installed and fully charged. Also insure that the batteries are fully charged.

B. Select the desired mode of operation of the recorder by means of the slide switch on the left side.

C. Turn recorder power on and select the desired full scale range and zero point.

D. Select the desired mode of operation for the power supply, preferably to match that of the recorder, with the front panel MODE and POWER switches. The batteries in the power supply should be sufficient for approximately 4 hours of continuous operation. The front panel meter provides an indication of the charge state of the batteries. When the pointer indicates in the red portion, system performance may be compromised by insufficient DC power. At this point, the batteries should be recharged before continuing.

E. Select the desired filter high and low corner frequencies with the rotary switches on the front panel of the filter unit.

F. Set the MODE switch on the amplifier to LOG, and the FREQ/SLEW RATE switch to indicate the frequency equal to or less than the low corner of the filter.

G. Turn the recorder chart drive on and lower the pen.

A.4.2 System Calibration

An overall system calibration should be made for use prior to system operation.

The calibration procedure is as follows:

A. Connect the output of the cal oscillator to the BNC on the rear of the Filter. Set the oscillator to 1 KHz and 0.5 v rms sine wave.

B. Set the Filter for broadband response, and the Amplifier to the LOG mode.

C. Set the recorder to 10 volts full scale and set the indicator eight major chart divisions from the right edge of the chart with the recorder input shorted.

D. Reconnect the recorder to the system and observe the pen indication. Pen should fall on the extreme right line of the chart, and recorder input should measure 8 v dc.

E. Attenuate the CAL signal by 40 db. Pen should indicate 4 major chart division from the right border and its input should be 4 v dc.

F. Attenuate the CAL signal by 80 db. Pen should indicate 8 major chart divisions from the right border and its input should be 0 v dc. NOTE: Since the amplifier is operating at maximum gain, some errors may be observed due to noise in the system.

G. If the system does not satisfactorily meet the above requirements, each unit's calibration should be checked individually. If the system performs satisfactorily, remove the CAL connection between the oscillator and the filter and commence system operation.

A.4.3 Chart Interpretation

With the system calibrated as above, each major division from the right border of the chart represents 10 db of amplifier gain. Consequently, each major division from the right border indicates that the amplifier input is an additional 10 db below 0.5 v rms.

This relationship is as follows:

No. Divisions from right border	Amplifier Gain	Input Signal Level
0	0 db	500 mv rms (0.5v)
1	10	158
2	20	50

3	30	15.8
4	40	5
5	50	1.58
6	60	500 microvolts
7	70	158
8	80	50

For chart readings in between major divisions, the amplifier gain is given by 10 (chart reading), and the amplifier input signal found by multiplying the above value for the lesser whole integer by the factor given below:

Fraction of major division	Multiplier
0.1	0.89
0.2	0.79
0.3	0.71
0.4	0.63
0.5	0.56
0.6	0.50
0.7	0.45
0.8	0.40
0.9	0.35

For example, if chart reading is 3.7 divisions from right border, multiply 15.8 mv rms (corresponding to 3 whole divisions) by 0.45 (corresponding to 0.7 division) to get an input signal level of 7.11 mv rms.

NOTE: For operations purposes, the polarity of the inter-unit cabling between the amplifier and the recorder was reserved. This was done to aid the field staff in interpretation of the recorded information. This resulted in 8 divisions from the right border for the 500 mv rms signal level, 7 divisions for the 158 mv rms signal level, and so on, up to 0 divisions for the 50 microvolts input signal level.

APPENDIX B

Data from Direct

Field Measurements

1971 Discharge Measurement Data for Cross-section Six

Date	Time	Width ft.	Area sq.ft.	Mean Velocity fps	Gauge Height ft.(GSC)	Discharge cfs	A/b_w
June 22	11:20-13:00	285	1168	6.19	30.97	7240	4.1
June 18	8:05-09:05	265	945	4.85	30.07	4580	3.6
June 17	9:15-10:25	265	924	4.74	30.02	4380	3.5
June 16	8:00-09:30	255	945	4.94	30.10	4670	3.7
June 14	9:40-11:00	265	976	5.38	30.40	5250	3.7
June 9	7:50-09:10	270	995	5.43	30.43	5410	3.7
June 7	9:15-11:10	285	1136	5.89	30.84	6730	4.0
June 1	12:10-13:45	255	998	5.42	30.44	5400	3.9
May 31	13:30-15:10	265	989	5:02	30.39	4970	3.7
May 28	7:50-10:00	260	1132	6.00	30.88	6830	4.4

1972 Discharge Measurement Data for Cross-section Six

Date	Time	Width ft.	Area sq.ft.	Mean Velocity fps	Gauge Height ft.(GSC)	Discharge cfs	A/b_w
May 25	08:10-09:35	271	1080	5.20	30.43	5620	4.0
May 30	09:05-09:50	316	1660	7.10	32.20	12400	5.3
June 1	09:05-09:50	310	1510	5.96	31.83	9010	4.9
June 2	12:00-12:40	310	1410	5.87	31.54	8280	4.6
June 5	11:45-12:30	310	1410	5.57	31.54	7860	4.6
June 8	11:55-12:40	311	1530	6.53	32.02	9990	4.9
June 13	09:15-10:00	310	1420	5.26	31.60	7470	4.6
June 15	13:50-14:20	285	1160	5.22	31.21	6050	4.1
June 23	10:18-11:15	293	1140	4.99	31.02	5690	3.9
June 30	10:15-11:20	309	1330	5.39	31.41	7160	4.3
July 11	08:40-09:35	273	1010	4.63	29.05	4680	3.7

Thalweg Distances between River Cross-sections

From	To	Distance in Feet
11	10	2920
10	9	1660
9	8	2330
8	7	4180
7	6	2450
6	5	3070
5	4	2200
4	3	3690
3	2	3850
2	1	5610

Total Distance = 31,960' or 6.053 Miles

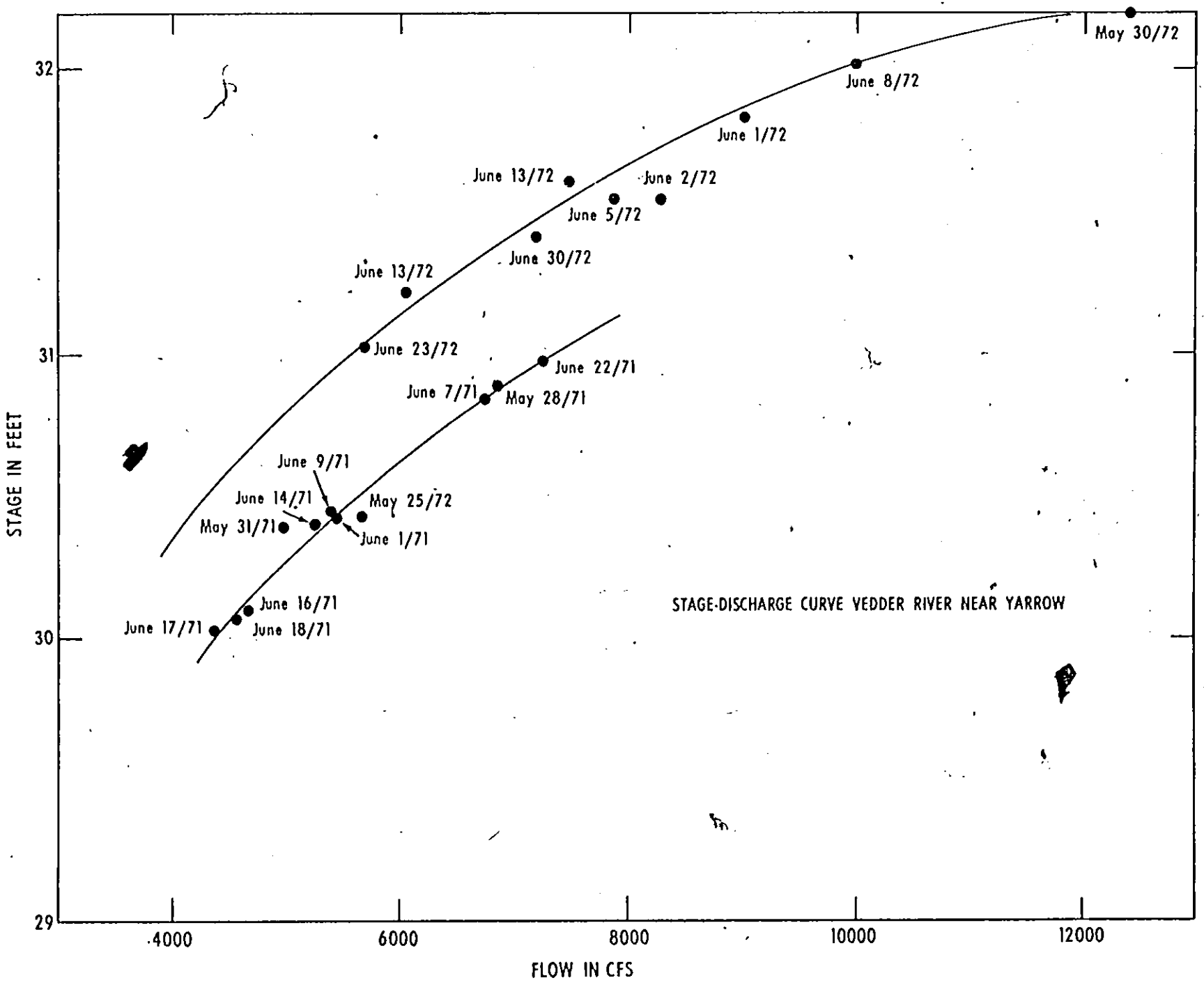
May 30/72
June 8/72
June 1/72
June 13/72
June 2/72
June 5/72
June 30/72
June 13/72
June 23/72
June 22/71
June 7/71
May 28/71
June 9/71
June 14/71
May 25/72
May 31/71
June 1/71
June 16/71
June 17/71
June 18/71
STAGE-DISCHARGE CURVE VEDDER RIVER NEAR YARROW
STAGE IN FEET
32
31
30
29
4000
6000
8000
10000
12000
FLOW IN CFS

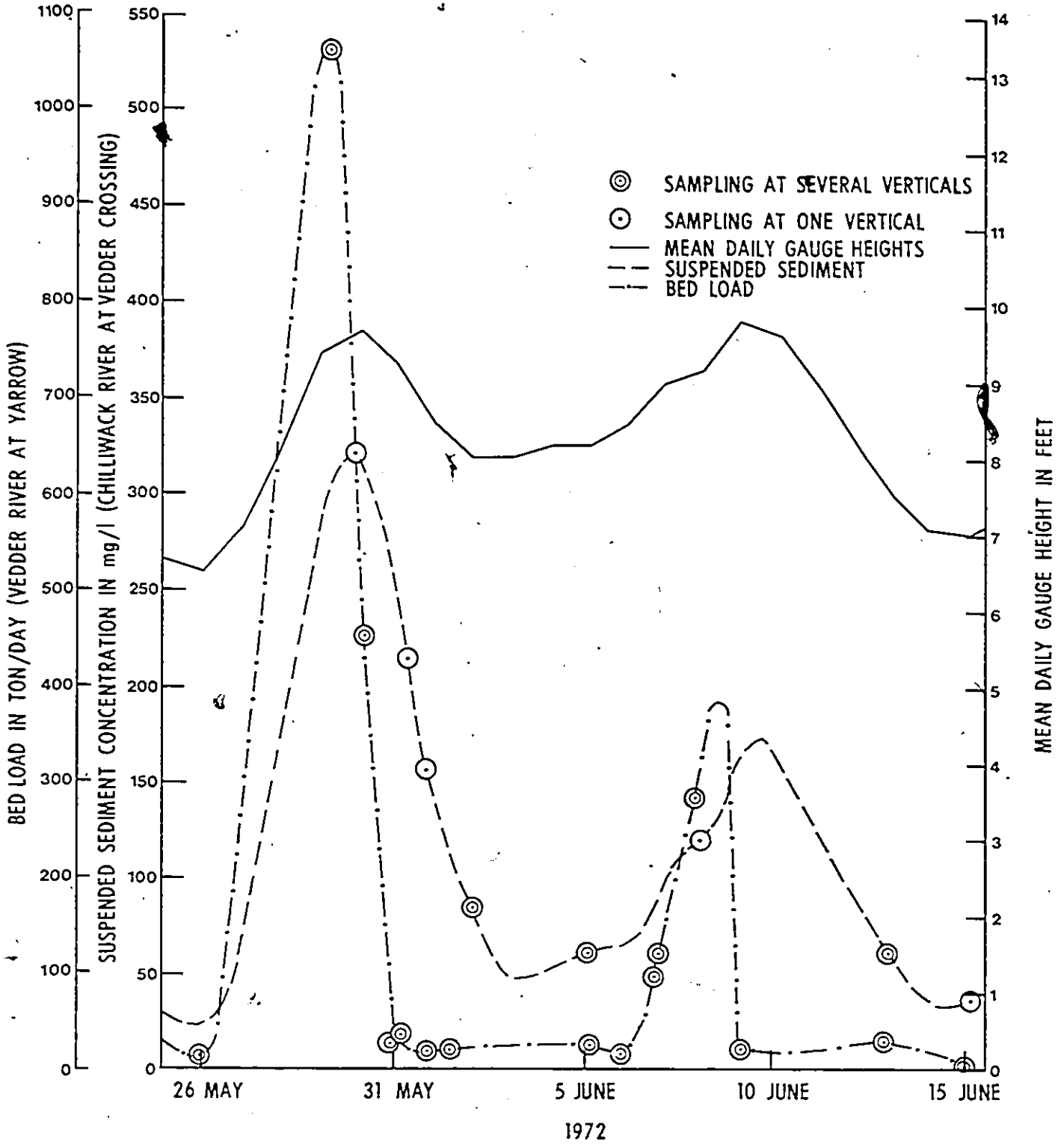

Bed Load and Suspended Sediment Hydrographs
(As Constructed from Sampling Results)
(from Tywoniuk et al, 1973)

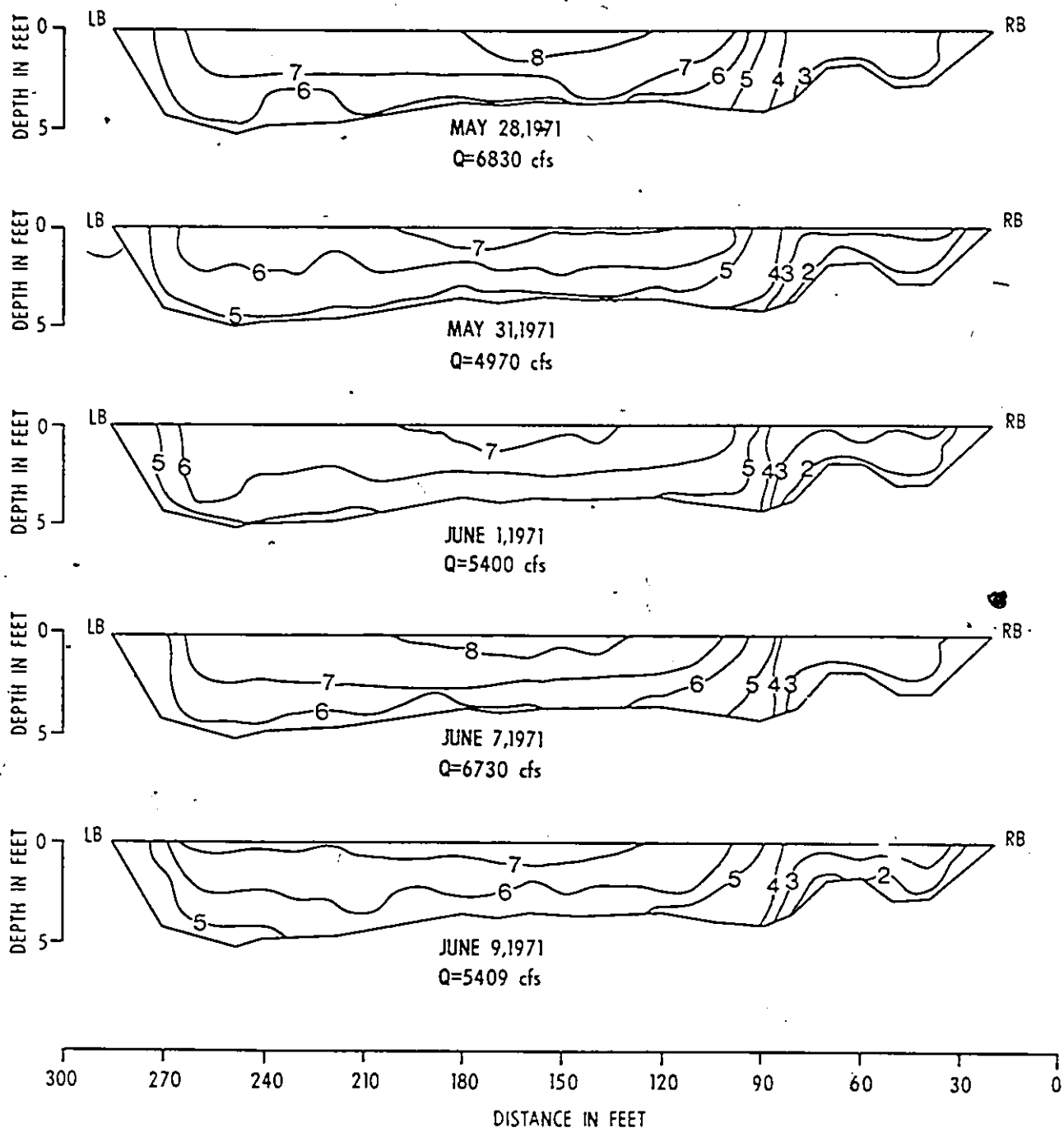

VELOCITY DISTIBUTION CURVES
CROSS SECTION SIX (VEDDER RIVER NEAR YARROW)
CONTOUR INTERVAL:ONE FOOT PER SECOND

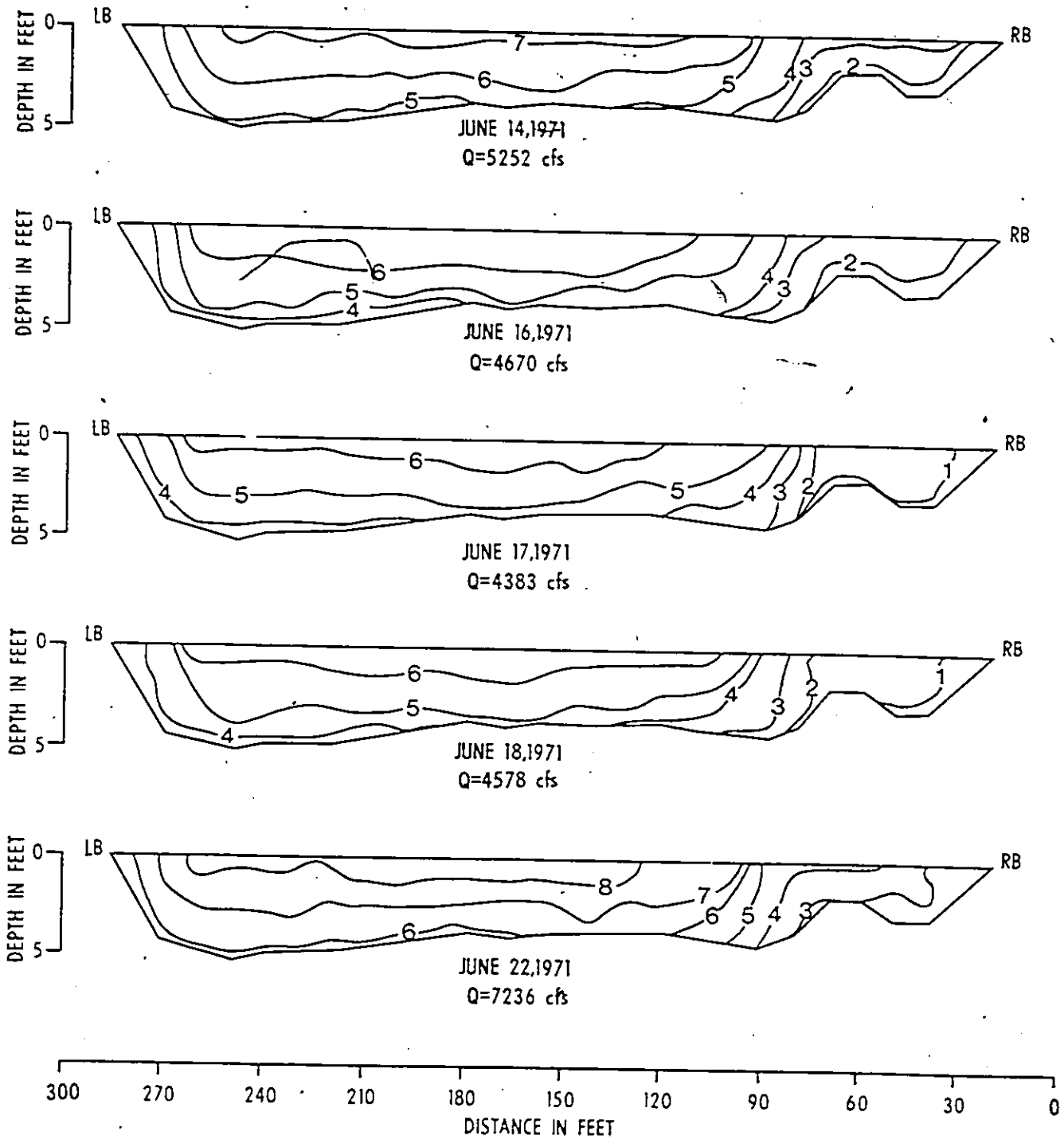

VELOCITY DISTIBUTION CURVES
CROSS SECTION SIX (VEDDER RIVER NEAR YARROW)
CONTOUR INTERVAL:ONE FOOT PER SECOND

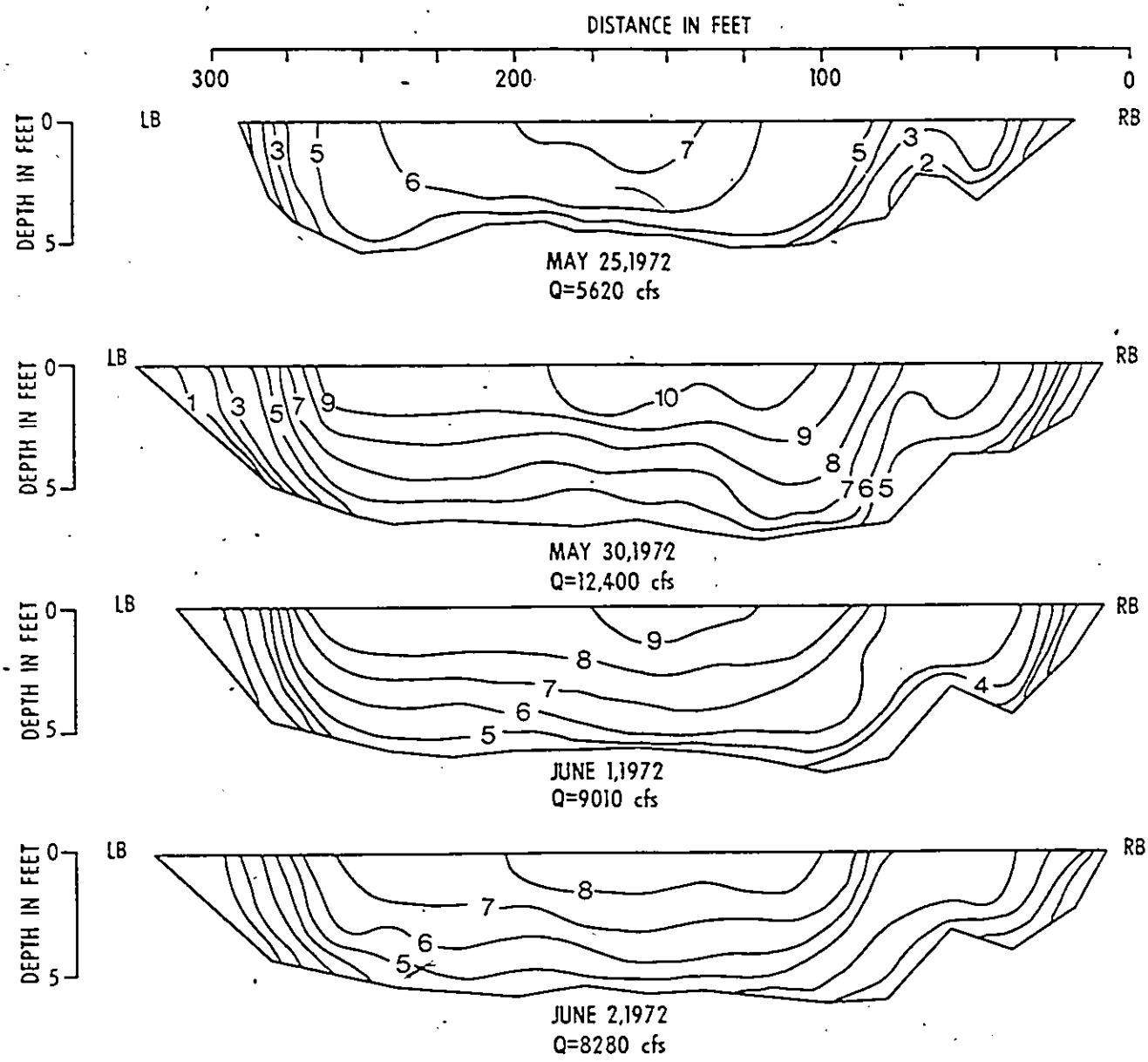

VELOCITY DISTIBUTION CURVES
CROSS SECTION SIX (VEDDER RIVER NEAR YARROW)
CONTOUR INTERVAL:ONE FOOT PER SECOND

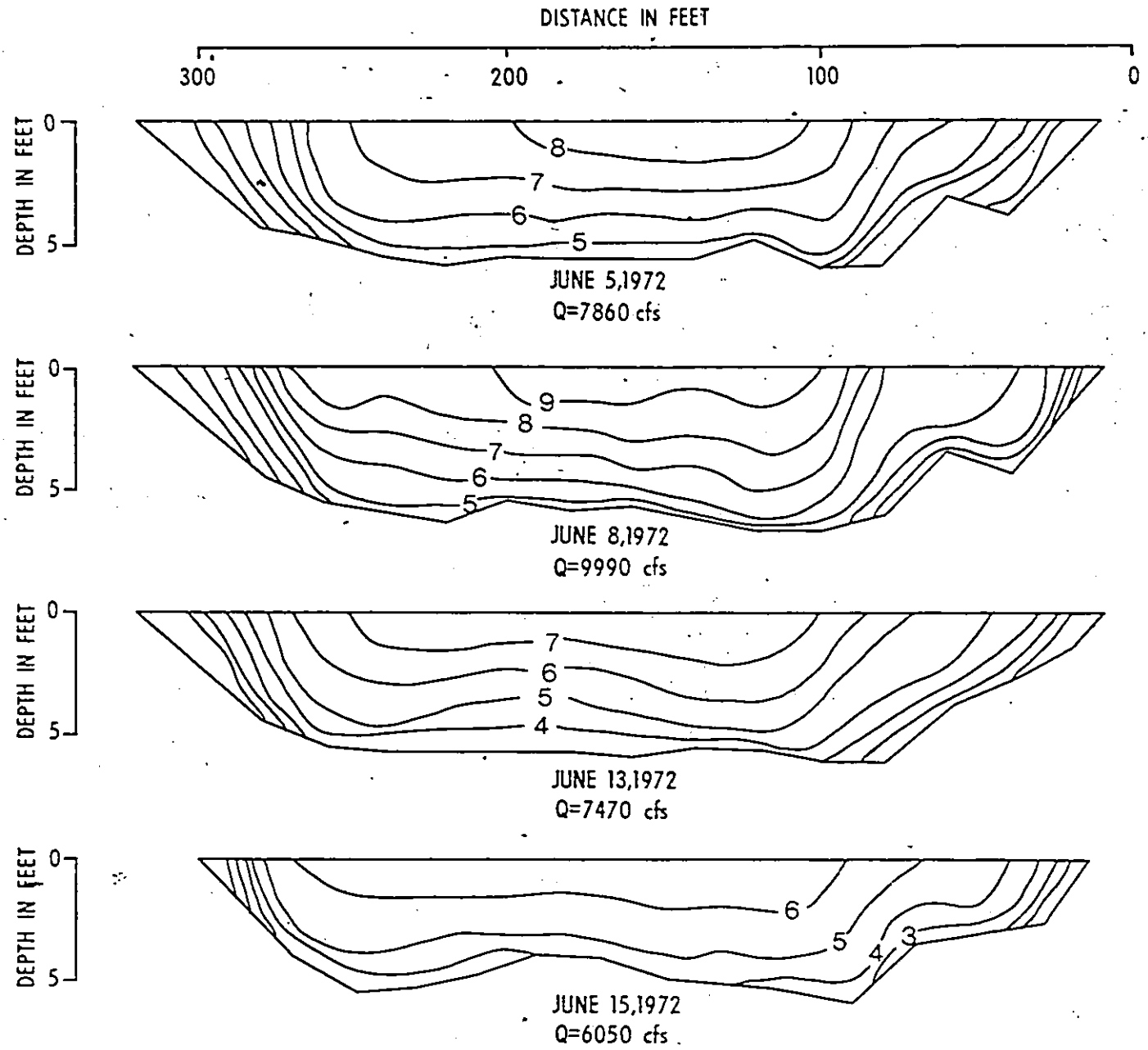

VELOCITY DISTIBUTION CURVES

CROSS SECTION SIX (VEDDER RIVER NEAR YARROW)
CONTOUR INTERVAL:ONE FOOT PER SECOND

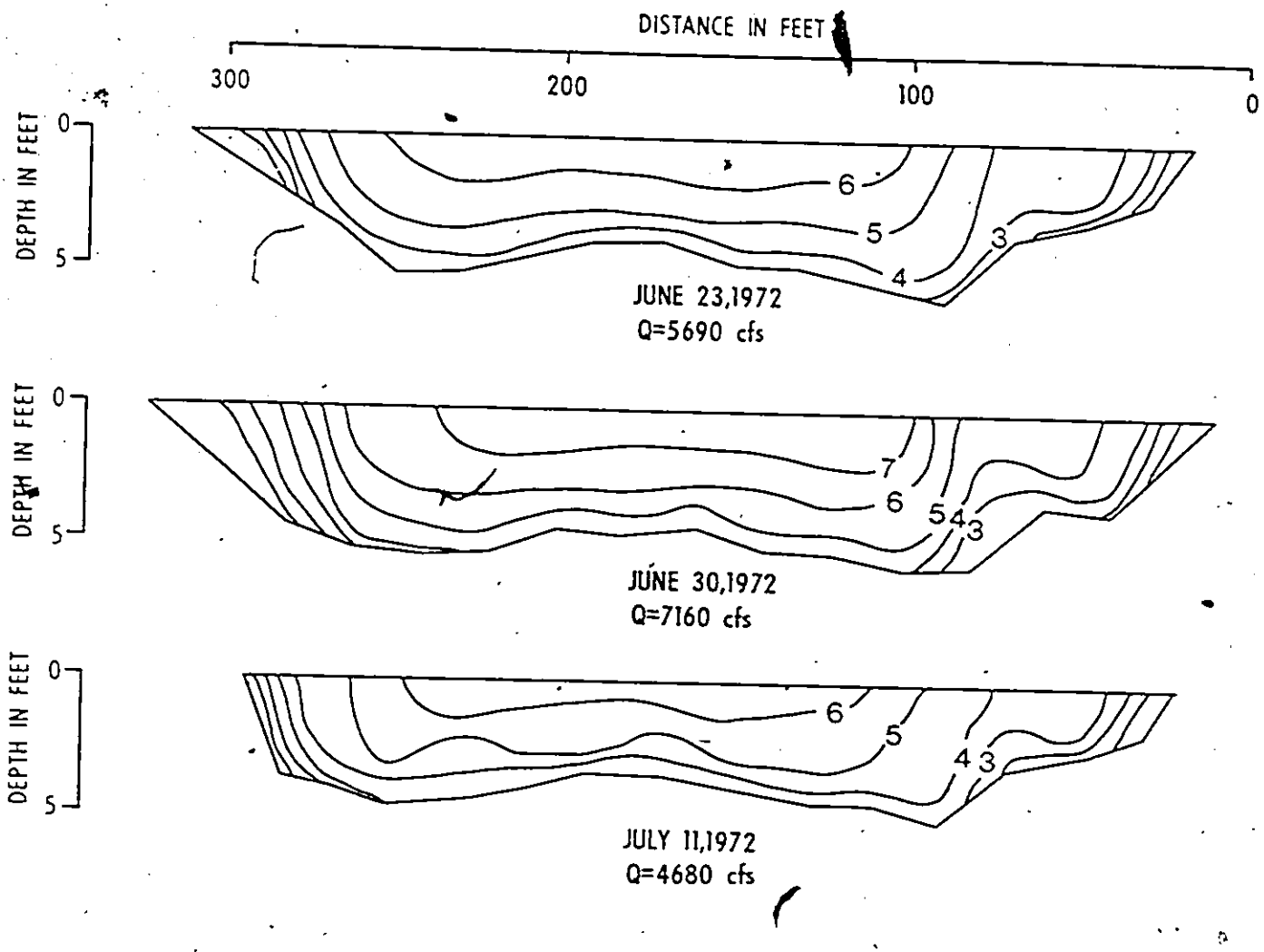

VELOCITY DISTIBUTION CURVES
CROSS SECTION SIX (VEDDER RIVER NEAR YARROW)
CONTOUR INTERVAL:ONE FOOT PER SECOND

Hydrophone Data, May 26, 1972

Test	Location	Freq. Range CPS	Chart Reading, Db Mean	Min	Max	Remarks
1	50	400-20K	35	32	40	
2	75	400-20K	44	43	45	
3	100	400-20K	47	46	48	
4	100	400-800	37	33	40	
5	100	800-1.6K	37	36	40	
6	100	1.6K-3.15K	40	38	42	
7	100	3.15K-6.3K	43	42	44	
8	100	6.3K-12.5K	42	41	44	
9	100	12.5K-25K	30	29	32	
10	125	400-20K	53	51	55	
11	150	400-20K	54	52	58	
12	150	400-20K	54	51	60	
13	150	8.0K-20K	52	49	55	
14	150	16K-20K	46	43	51	
15	200	400-20K	47	46	48	
16	200	400-2.0K	18	16	19	
17	200	400-1.25K	4	3	6	

Hydrophone Data, May 29, 1972

Test	Location	Freq. Range CPS	Chart Reading, Db			Remarks
			Mean	Min	Max	
1	150	200-400	54	50	60	
2	140	200-400	54	50	70	
3	130	200-400	65	55	78	
4	130	200-4K	76	70	83	
5	120	200-400	60	53	70	
6	120	400-800	65	57	80	
7	120	800-1.6K	63	61	66	
8	110	200-400	55	49	62	
9	110	400-800	53	51	55	
10	100	200-400	53	50	58	
11	90	200-400	50	43	60	
12	80	200-400	49	48	51	
13	70	200-400	42	38	48	

Hydrophone Data, May 31, 1972

Test	Location	Freq. Range CPS	Chart Reading, Db Mean	Min	Max	Remarks
1	120	100-200	54	45	60	
2	120	200-400	56	52	62	
3	120	400-800	60	58	64	
4	120	800-1.6K	65	65	66	
5	120	1.6K-3.15K	69	69	70	
6	120	3.15K-6.3K	69	68	72	
7	120	6.3K-12.5K	68	67	70	
8	120	200-400	55	50	61	
9	130	100-200	55	46	62	
10	130	200-400	55	51	59	
11	130	400-800	60	58	64	
12	130	800-1.6K	64	64	65	
13	110	800-1.6K	64	63	66	
14	110	400-800	60	57	64	
15	110	200-400	54	50	58	
16	110	100-200	54	47	62	
17	110	200-400	54	51	56	Test numbers 17 to 21 inclusive were taken at 1/2, 1-1/2, 2-1/2, 3-1/2 and 4-1/2 feet from the bottom respectively.
18	110	200-400	53	49	56	
19	110	200-400	53	50	56	
20	110	200-400	48	48	51	
21	110	200-400	49	48	51	
22	80	100-200	45	40	53	
23	80	200-400	51	48	56	
24	80	400-800	49	48	50	
25	80	800-1.6K	59	58	60	
26	90	100-200	62	55	71	
27	90	200-400	52	45	59	
28	90	400-800	50	48	51	
29	90	800-1.6K	56	55	57	
30	100	100-200	51	45	60	
31	100	200-400	51	48	55	
32	100	400-800	57	56	58	
33	100	800-1.6K	62	61	63	
34	140	100-200	48	42	55	
35	140	200-400	54	50	68	
36	140	400-800	60	58	64	
37	140	800-1.6K	64	64	65	
38	150	100-200	48	41	54	
39	150	200-400	51	49	55	
40	150	400-800	59	58	61	
41	150	800-1.6K	65	63	66	
42	160	100-200	48	41	54	
43	160	200-400	51	48	58	
44	160	400-800	59	58	61	
45	160	800-1.6K	64	64	65	

Hydrophone Data, June 2, 1972

Test	Location	Freq. Range, CPS	Chart Reading, Db			Remarks
			Mean	Min	Max	
1	50	100-200	30	24	42	
2	50	200-400	35	29	49	
3	50	400-800	44	42	46	
4	50	800-1.6K	46	45	47	
5	100	100-200	44	40	50	
6	100	200-400	44	40	50	
7	100	400-800	45	44	46	
8	100	800-1.6K	49	48	51	
9	125	100-200	48	44	55	
10	125	200-400	44	38	55	
11	125	400-800	40	37	44	
12	125	800-1.6K	46	44	58	
13	150	100-200	40	32	48	
14	150	200-400	43	38	48	
15	150	400-800	47	45	49	
16	150	800-1.6K	51	50	52	Test numbers 17 to 21 inclusive were taken at 1/2, 1-1/2, 3-1/2 and 4-1/2 feet from the bottom respectively.
17	150	200-400	43	40	45	
18	150	200-400	43	36	46	
19	150	200-400	41	39	43	
20	150	200-400	41	36	45	
21	150	200-400	45	40	52	
22	175	100-200	45	39	51	
23	175	200-400	37	32	42	
24	175	400-800	37	35	39	
25	175	800-1.6K	43	42	44	
26	225	100-200	46	40	51	
27	225	200-400	37	31	43	
28	225	400-800	37	36	38	
29	225	800-1.6K	43	42	44	

Hydrophone Data, June 7, 1972

Test	Location	Freq. Range CPS	Chart Reading, Db			Remarks
			Mean	Min	Max	
1	50	800-1.6K	59	57	61	
2	50	400-800	49	48	51	
3	50	200-400	42	37	48	
4	50	100-200	40	35	47	
5	100	200-400	48	44	55	
6	125	100-200	56	51	56	
7	125	200-400	54	49	60	
8	125	400-800	58	54	63	
9	125	800-1.6K	62	60	66	
10	150	200-400	52	47	58	
11	175	100-200	50	48	53	
12	175	200-400	52	45	56	
13	175	400-800	57	54	59	
14	175	800-1.6K	60	57	62	
15	200	100-200	55	44	64	
16	225	200-400	53	46	60	
17	35	100-200	15	9	34	
18	35	200-400	10	1	21	
19	35	400-800	38	33	41	
20	35	800-1.6K	52	49	54	
21	35	200-400	20	11	40	
22	35	100-200	14	2	32	

Hydrophone Data, June 8, 1972

Test	Location	Freq. Range CPS	Chart Reading, Db			Remarks
			Mean	Min	Max	
1	50	100-200	36	27	44	
2	50	200-400	45	39	51	
3	100	200-400	35	30	40	
4	100	100-200	45	37	53	
5	112	100-200	43	36	50	
6	112	200-400	46	42	50	
7	125	100-200	46	40	51	
8	125	200-400	40	35	47	
9	125	400-800	43	41	46	
10	125	800-1.6K	51	50	53	
11	137	800-1.6K	47	45	50	
12	137	400-800	42	40	47	
13	137	200-400	39	35	45	
14	137	100-200	52	42	60	
15	150	100-200	45	37	50	
16	150	200-400	48	45	51	
17	175	200-400	50	48	53	
18	175	100-200	48	44	55	
19	200	100-200	50	42	58	
20	200	200-400	37	33	41	

Hydrophone Data, June 12, 1972

Test	Location	Freq. Range CPS	Chart Reading, Db			Depth from bottom (feet)
			Mean	Min	Max	
1	125	100-200	45	40	49	0.1
2	125	200-400	45	42	49	0.1
3	125	400-800	46	45	47	0.1
4	125	800-1.6K	51	50	52	0.1
5	125	100-200	44	42	46	0.3
6	125	200-400	47	43	51	0.3
7	125	400-800	46	46	46	0.3
8	125	800-1.6K	51	50	52	0.3
9	125	100-200	44	40	48	0.6
10	125	200-400	48	46	50	0.6
11	125	400-800	47	46	48	0.6
12	125	800-1.6K	50	49	51	0.6
13	125	100-200	43	41	45	1.0
14	125	200-400	46	44	48	1.0
15	125	400-800	46	44	47	1.0
16	125	800-1.6K	48	48	49	1.0
17	125	100-200	44	43	45	1.5
18	125	200-400	47	43	49	1.5
19	125	400-800	46	46	47	1.5
20	125	800-1.6K	49	48	50	1.5
21	125	100-200	43	41	45	2.0
22	125	200-400	45	44	47	2.0
23	125	400-800	45	43	46	2.0
24	125	800-1.6K	49	49	49	2.0
25	125	100-200	42	39	45	3.0
26	125	200-400	40	39	41	3.0
27	125	400-800	45	43	45	3.0
28	125	800-1.6K	48	47	49	3.0
29	125	100-200	43	41	46	4.0
30	125	200-400	39	37	40	4.0
31	125	400-800	44	42	46	4.0
32	125	800-1.6K	50	46	50	4.0
33	125	100-200	44	43	45	5.0
34	125	200-400	40	39	42	5.0
35	125	400-800	39	39	40	5.0
36	125	800-1.6K	50	49	51	5.0
37	225	100-200	42	40	44	0.1
38	225	200-400	43	41	46	0.1
39	225	400-800	47	45	49	0.1
40	225	800-1.6K	50	49	51	0.1

Hydrophone Data, June 12, 1972 ...cont'd

Test	Location	Freq. Range CPS	Chart Reading, Db Mean	Min	Max	Depth from bottom (feet)
41	225	100-200	39	34	44	0.3
42	225	200-400	45	40	47	0.3
43	225	400-800	46	44	47	0.3
44	225	800-1.6K	49	50	50	0.3
45	225	100-200	42	38	45	0.6
46	225	200-400	44	41	48	0.6
47	225	400-800	46	45	47	0.6
48	225	800-1.6K	49	49	50	0.6
49	225	100-200	43	39	44	1.0
50	225	200-400	45	43	46	1.0
51	225	400-800	46	46	47	1.0
52	225	800-1.6K	49	48	49	1.0
53	225	100-200	42	41	44	1.5
54	225	200-400	44	41	45	1.5
55	225	400-800	47	46	48	1.5
56	225	800-1.6K	47	47	48	1.5
57	225	100-200	42	41	43	2.0
58	225	200-400	42	41	43	2.0
59	225	400-800	45	45	46	2.0
60	225	800-1.6K	47	47	48	2.0
61	225	100-200	42	40	44	3.0
62	225	200-400	39	39	40	3.0
63	225	400-800	46	44	46	3.0
64	225	800-1.6K	48	46	49	3.0
65	225	100-200	41	39	42	4.0
66	225	200-400	37	36	38	4.0
67	225	400-800	41	41	42	4.0
68	225	800-1.6K	48	48	49	4.0
69	225	100-200	43	42	44	5.0
70	225	200-400	40	39	40	5.0
71	225	400-800	41	40	42	5.0
72	225	800-1.6K	47	47	48	5.0

Hydrophone Data, June 15, 1972

Test	Location	Freq. Range CPS	Chart Reading, Db			Depth from bottom (feet)
			Mean	Min	Max	
1	125	100-200	45	38	53	0.3
2	125	200-400	49	43	54	0.3
3	125	400-800	38	35	42	0.3
4	125	800-1.6K	36	34	38	0.3
5	125	100-200	47	41	55	0.6
6	125	200-400	49	44	57	0.6
7	125	400-800	39	37	40	0.6
8	125	800-1.6K	35	33	38	0.6
9	125	100-200	46	40	53	1.0
10	125	200-400	49	41	59	1.0
11	125	400-800	38	33	42	1.0
12	125	800-1.6K	35	32	39	1.0
13	125	100-200	46	39	55	1.5
14	125	200-400	50	42	60	1.5
15	125	400-800	39	35	41	1.5
16	125	800-1.6K	35	34	47	1.5
17	125	100-200	42	39	45	2.0
18	125	200-400	44	40	48	2.0
19	125	400-800	46	45	47	2.0
20	125	800-1.6K	33	33	33	2.0
21	125	100-200	42	39	44	3.0
22	125	200-400	41	40	42	3.0
23	125	400-800	35	34	36	3.0
24	125	800-1.6K	35	35	35	3.0
25	125	100-200	45	43	49	4.0
26	125	200-400	47	41	52	4.0
27	125	400-800	36	31	39	4.0
28	125	800-1.6K	35	34	36	4.0
29	225	100-200	35	30	40	0.3
30	225	200-400	39	34	43	0.3
31	225	400-800	42	41	43	0.3
32	225	800-1.6K	41	39	43	0.3
33	225	100-200	40	35	44	0.6
34	225	200-400	43	36	48	0.6
35	225	400-800	41	39	42	0.6

Hydrophone Data, June 15, 1972 ...cont'd

Test	Location	Freq. Range CPS	Chart Reading, Db Mean	Min	Max	Depth from bottom (feet)
36	225	800-1.6K	42	41	42	0.6
37	225	100-200	39	33	44	1.0
38	225	200-400	45	41	48	1.0
39	225	400-800	43	42	44	1.0
40	225	800-1.6K	40	39	41	1.0
41	225	100-200	43	41	45	1.5
42	225	200-400	46	44	48	1.5
43	225	400-800	43	42	44	1.5
44	225	800-1.6K	41	40	42	1.5
45	225	100-200	37	33	40	2.0
46	225	200-400	39	37	41	2.0
47	225	400-800	42	42	43	2.0
48	225	800-1.6K	39	38	39	2.0
49	225	100-200	34	32	35	3.0
50	225	200-400	36	33	39	3.0
51	225	400-800	40	37	42	3.0
52	225	800-1.6K	39	38	40	3.0
53	225	100-200	40	39	41	4.0
54	225	200-400	40	35	43	4.0
55	225	400-800	40	37	41	4.0
56	225	800-1.6K	40	39	41	4.0

1971 BED LOAD MEASUREMENT DATA
(Cross-section six)

DATE	TIME	FLOW cfs.	SAMPLE LOCATION	SAMPLE TYPE	BED LOAD Tons/Day
June 1	08:45-10:20	5400	50	Basket	nil
			105		nil
			150		nil
			200		nil
			250		nil
June 2	10:20-11:00	5690	50	Basket	nil
			75		nil
			100		nil
			125		nil
			150		nil
			175		nil
			200		nil
			225		nil
			250		nil
June 7	12:50-13:25	6710	50	Basket	nil
			75		nil
			100		nil
			125		nil
			150		nil
			175		nil
			200		nil
			225		nil
			250		nil
June 22	13:30-15:05	7640	50	VUV	.2008
			75		.0135
			100		.1332
			125		.0979
			150		.1716
			175		.0064
			200		.0004
			225		.0015
			250		.0015

1971 BED LOAD MEASUREMENT DATA

DATE	TIME	FLOW cfs.	SAMPLE LOCATION	SAMPLE TYPE	BED LOAD Tons/Day
June 23	09:35-11:05	8040	50	VUV	.0635
			75		.0128
			100		.1416
			120		.0821
			140		.4995
			160		.4761
			180		.0014
			150		.1116
			130		.0921
			170		.1168
			200		.0130
			230		.0154
June 23	12:50-16:00	8040	140	Basket	nil
			140		nil
			140		0.30
			150		nil
			140		3.03
			130		0.32
			160		nil
			120		nil
			130		nil
			140		6.34
			135		0.65
			145		3.75
			150		nil
June 24	08:30-09:35	6990	140	Basket	nil
			130		nil
			150		nil
			135		nil
			125		nil

1971 BED LOAD MEASUREMENT DATA

DATE	TIME	FLOW cfs.	SAMPLE LOCATION	SAMPLE TYPE	BED LOAD Tons/Day
June 24	11:40-13:35	6990	70	¼VUV	.0096
			100		.0912
			120		.2760
			140		.0161
			140		.0774
			160		.0091
			200		.0066
			240		.0044
			50		.0249
			70		.0074
			90		.0315
			100		.1929
			110		.1782
			120		.1902
			130		.1123
			140		.1148
			200		.0118
June 25	08:50-10:45	6970	50	¼VUV	.0723
			30		.0051
			70		.0123
			90		.0351
			100		.0615
			110		.2817
			120		.1351
			130		.0671
			150		.0327
			140		.0385
			160		.0028
			200		.0016
			240		.0015
			100		.0991
			120		.0104
			120		.0503
			140		.0037

1972 BED LOAD MEASUREMENT DATA
(Cross-section six)

DATE	TIME	FLOW cfs.	SAMPLE LOCATION	SAMPLE TYPE	BED LOAD Tons/Day
May 26	10:05-10:50	5210	50	VUV	.0107
			100		.0153
			150		.0439
			200		.0006
			250		.0007
			50		.0103
May 29	15:20-16:38	11220	50	Basket	nil
			100		nil
			100		nil
			125		29.5
			112		nil
			112		5.76
			137		0.12
May 30	12:15-15:26	12480	50	Basket	nil
			75		nil
			100		nil
			125		nil
			150		0.72
			175		2.52
			200		nil
			225		nil
			225		0.60
			250		0.60
			225		nil
			200		3.00
			187		nil
			175		0.06
			162		0.12
			150		0.03
			137		5.04
			125		0.12
			112		0.12
			100		1.80

1972 BED LOAD MEASUREMENT DATA

DATE	TIME	FLOW cfs.	SAMPLE LOCATION	SAMPLE TYPE	BED LOAD Tons/Day
May 31	11:50-12:37	11640	50	Basket	nil
			100		nil
			125		0.24
			150		0.06
			137		0.48
			175		nil
			200		nil
			225		nil
	13:20-14:32	11300	50	¼VUV	.0298
			100		0.233
			125		.0037
			150		.0065
			175		.0153
			200		.0211
			225		.0020
June 1	10:07-10:40	9630	50	Basket	nil
			100		nil
			125		nil
			150		0.06
			175		nil
			225		nil
	11:30-12:37	9630	50	¼VUV	.0544
			100		.0161
			125		.1052
			150		.0066
			175		.0029
			225		.0167
June 2	10:21-11:10	8250	50	¼VUV	.0387
			100		.1277
			125		.0247
			150		.0067
			175		.0075
			225		.0077

1972 BED-LOAD MEASUREMENT DATA

DATE	TIME	FLOW cfs.	SAMPLE LOCATION	SAMPLE TYPE	BED LOAD Tons/Day
June 5	13:56-14:35	8330	50	¼VUV	.0467
			100		.0811
			125		.1042
			150		.0204
			175		.0043
			225		.0042
June 6	08:12-08:41	9400	50	Basket	nil
			100		nil
			125		nil
			150		nil
			175		nil
			225		nil
	09:00-10:18	9350	50	¼VUV	.0883
			100		.0284
			125		.0062
			150		.0183
			175		.0147
			225		.0058
June 7	08:49-09:56	10800	50	¼VUV	.0453
			100		.1610
			125		.4043
			150		.1671
			137		.2292
			175		.4015
			200		.0110
			225		.0044
	10:24-11:41	10800	50	Basket	nil
			100		0.60
			125		nil
			125		1.2
			150		nil
			150		nil

1972 BED LOAD MEASUREMENT DATA

DATE	TIME	FLOW cfs.	SAMPLE LOCATION	SAMPLE TYPE	BED LOAD Tons/Day
June 7	(continued)	10800	137		0.09
			137		0.03
			175		0.24
			175		0.60
			162		1.20
			162		0.06
			200		nil
			225		nil
June 8	08:27-09:53	11020	50	Basket	nil
			100		nil
			125		0.24
			125		6.0
			125		7.2
			112		1.2
			112		0.36
			100		0.36
			137		nil
			137		0.06
			150		nil
			175		nil
			200		0.06
			225		nil
June 9	14:06-14:51	13120	50	Basket	nil
			100		nil
			125		0.72
			125		0.12
			125		0.48
			150		nil
			150		nil
			175		nil
			175		nil

1972 BED LOAD MEASUREMENT DATA

DATE	TIME	FLOW cfs.	SAMPLE LOCATION	SAMPLE TYPE	BED LOAD Tons/Day
June 13	08:17-09:01	7400	50	¼VUV	.0179
			100		.2045
			125		.0096
			150		.0035
			175		.0029
			225		.0035
June 15	11:30-12:28	6200	50	¼VUV	.0131
			100		.0334
			125		.0210
			150		.0053
			175		.0035
			225		.0014
June 23	09:03-09:50	5860	50	¼VUV	.0204
			75		.0120
			100		.1548
			125		.0321
			150		.0111
			175		.0037
			225		.0032
June 30	08:45-10:04	7360	50	¼VUV	.0161
			100		.0149
			75		.0334
			125		.0985
			125		.0522
			150		.0154
			137		.0019
			175		.0072
			200		.0045
			225		.0058

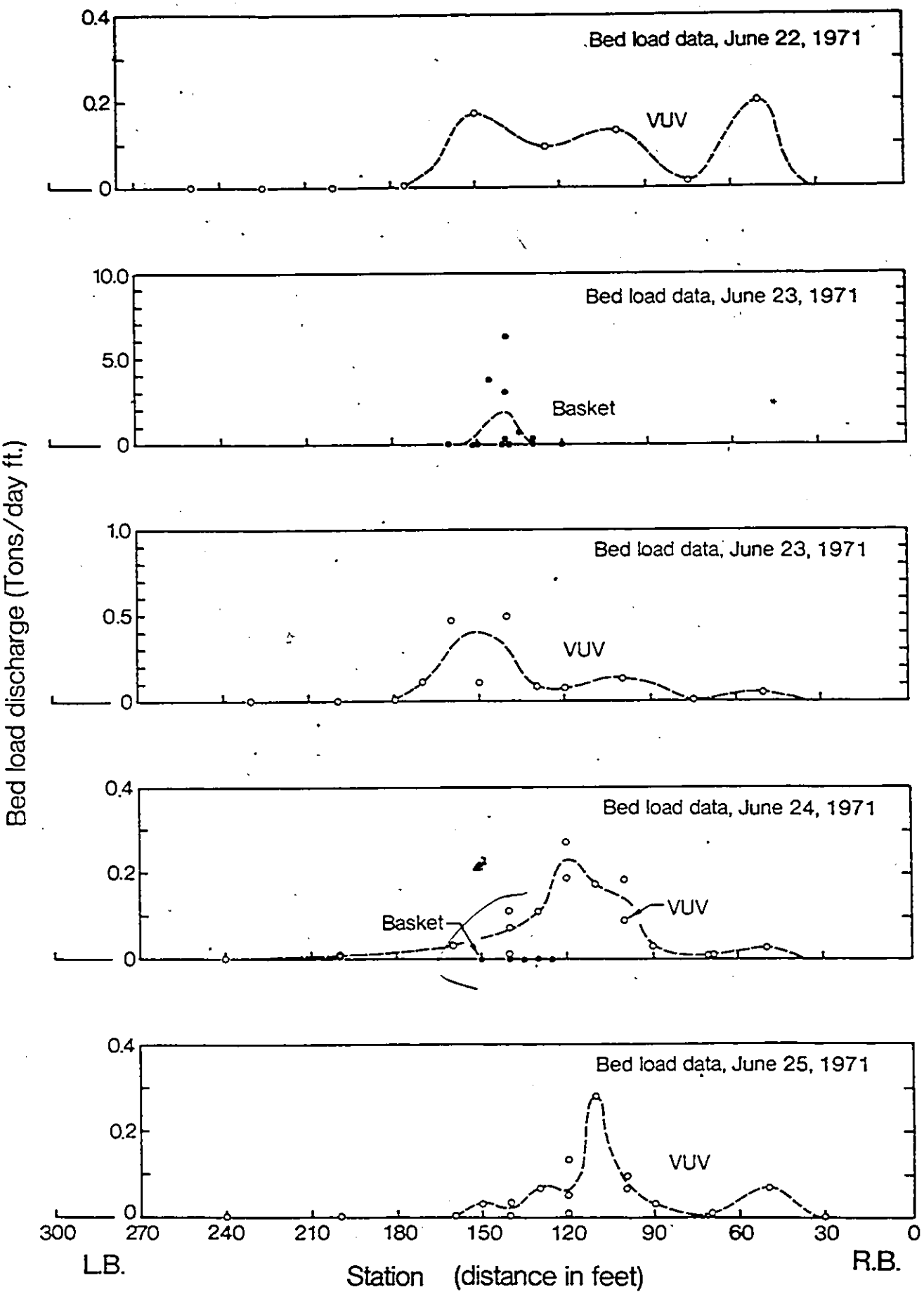
Bed load data, June 22, 1971
VUV
0.4
0.2
0
Bed load data, June 23, 1971
Basket
10.0
5.0
0
Bed load data, June 23, 1971
VUV
1.0
0.5
0
Bed load data, June 24, 1971
Basket
VUV
0.4
0.2
0
Bed load data, June 25, 1971
VUV
0.4
0.2
0
Bed load discharge (Tons/day ft.)
300 270 240 210 180 150 120 90 60 30 0
L.B.
Station (distance in feet)
R.B.

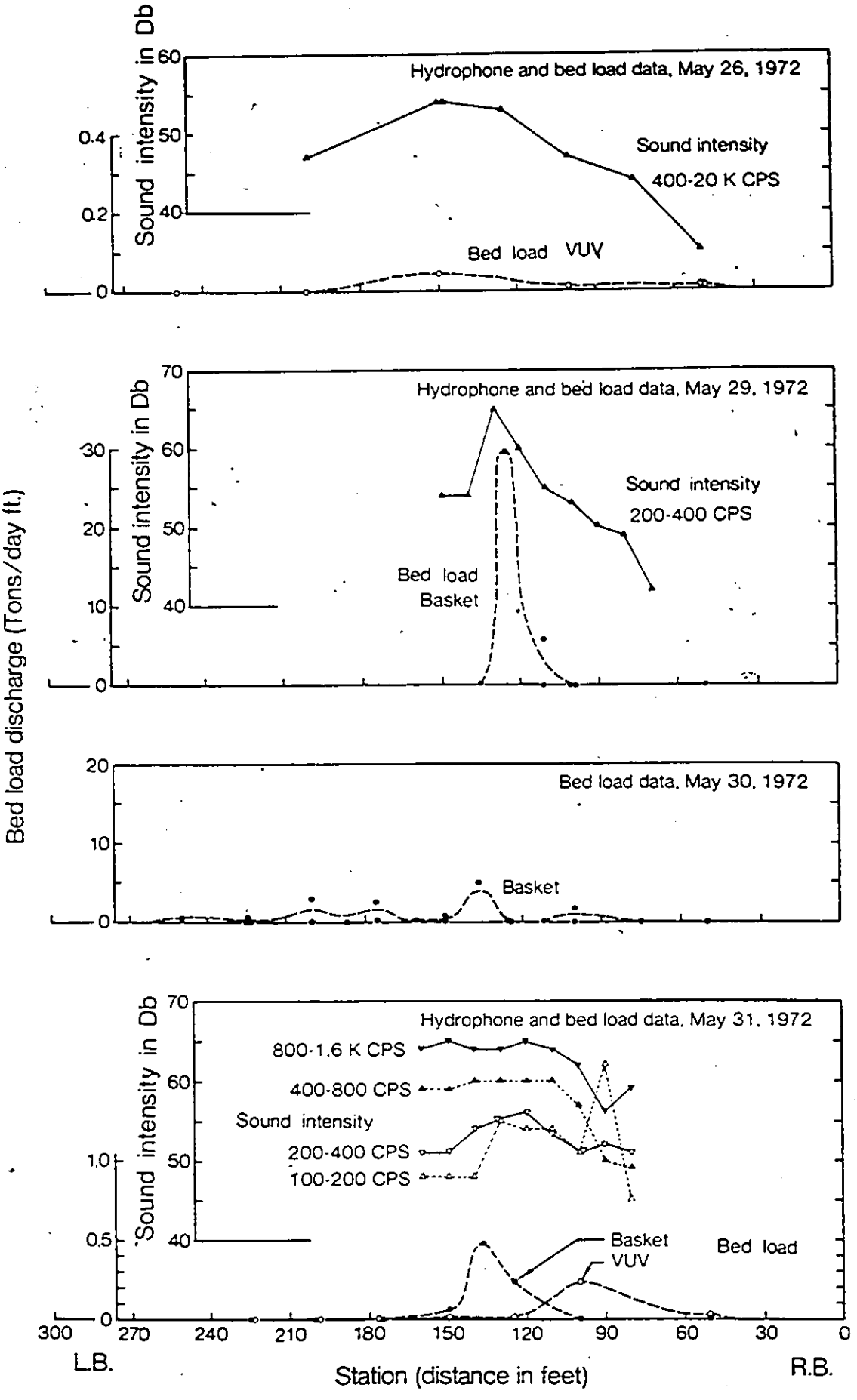
Hydrophone and bed load data, May 26, 1972
Sound intensity in Db
Sound intensity
400-20 K CPS
Bed load VUV
Hydrophone and bed load data, May 29, 1972
Sound intensity
200-400 CPS
Bed load
Basket
Bed load data, May 30, 1972
Basket
Hydrophone and bed load data, May 31, 1972
800-1.6 K CPS
400-800 CPS
Sound intensity
200-400 CPS
100-200 CPS
Basket
VUV
Bed load
Bed load discharge (Tons/day ft.)
L.B.
R.B.
Station (distance in feet)

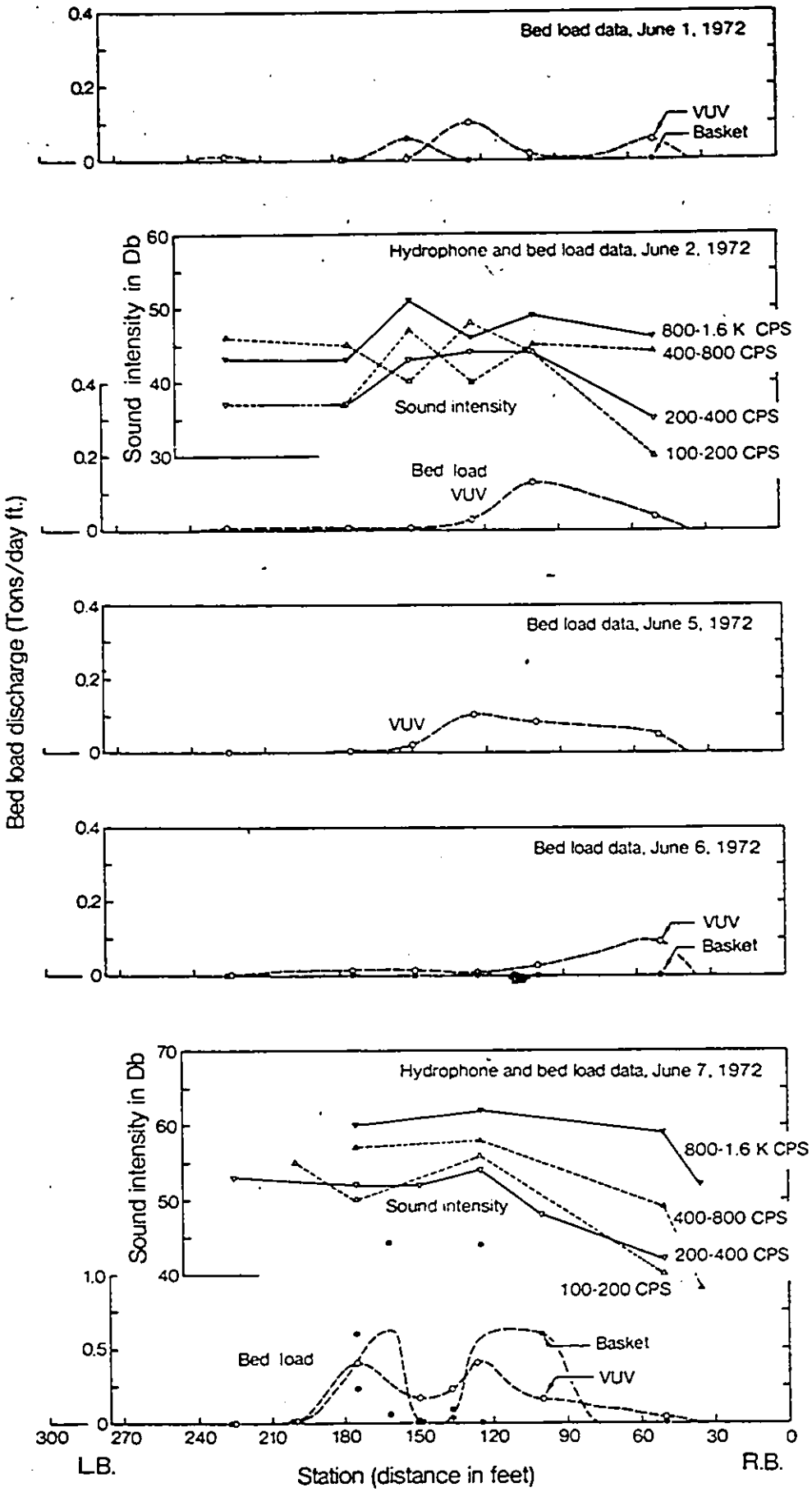
Bed load data, June 1, 1972
VUV
Basket
Hydrophone and bed load data, June 2, 1972
Sound intensity in Db
800-1.6 K CPS
400-800 CPS
Sound intensity
200-400 CPS
100-200 CPS
Bed load
VUV
Bed load data, June 5, 1972
VUV
Bed load data, June 6, 1972
VUV
Basket
Hydrophone and bed load data, June 7, 1972
Sound intensity in Db
800-1.6 K CPS
Sound intensity
400-800 CPS
200-400 CPS
100-200 CPS
Bed load
Basket
VUV
Bed load discharge (Tons/day ft.)
LB.
Station (distance in feet)
R.B.

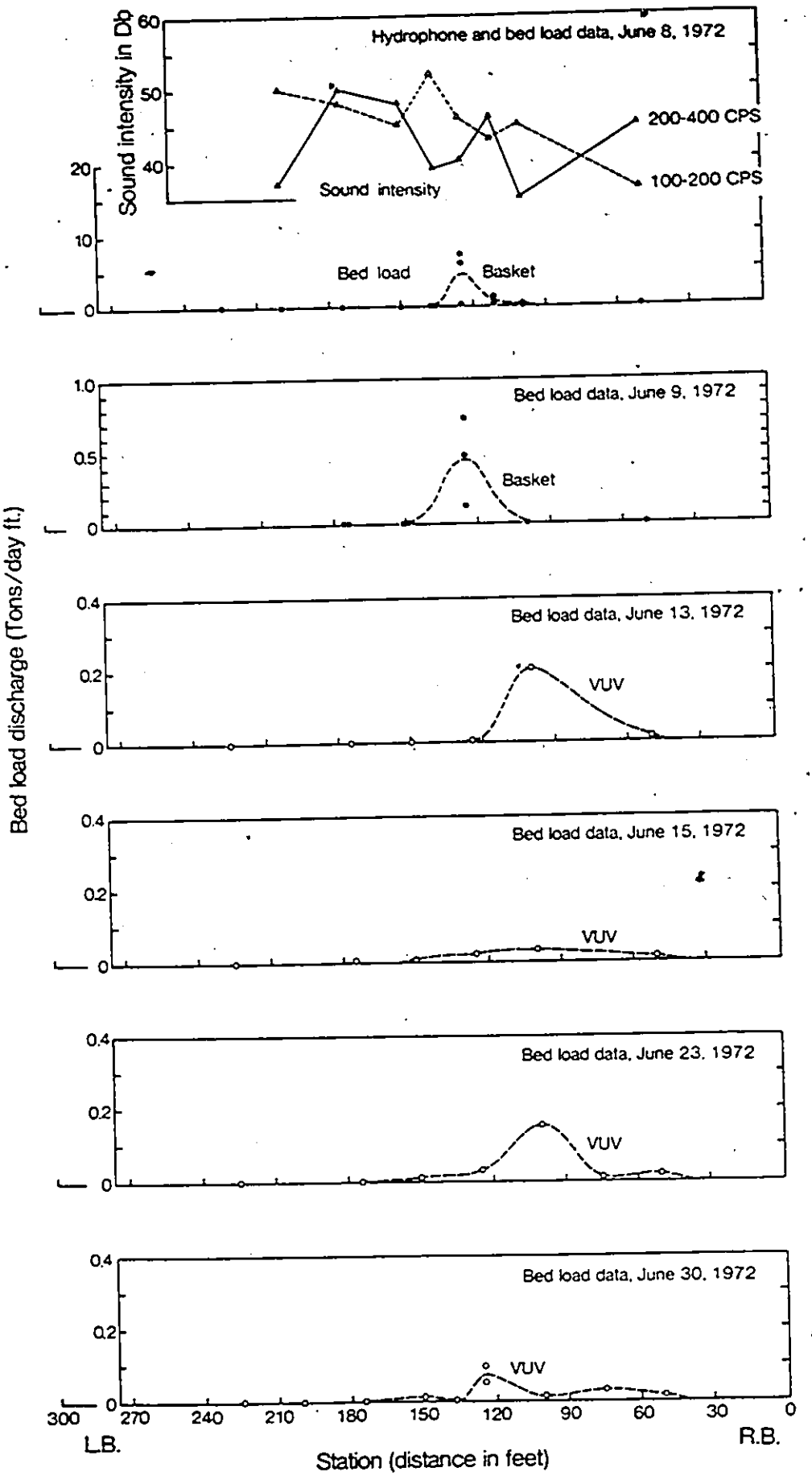
Hydrophone and bed load data, June 8, 1972
Sound intensity in Db
60
50
40
20
10
0
200-400 CPS
100-200 CPS
Sound intensity
Bed load
Basket
Bed load data, June 9, 1972
1.0
0.5
0
Basket
Bed load data, June 13, 1972
0.4
0.2
0
VUV
Bed load data, June 15, 1972
VUV
Bed load data, June 23, 1972
VUV
Bed load data, June 30, 1972
VUV
Bed load discharge (Tons/day ft.)
300
270
240
210
180
150
120
90
60
30
0
L.B.
R.B.
Station (distance in feet)

Sound Intensities (Decibels), Bed Load (VUV) and Velocity Data, 1972

Date	Station	Bed Load T/d.f	Freq. Range, CPS (Field)				Botton Velocity ft./sec.	Freq. Range, CPS (Background)				Freq. Range, CPS (Difference)			
			100-200	200-400	400-800	800-1.6K		100-200	200-400	400-800	800-1.6K	100-200	200-400	400-800	800-1.6K
May 31	80	.12	45	51	49	59	3.6	49	36	22	21	--	50.9	49.0	59.0
	90	.20	62	52	50	56	6.3	51	42	29	34	61.6	51.5	50.0	56.0
	100	.24	51	51	57	62	5.4	49	40	28	29	46.7	50.6	57.0	62.0
	110	.14	54	54	60	64	5.6	49	40	28	30	52.4	53.8	60.0	64.0
	120	.04	54	56	60	65	5.5	49	40	28	30	52.4	55.9	60.0	65.0
	130	.01	54	54	60	64	6.2	50	41	28	34	51.8	53.8	60.0	64.0
	140	.01	48	54	60	64	6.3	51	42	29	34	--	53.7	60.0	64.0
	150	.01	48	51	59	65	7.0	52	42	30	31	--	50.4	59.0	65.0
	160	0	48	51	59	63	6.8	51	42	30	32	--	50.4	59.0	63.0
June 2	50	.04	30	35	44	46	4.2	49	38	23	25	--	--	44.0	46.0
	60	.06	39	37	44	46	4.5	49	38	24	26	--	--	44.0	46.0
	70	.08	36	39	44	47	3.8	49	36	22	22	--	36.0	44.0	47.0
	80	.10	39	41	45	48	3.1	49	34	22	18	--	40.0	45.0	48.0
	90	.12	41	42	45	48	3.8	49	36	22	22	--	40.7	45.0	48.0
	100	.13	44	44	45	49	4.4	49	38	24	25	--	42.7	45.0	49.0
	110	.10	46	44	43	48	5.0	48	39	27	27	--	42.4	42.9	48.0
	120	.04	48	44	41	46	5.6	49	40	28	30	--	41.8	40.8	45.9
	130	.02	47	44	42	47	5.8	50	40	28	32	--	41.8	41.8	46.9
	140	.01	44	44	45	49	5.9	50	41	29	32	--	41.0	44.9	48.9
	150	.01	40	43	47	51	6.1	50	41	29	34	--	38.7	46.9	50.9
	160	.01	42	41	44	48	6.2	50	41	29	34	--	--	43.9	47.8
	170	.01	44	38	39	45	5.9	50	41	29	32	--	--	38.5	44.8
	180	.01	45	37	37	43	5.6	49	40	28	30	--	--	36.4	42.8
	190	.01	45	37	37	43	5.3	49	40	28	28	--	--	36.4	42.9
	200	.01	45	37	37	43	5.0	48	39	27	27	--	--	36.5	41.9
	210	.01	46	37	37	43	5.2	49	39	28	28	--	--	36.4	42.9
	220	.01	46	37	37	43	5.4	49	40	28	29	--	--	36.4	42.8

Sound Intensities (Decibels), Bed Load (VUV) and Velocity Data, 1972 Cont'd

Date	Station	Bed Load T/d.f	Freq. Range, CPS (Field)				Bottom Velocity ft./sec.	Freq. Range, CPS (Background)				Freq. Range, CPS (Difference)			
			100-200	200-400	400-800	800-1.6K		100-200	200-400	400-800	800-1.6K	100-200	200-400	400-800	800-1.6K
June 7	40	.01	—	—	41	54	4.5	49	38	24	26	--	40.4	40.9	54.0
	50	.02	40	42	49	59	4.0	49	37	22	24	—	40.8	49.0	59.0
	60	.02	42	43	50	59	5.1	49	39	28	27	--	44.0	50.0	59.0
	70	.04	45	45	52	60	4.5	49	38	24	26	--	45.4	52.0	60.0
	80	.04	46	46	53	60	3.8	49	37	22	22	—	45.4	53.0	60.0
	90	.06	49	47	54	61	5.0	49	39	27	27	—	46.3	54.0	61.0
	100	.07	51	48	55	61	6.3	51	42	29	34	--	46.7	55.0	61.0
	110	.09	53	50	56	61	6.6	51	42	29	34	48.7	49.3	56.0	61.0
	120	.15	55	53	57	62	6.8	51	42	30	32	52.8	52.6	57.0	62.0
	130	.15	55	54	58	62	6.5	51	42	29	34	52.8	53.7	58.0	62.0
	140	.08	54	53	58	61	6.2	50	41	29	34	51.8	52.7	58.0	61.0
	150	.07	53	52	58	61	6.2	50	41	29	34	48.7	51.6	58.0	61.0
	160	.11	52	52	57	62	6.8	51	42	30	32	45.1	51.5	57.0	62.0
	170	.15	51	52	57	60	6.5	51	42	29	34	--	51.5	57.0	60.0
	180	.15	51	52	57	60	6.1	50	41	29	34	44.1	51.6	57.0	60.0
	190	.06	53	52	--	--	6.1	50	41	29	34	48.7	51.6	—	--
	200	.01	55	53	—	--	6.1	50	41	29	34	53.4	52.7	—	—

NOTES: 1. Bed load and sound intensity data were taken from Appendix B. Hydrometric measurement data were utilized in determining bottom velocities.
2. "Background" sound intensities were obtained from figure 3.4(a); "difference" values were computed by subtracting "background" from "field" or insitu values utilizing equation 2.31.

Sound Intensities (Decibels), Bed Load (Basket) and Velocity Data, 1972

Date	Station	Bed Load T/d.f	Freq. Range, CPS (Field)				Bottom Velocity ft./sec.	Freq. Range, CPS (Background)				Freq. Range, CPS (Difference)			
			100-200	200-400	400-800	800-1.6K		100-200	200-400	400-800	800-1.6K	100-200	200-400	400-800	800-1.6K
May 29	100	0	—	53	—	—	7.2	—	42	—	—	—	52.6	—	—
	110	3.0	—	55	—	—	7.2	—	42	—	—	—	54.8	—	—
	120	14.0	—	60	—	—	7.1	—	42	—	—	—	59.9	—	—
	130	25.0	—	65	—	—	6.7	—	42	—	—	—	65.0	—	—
	140	0	—	54	—	—	6.3	—	41	—	—	—	53.8	—	—
May 31	100	0	51	51	57	62	5.4	49	40	28	29	46.7	50.6	57.0	62.0
	110	0.10	54	54	60	64	5.6	49	40	28	30	52.4	53.8	60.0	64.0
	120	0.16	54	56	60	65	5.5	49	50	28	30	52.4	54.7	60.0	65.0
	130	0.35	54	54	60	64	6.2	50	41	29	34	51.8	53.8	60.0	64.0
	140	0.43	48	54	60	64	6.3	51	42	29	34	—	53.7	60.0	64.0
	150	0.13	48	51	59	65	7.0	52	42	30	31	—	50.4	59.0	65.0
	160	0.06	48	51	59	63	6.8	52	42	30	32	—	50.4	59.0	63.0
June 7	80	0	46	46	53	60	3.8	49	37	22	22	—	45.4	53.0	60.0
	90	0.30	49	47	54	61	5.0	49	39	27	27	—	46.3	53.0	61.0
	100	0.60	51	48	55	61	6.3	51	42	29	34	—	46.7	55.0	61.0
	110	0.63	53	50	56	61	6.6	51	42	29	33	48.7	49.3	56.0	61.0
	120	0.62	55	53	57	62	6.8	52	42	30	32	52.0	52.6	57.0	62.0
	130	0.40	55	54	58	62	6.5	51	42	29	34	52.8	53.7	58.0	62.0
	140	0	54	53	58	61	6.2	50	41	29	34	51.8	52.7	58.0	61.0
	150	0	53	52	58	61	6.2	50	41	29	34	50.0	51.6	58.0	61.0
	160	0.62	52	52	57	62	6.8	52	42	30	32	—	51.5	57.0	62.0
	170	0.54	51	52	57	60	6.5	51	42	29	34	—	51.5	57.0	60.0
	180	0.32	51	52	57	60	6.1	50	41	29	34	44.1	51.6	57.0	60.0
	190	0.10	53	52	—	—	6.1	50	41	—	—	50.0	51.6	—	—
	200	0.02	55	53	—	—	6.1	50	41	—	—	53.4	52.7	—	—
	210	0	—	53	—	—	5.9	50	41	—	—	—	52.7	—	—

Sound Intensities (Decibels), Bed Load (Basket) and Velocity Data, 1972 Cont'd

Date 1972	Station	Bed Load T/d.f	Freq. Range, CPS (Field)				Botton Velocity ft./sec.	Freq. Range, CPS (Background)				Freq. Range, CPS (Difference)			
			100-200	200-400	400-800	800-1.6K		100-200	200-400	400-800	800-1.6K	100-200	200-400	400-800	800-1.6K
June 8	100	0.2	45	35	—	—	6.3	51	42	—	—	--	—	—	—
	110	0.8	43	46	—	—	6.6	51	42	—	—	--	43.8	—	—
	120	3.3	45	42	—	—	6.8	51	42	—	—	--	—	—	—
	130	2.6	49	40	—	—	6.5	51	42	—	—	--	—	—	—
	140	0	50	42	—	—	6.2	50	41	—	—	--	35.1	—	—

NOTES: 1. Bed load and sound intensity data were taken from Appendix B. Hydrometric measurement data were utilized in determining bottom velocities.
2. "Background" sound intensities were obtained from figure 3.4(a); "difference" values were computed by subtracting "background" from "field" or insitu values utilizing equation 2.31.

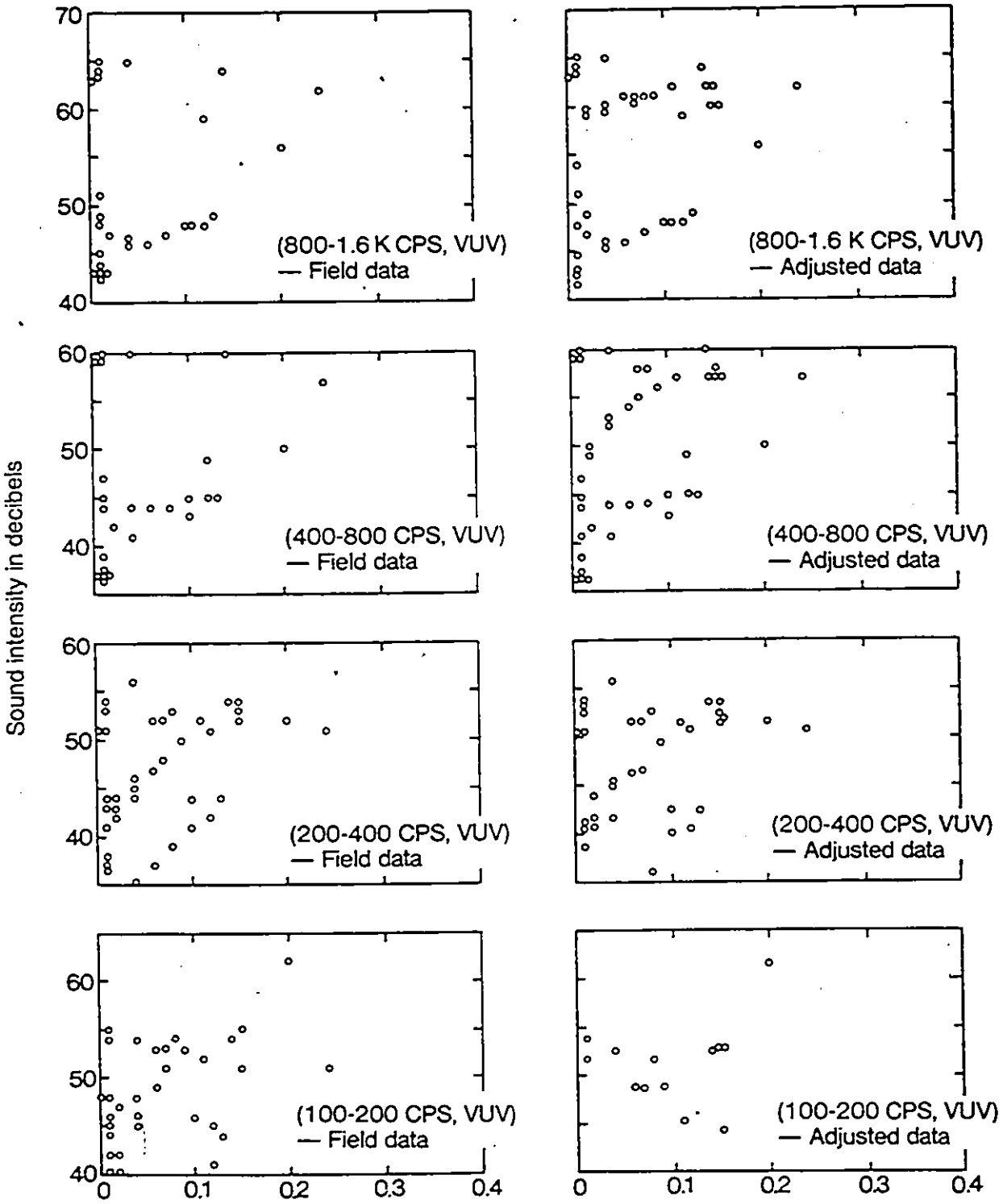
(800-1.6 K CPS, VUV)
— Field data
(800-1.6 K CPS, VUV)
— Adjusted data
(400-800 CPS, VUV)
— Field data
(400-800 CPS, VUV)
— Adjusted data
(200-400 CPS, VUV)
— Field data
(200-400 CPS, VUV)
— Adjusted data
(100-200 CPS, VUV)
— Field data
(100-200 CPS, VUV)
— Adjusted data
Sound intensity in decibels
Bed load discharge, Tons/day ft.

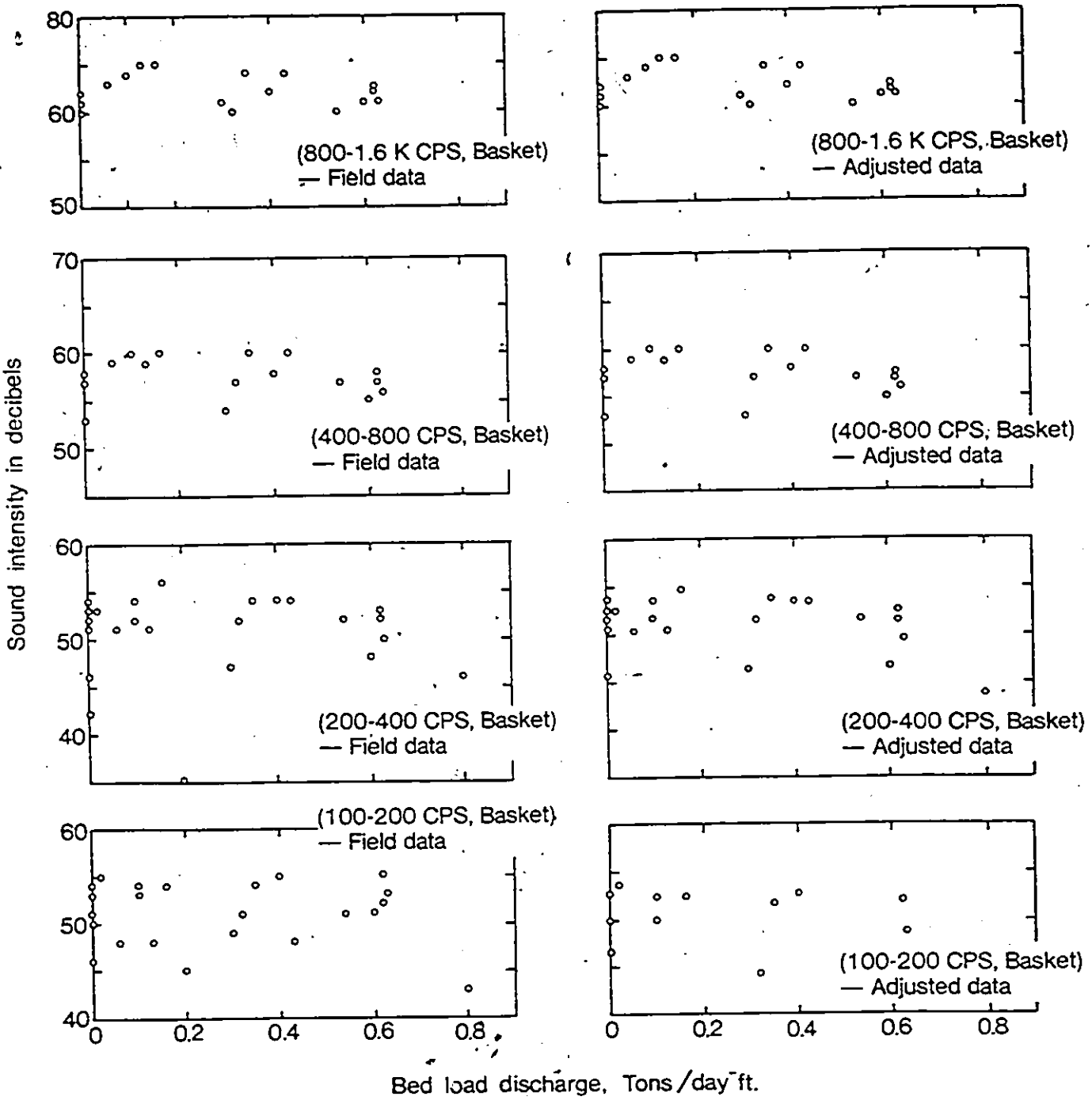
(800-1.6 K CPS, Basket)
— Field data
(800-1.6 K CPS, Basket)
— Adjusted data
(400-800 CPS, Basket)
— Field data
(400-800 CPS, Basket)
— Adjusted data
(200-400 CPS, Basket)
— Field data
(200-400 CPS, Basket)
— Adjusted data
(100-200 CPS, Basket)
— Field data
(100-200 CPS, Basket)
— Adjusted data
Sound intensity in decibels
Bed load discharge, Tons/day ft.

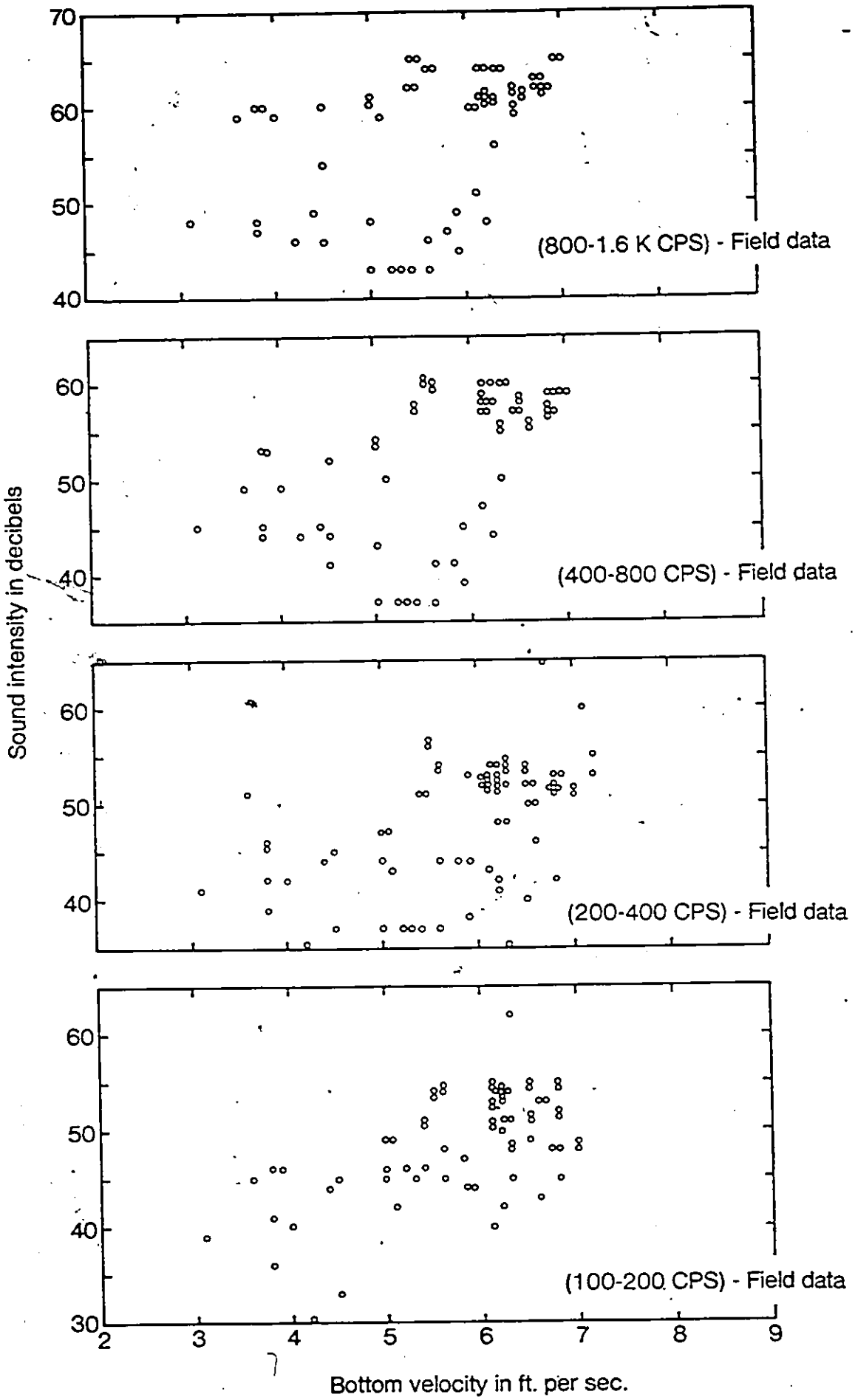
70
60
50
40
(800-1.6 K CPS) - Field data
60
50
40
(400-800 CPS) - Field data
60
50
40
(200-400 CPS) - Field data
60
50
40
30
(100-200 CPS) - Field data
2
3
4
5
6
7
8
9
Sound intensity in decibels
Bottom velocity in ft. per sec.

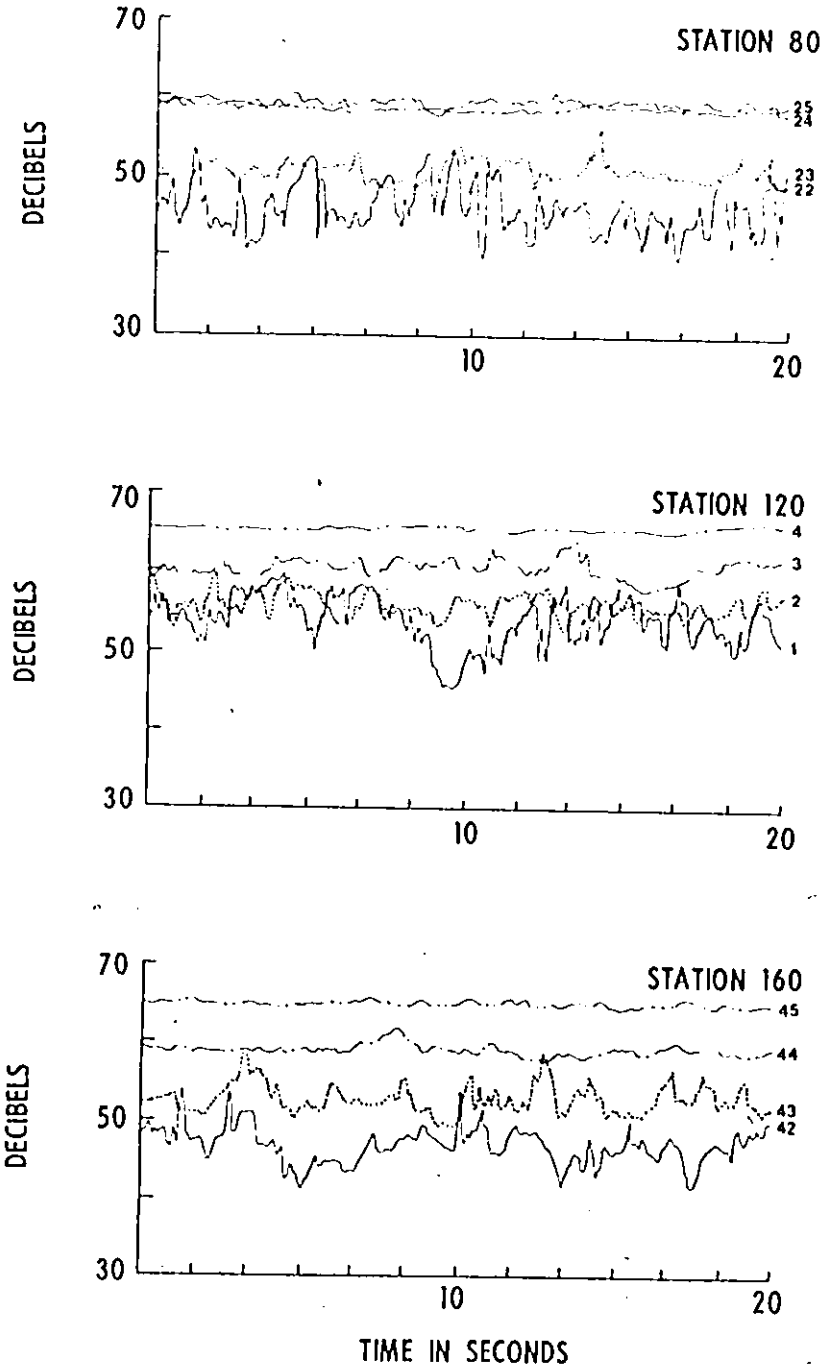

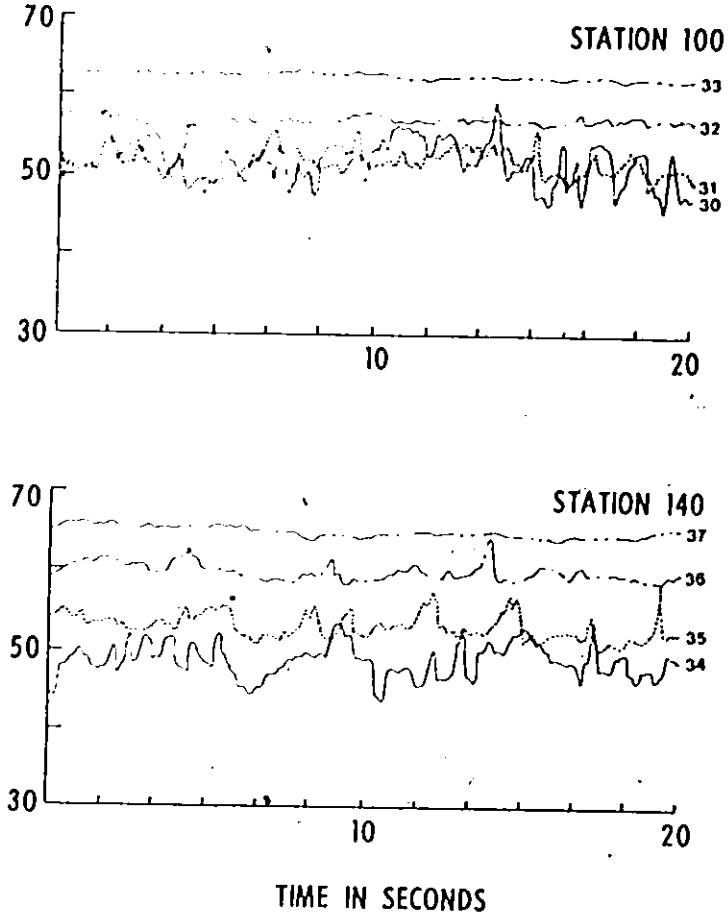

HYDROPHONE DATA MAY 31, 1972

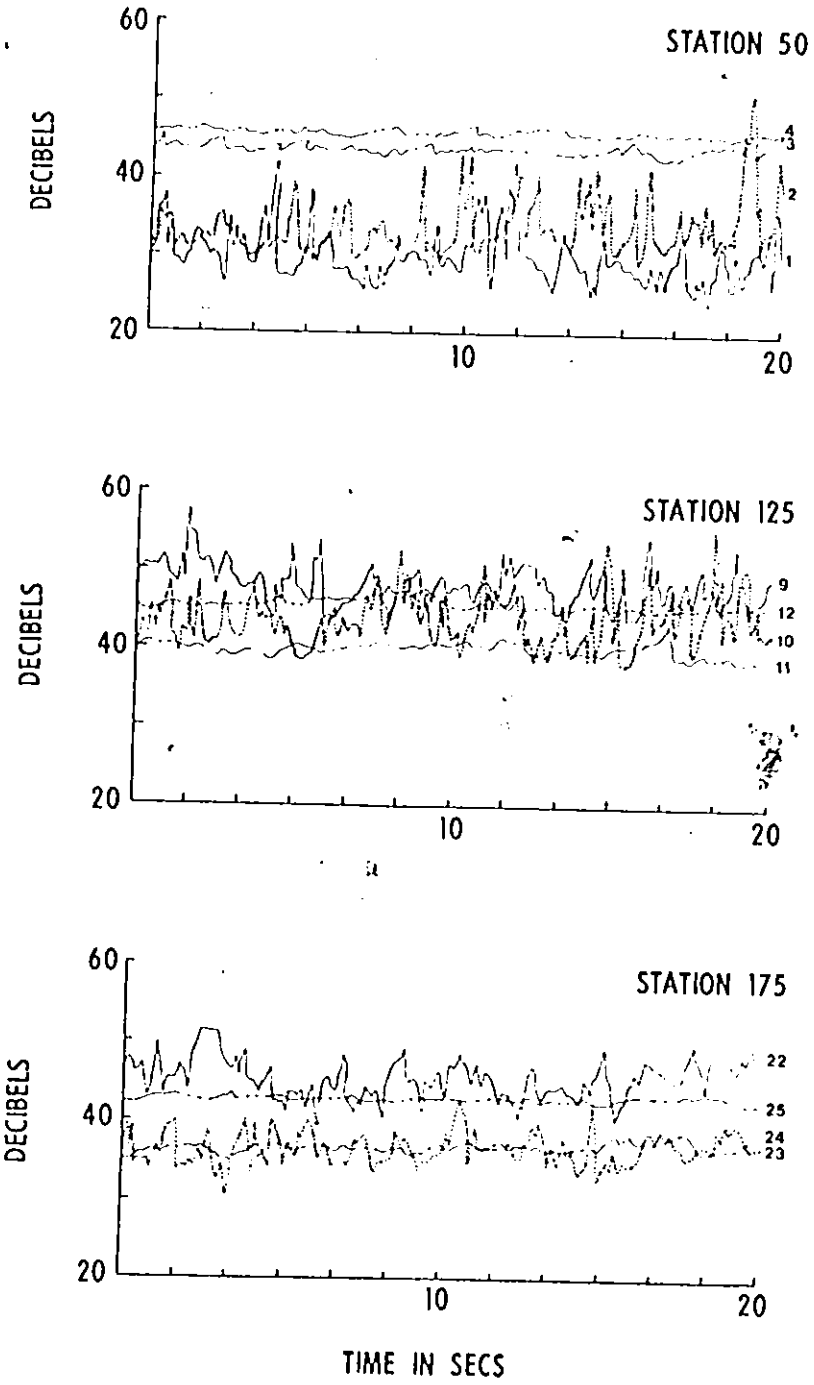

HYDROPHONE DATA JUNE 2, 1972

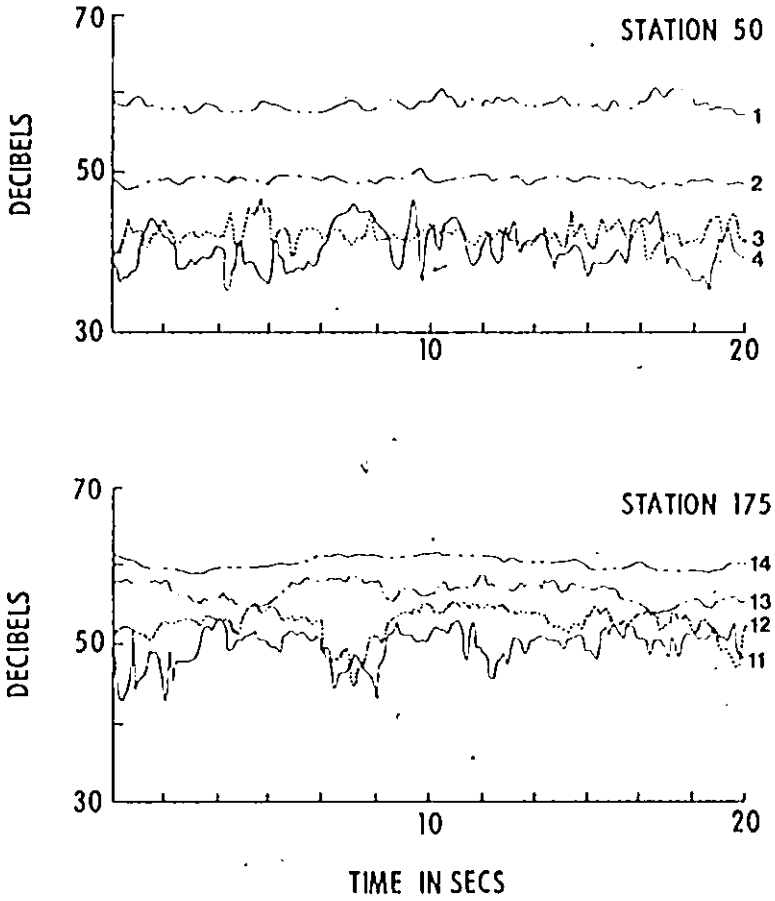

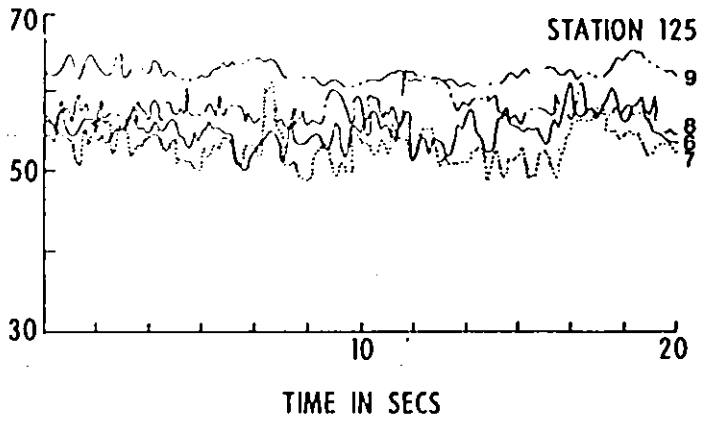

HYDROPHONE DATA JUNE 7, 1972

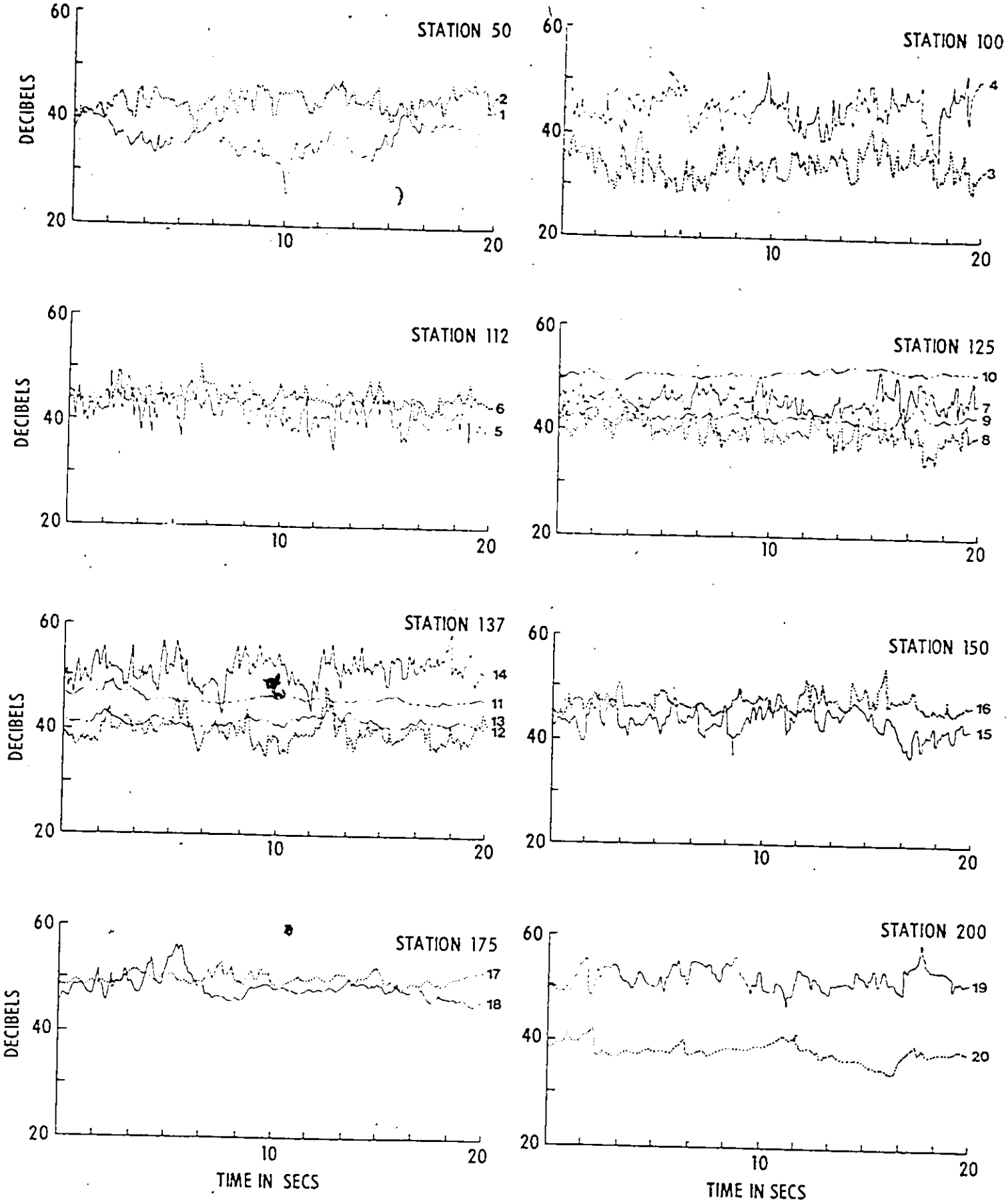

HYDROPHONE DATA JUNE 8, 1972

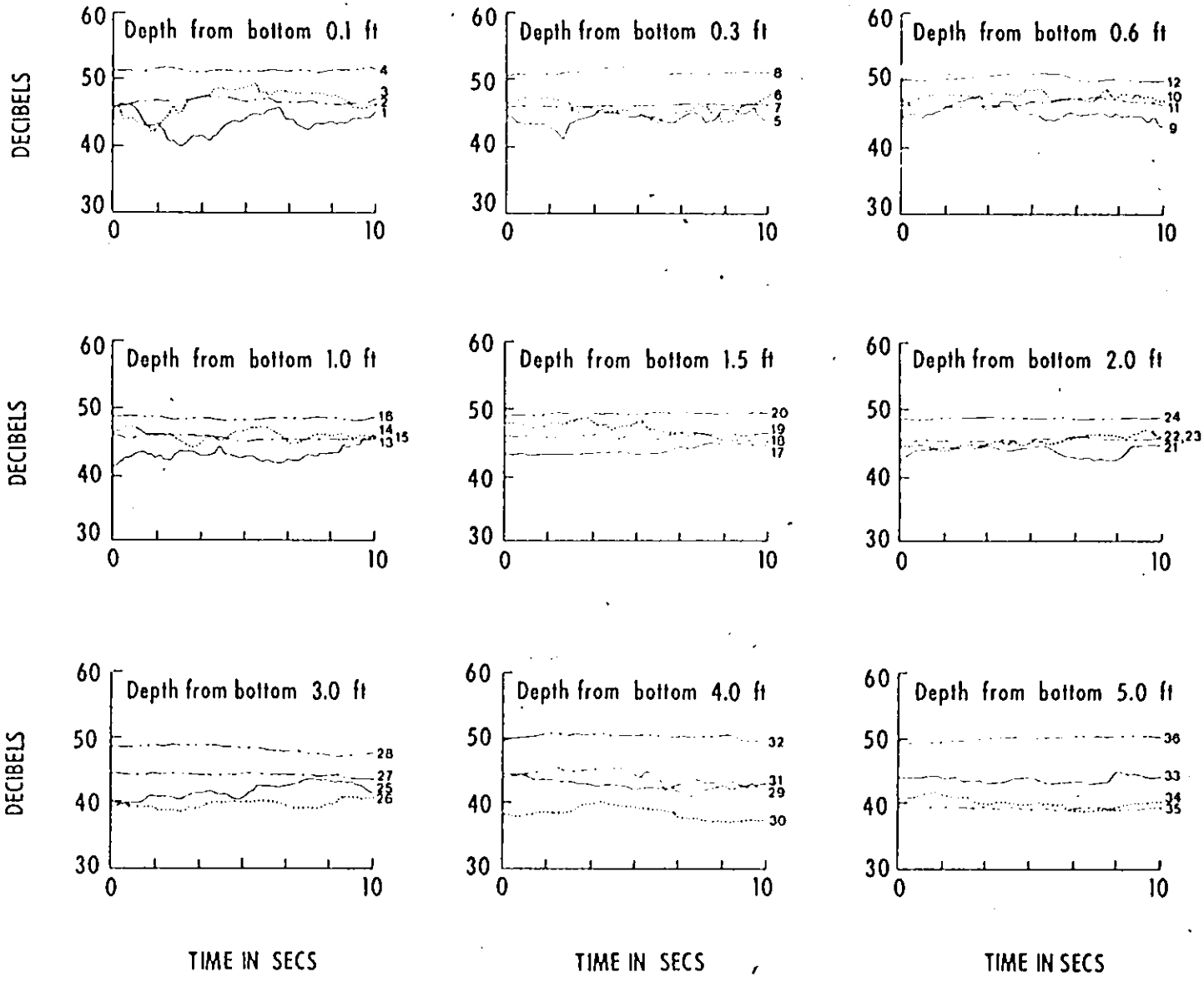

HYDROPHONE DATA JUNE 12, 1972. STATION 125

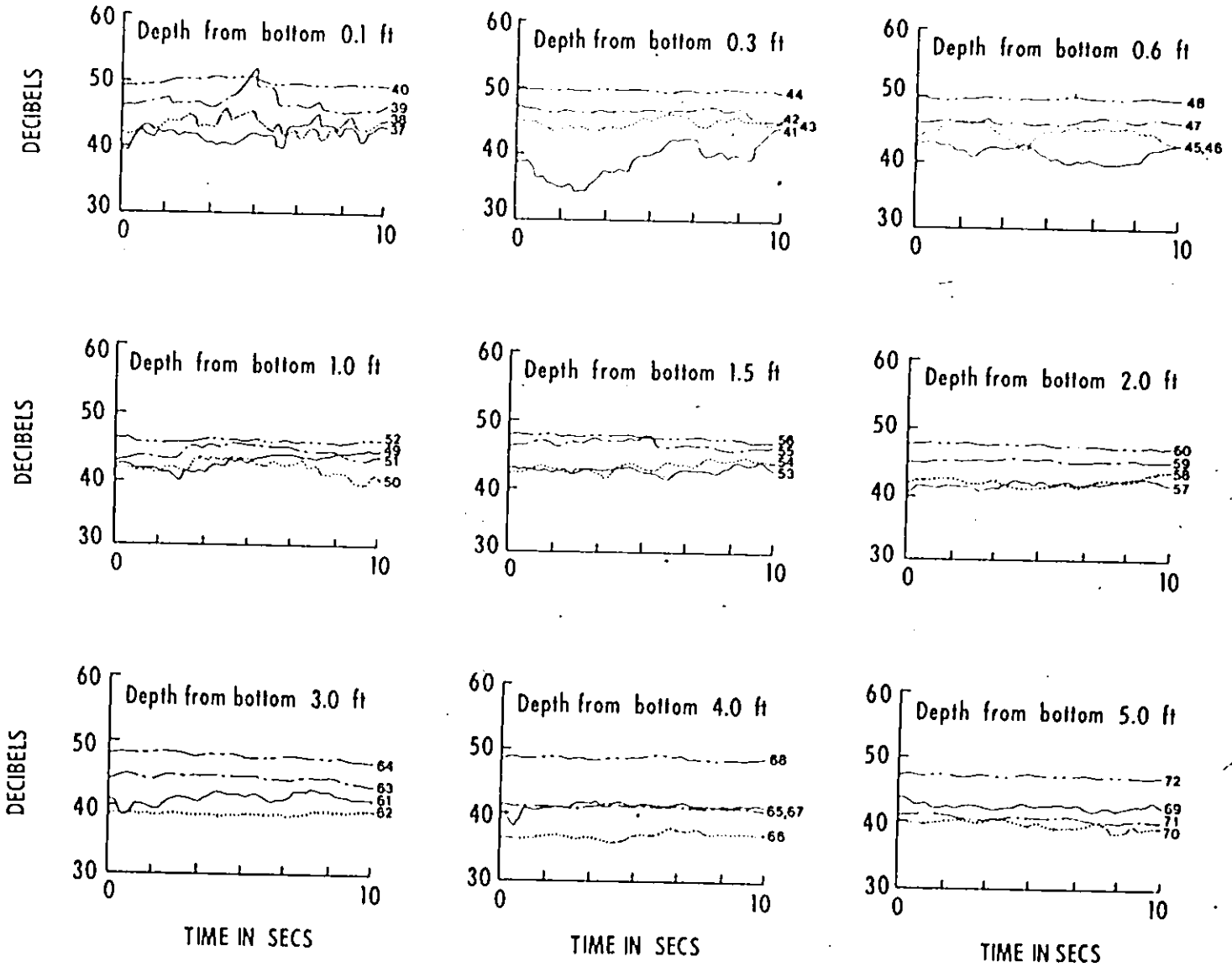

HYDROPHONE DATA JUNE 12, 1972. STATION 225

APPENDIX C

Photographs Illustrating Instrumentation and Site Conditions

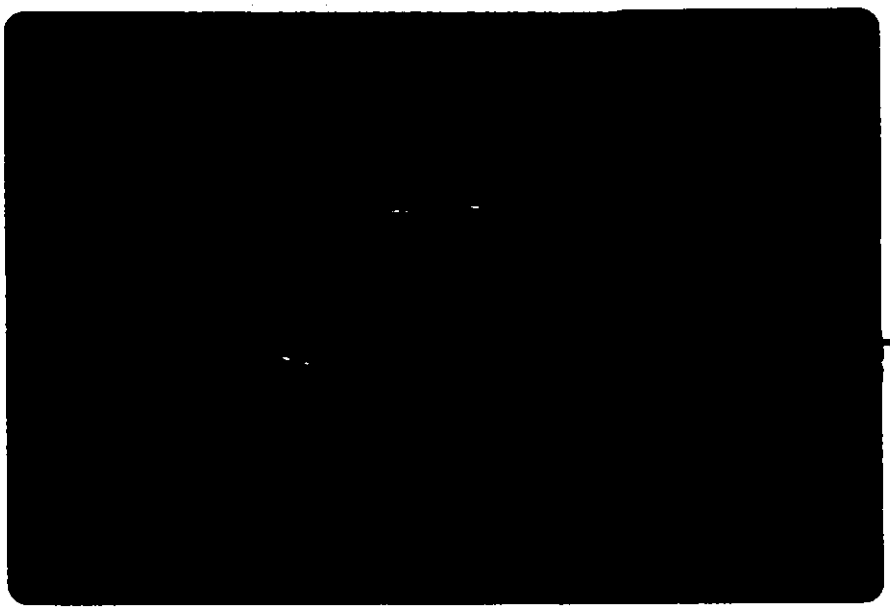

1. Vedder River: Upstream view from cross-section six, June, 1972.

2. Vedder River: Downstream view from cross-section six, June, 1972.

3. Upstream view of right bank at cross-section six, June, 1971.

4. Upstream view of right bank at cross-section six, June, 1972.

5. Downstream view of right bank at cross-section six, June, 1972.

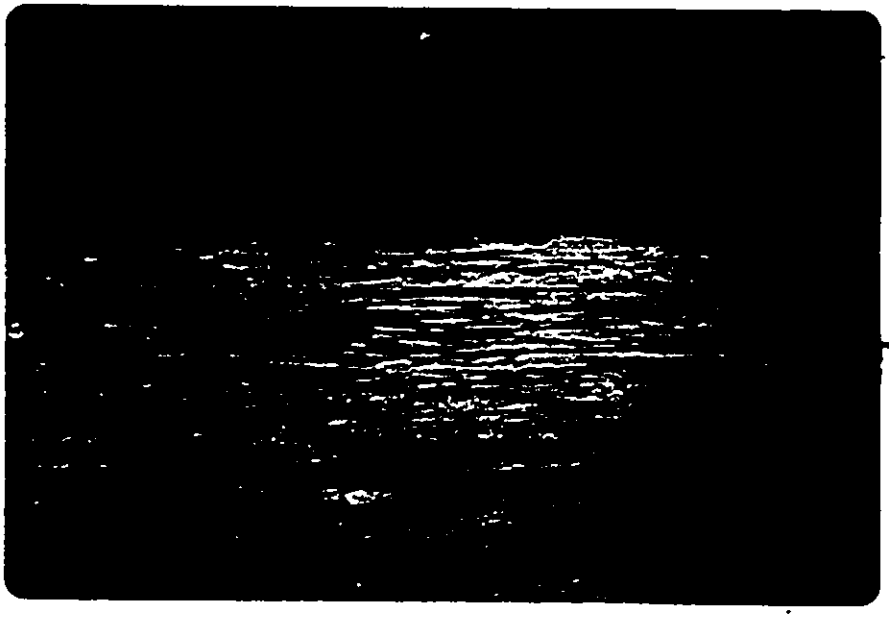

6. Cross-sectional view from right bank at cross-section six, June, 1972.

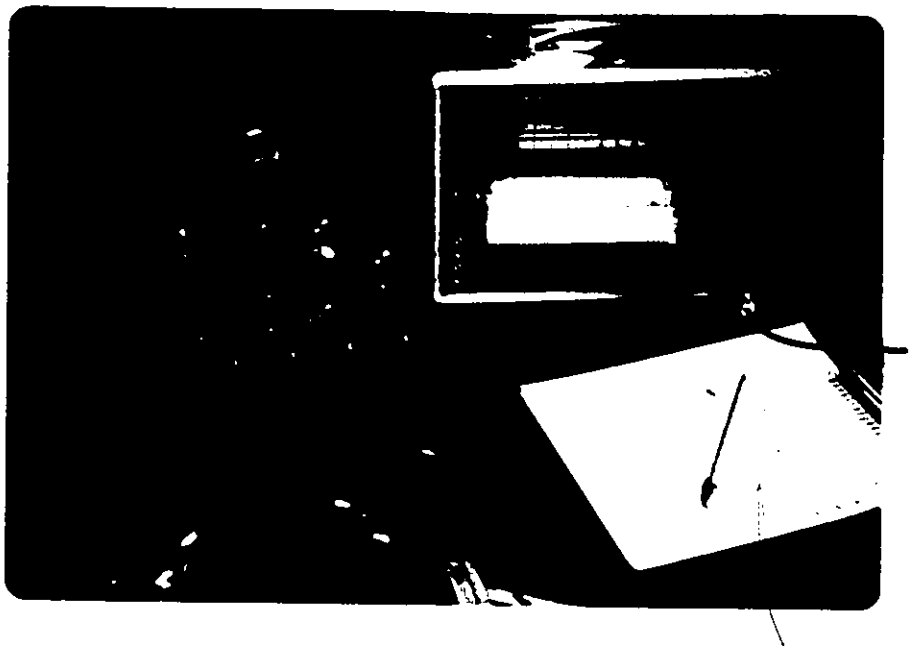

7. Signal conditioning (power supply, electronic filter, logarithmic amplifier and monitor panels) and recording components of the hydrophone system.

8. C-150 lead weight encompassing the hydrophone or data acquisition component of the hydrophone system.

9. Bed load sampling operations at cross-section six, utilizing a basket-type sampler and cable car, June, 1972.

10. Hydroscale and motorized reel utilized for bed load and other sampling operations at cross-section six, June, 1972.